Liquid Scintillation Analysis of the Main Environmental Radioisotopes in Air Using a Liquid Collector with Absorption Properties

Takahisa Kato

2023

Contents

Liquid Scintillation Analysis of the Main Environmental Radioisotopes in Air Using a Liquid Collector with Absorption Properties

Takahisa Kato

General Introduction

1. Historical background of radiation measurement

Humans, as well as all living species on Earth, must breathing. Breathing air is a fundamental function for sustaining life. Air containing various impurities, dusts, harmful gases and radioactive materials that can cause serious injury. Various kinds of radioisotopes in the atmosphere can have dire consequences, e.g., cause bodily injury due to radiation. In fact, such hazardous conditions occurred in the sixteenth century. In mines, radioactive radon was present in the mine tunnel air, and radon emits α-radiation, which can injure living things. Such hazards for mine workers were not understood at the time. Therefore, many mine workers in Europe died from pulmonary disease with no apparent explanation. Pulmonary disease was not connected with lung cancer and radon radiation because it was not known that radon was present at high concentrations in mines. Many people at that time believed that pulmonary disease was caused by unhealthy lifestyle, excess alcohol consumption and smoking tobacco in addition to the dust and poison gas in and mines. Only later was this disease actually diagnosed as lung cancer. In the 1920s, the relationship between pulmonary disease and lung cancer was demonstrated in animal experiments. Additional links between radiation and bodily injury were revealed after the discoveries of X-rays by W.C. Röentgen in 1895 and radionuclides by A.H. Becquel in 1896. Radiation was not initially thought to be the cause of lung cancer. It was later discovered that radon is a nuclide that emits α-radiation. As a result of the discovery of the correlation between α-radiation and bodily injury, it was recognized that lung cancer was induced by lung exposure to α-radiation from radon and its daughter species, polonium, bismuth and lead, because these nuclides were inhaled by miners in underground mines 1).

The measurement of radioactivity in the atmosphere is the first step in protecting the human body from internal exposure to radiation. First, the drift patterns of radioisotopes and the concentration of radioisotopes in the air must be determined, as humans cannot detect radioisotopes drifting in the air with our five major senses. By measuring the patterns and concentrations, we can determine the best way to protect ourselves against such hazards and take the appropriate actions in the future. When a serious accident, such

as the Fukushima nuclear power plant accident, which was caused by a tidal wave, at an atomic power plant or an atomic explosion occurs, the hazards (risks) are first recognized on the basis of radiation measurements. The hazards of radioisotopes in the air, however, have been thoroughly recorded throughout history.

2. Trends in regulations and the establishment of safe limits

The necessity of defining safe limits for internal and external exposure to protect humans was recognized based on these facts. As a consequence, a meeting was held in 1928 to discuss such safe limits. After that meeting, the International Commission on Radiological Protection (ICRP) was established in 1951. The ICRP began to examine occupational risks, and then in 1960, Committee II of the ICRP, 'Permissible dose for internal radiation', provided limits for the maximum permissible concentrations of individual radionuclides in air and water 2). An annual dose-equivalent limit was set for radioisotopes with radioactive half-lives in excess of 10 min. Then, based on a recommendation to define new criteria, the derived air concentration (DAC) and the annual limit on intake (ALI) 3) were calculated and published in 1979~1982 in ICRP Publication 30 4).

3. Necessity of measurement

The measurement of radioactivity in air originated from miner deaths due to lung cancer, and the public recognized the importance of this measurement. In Japan, the concepts of DAC and ALI are reflected in "The Law Concerning the Prevention of Radiation Hazards Due to Radioisotopes" (LPRHR) 5) and "Regulation Concerning the Prevention of Radiation Hazards Due to Ionizing Radiation" (RPRHIR) 6). The standard safe limits for every radioisotope in air and water based on the DAC and ALI for almost all radionuclides are presented in Tables G-1 and -2 of the additional appendixes of LPRHR. To apply the DAC and ALI values to safety requirements, exact measurements are necessary. Measuring the airborne radionuclide concentrations makes it possible to evaluate internal and external radiation exposure in humans. Moreover, monitoring and controlling the concentrations indoors or in limited space environments can increase occupational safety for everyone involved. To satisfy the purpose of the ICRP publications, we must establish a suitable daily measurement method and select a suitable apparatus for the accurate measurement of radionuclides and radiochemical compounds.

4. Measuring the main relative radionuclides and their safety limits

At this point, all radionuclides can be measured. The individual radioactivities of the 401 radionuclides shown in Tables G-1 and -2 attached in the LPRHR are measurable when the nuclide exists as a material in air, water, or solid materials using the appropriate apparatus, method or device. For simple daily measurements, when multiple

radionuclides are present, individual radioactivities sometimes cannot be measured. However, not all the radionuclides mentioned in LPRHR need to be measured at radiation facilities, reactor facilities, nuclear fusion facilities or dwellings. The radionuclides that require measurement and are easily multiplied were selected and classified, and these classifications are summarized in Table G-1.

Table G-1 Selected and classified easily multiplied radionuclides that require measurement.

Radiation	Nuclide being measured (limit in air, Bq cm^{-3})	Format or Phase of Materials	Measurement Method or Apparatus	Measurement limit in air (Bq cm^{-3})
α-particle	^{220}Rn, ^{222}Rn and their progenys, ^{235}U (3×10^{-6}), ^{238}U (4×10^{-6})	Gas, Aerosols	Gas flow scintillaion counter (ZnS(Ag)), Gas flow ionization chamber, Proportional counter (collected by filter)	$< 5.0\times10^{-8}$
β-emitter	^{14}C (4×10^{-2}), ^{32}P (4×10^{-5}), ^{33}P (8×10^{-5}), ^{35}S (2×10^{-4})	Gas, Chemical compound (volatilized)	Gas flow ionization chmber	2.0×10^{-4} (^{14}C)
	$^{3}H(5\times10^{-1})$	Gas, Chemical compound (volatilized)	Gas flow ionization chmber	
γ- or X- ray	^{125}I (1×10^{-3}), ^{131}I (1×10^{-3}), ^{18}F (2×10^{-1})	Gas, Chemical compound (volatilized)	NaI γ counter, Gas flow ionization chamber	2.9×10^{-7} (^{125}I), 1.4×10^{-6} (^{131}I), 7.2×10^{-4} (^{18}F)

As shown in Table G-1, the most common α-decay radionuclides present in air are ^{222}Rn, ^{220}Rn and their progenies, and these species originate underground. The radionuclides decaying with β-emission present in air are ^{3}H (tritium), ^{14}C, ^{32}P, ^{33}P, ^{35}S and ^{18}F, which are frequently used by researchers in radiation facilities. The X-ray emitting radioactive radionuclides present in air are derived from chemical compounds bearing ^{125}I and ^{131}I 7, 8).

5. Approach to measurement – selection of measurement apparatus

Instruments and methods for measuring nuclear radiation have been discussed by many researchers. As shown in Table G-1, ^{3}H, ^{14}C, ^{35}S and ^{18}F are easily detectable in air. Of the weak β-emitters, ^{3}H, ^{14}C, and ^{3}HHO (THO, tritiated water) are volatilized in fusion facilities, and ^{3}H- and ^{14}C-labeled chemical compounds are evaporated in radiation facilities. These nuclides cannot be measured with a GM monitor or a well-type scintillation counter. For ^{35}S, the self-decomposition components of ^{35}S gas can be effectively isolated in special cases involving the high specific activity of ^{35}S-labeled amino acids due to β-emissions 9). Other ^{35}S-labeled chemical compounds are not easily isolated. ^{32}P, a β-emitting radionuclide of high energy (1.711 MeV), and ^{33}P are difficult to identify. Only small amounts of ^{32}P and ^{33}P are present in the air and only for a short

time. ^{33}P is a β-emitting radionuclide with a comparatively weak energy (0.249 MeV). ^{18}F is a short-lived radionuclide (half-life of 109.771 min), that is used for PET analysis in humans, and its can be easily measured with a GM monitor. ^{125}I and ^{131}I are easily identified and can be collected by filtration and easily measured with a well-type scintillation counter or GM monitor; these isotopes can also be measured with a gas flow ionization counter but with low sensitivity. The α-particle emitters radon (^{222}Rn) and thoron (^{220}Rn), which are constantly released from the ground, cannot be collected by filtration, but they can be measured by a gas flow ionization counter or a liquid scintillation counter. When the radioactivities of ^{3}H, ^{14}C, ^{35}S, ^{222}Rn and ^{220}Rn in air are measured with a gas flow ionization monitor, the weak β particles from ^{3}H (18.6 keV), ^{14}C (156 keV), and ^{35}S (167 keV) are masked by the strong α particles from radon (5.48 MeV). Therefore, the nuclides cannot be independently measured.

LPRHR and RPRHIR noted that an ^{3}H concentration of 5×10^{-1} Bq cm^{-3} cannot be measured satisfactorily except by using a specifically designed gas flow ionization chamber 10,11) or a portable gas flow tritium air monitor attached to a plastic scintillator 12). These apparatuses are not commercially available.

Based on these factors, when the radioisotopes ^{3}H, ^{14}C, ^{222}Rn and ^{220}Rn are present in air at the same time, individually measuring these isotopes with a gas flow ionization chamber counter is very difficult. However, a liquid scintillation counter is a good detector for measuring these nuclides.

6. Characteristics of liquid scintillation measurements

Liquid scintillation spectrometers are one of the most powerful detectors for determining the type of radionuclide by the energy spectrum of the α-particles and/or β-emitters, especially for tritium 13-18). This instrument has a higher sensitivity for α-particles and low-energy β-emitters than a windowless gas flow-through proportional counter or ionization chamber. Each nuclide can be determined based on a number of useful quench correction methods 19~21) and can be identified from the resulting spectrum.

The most attractive characteristic of liquid scintillation measurements is the ability to record the energy spectra of α-particles and β-emitters. The resolution of the α-particle and β-emitter spectra recorded by the channel analyzer makes it possible to obtain separate energy spectra to determine the radioactivity of each radionuclide. Fig. G-1 shows the spectra of ^{3}H, ^{14}C and ^{222}Rn. The region between lines A and B shows the tritium spectrum and the radioactivity, the region between lines A and C shows the ^{14}C spectrum, the region between lines D and E shows the spectra of ^{222}Rn and its daughter radionuclide ^{218}Po, and the region between lines E and F shows the spectrum of ^{222}Rn

great-great-granddaughter ^{214}Po. The resolution of the energy spectrum of each radionuclide makes it possible to resolve the radioactivity of each radionuclide.

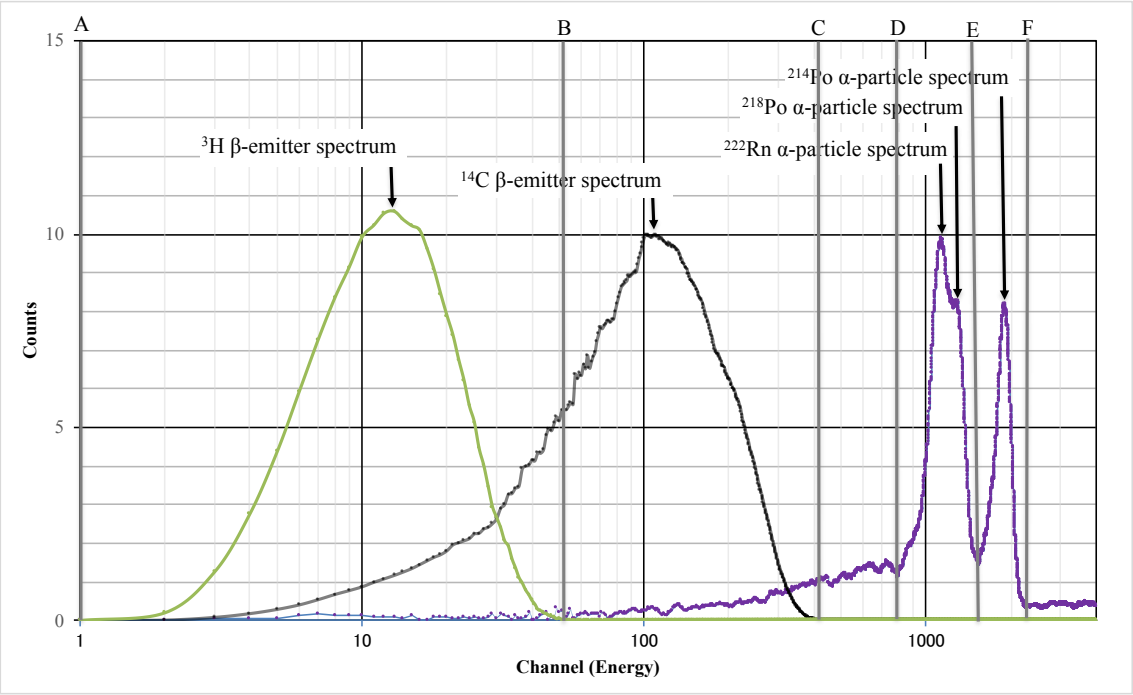

Figure G-1 Logarithmic plots of the α-particles and β-emitters tritium, ^{14}C, and ^{222}Rn and their daughter products ^{218}Po and ^{214}Po.

Due to these advantages, the radioactivities of ^{3}H, ^{14}C, and radon (^{222}Rn) gases can be measured independently. Therefore, a liquid scintillation counter is the most suitable instrument for determining the radioactivities of these radionuclides.

7. Measurement methods and conditions on Liquid Scintillation Measurements

In reactor facilities, large quantities of tritiated water (THO) evaporates from the pool that surrounds and shields the reactor core. Tritium-labeled chemical compounds are commonly used in radiation facilities. They are volatilized when using the tracer technique 22~30). A large volume of H_2 gas is used in nuclear fusion facilities. Such facilities condense airborne tritiated substances in measurable concentration ranges, which allows convenient sampling for practical indoor environmental monitoring. An adequate technique and suitable method are needed for these analyses.

8. Lowest concentration of collectible material

To measure radioactive chemical compounds in air through liquid scintillation measurements, the contaminated gases must be collected, and the sample for analysis in the liquid scintillator must be prepared. If the collection is based on adsorption to a solid

collector, e.g., activated carbon, silica gel or molecular sieves, the gaseous compounds can be measured, the results of which are shown in Fig. G-2-1 and -2; however, the sample

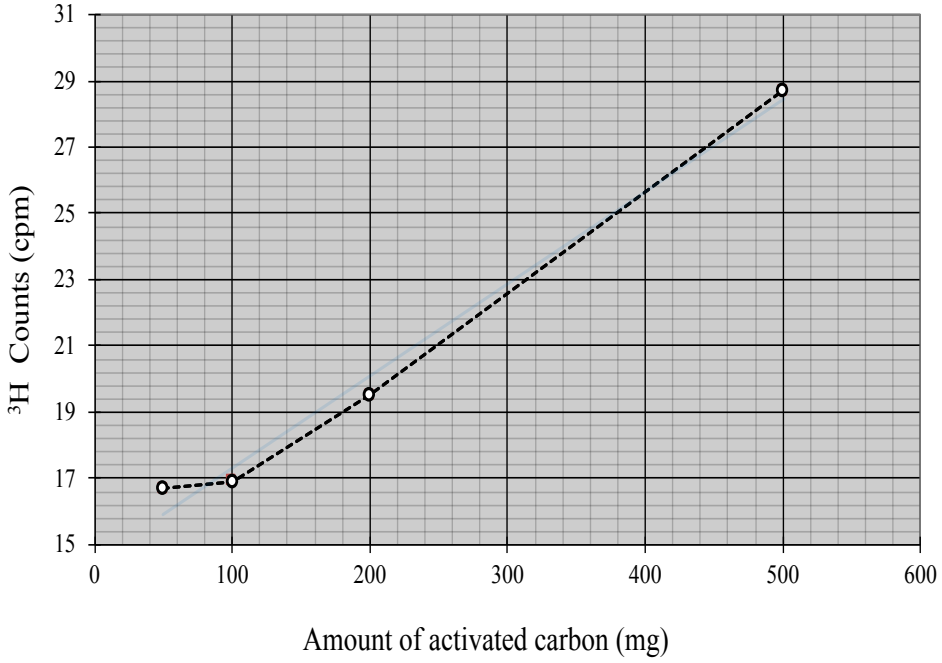

Figure G-2-1 Count rate of ^{3}H vs the amount of activated carbon mixed in the liquid scintillator

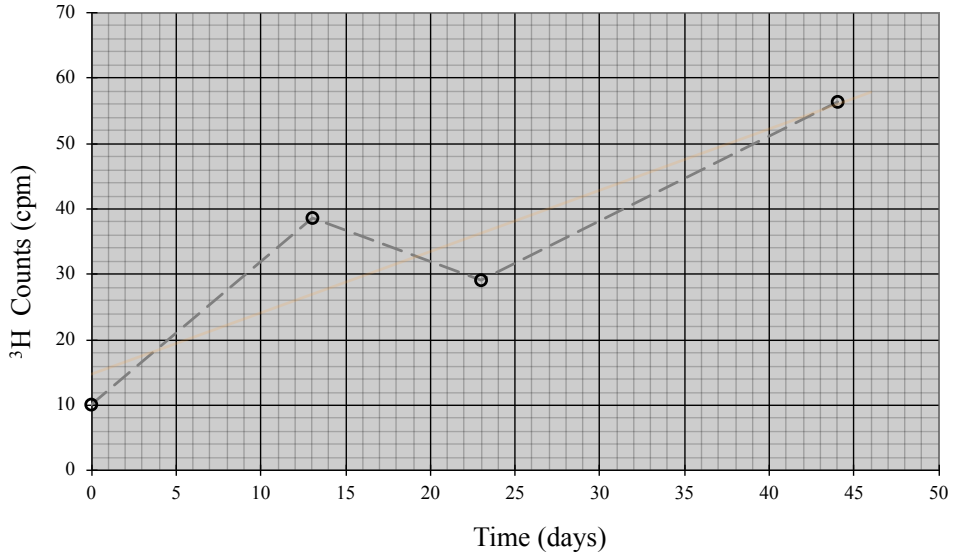

Figure G-2-2 Amount of ^{3}H adsorbed on activated carbon vs adsorption time (days)

cannot be mixed uniformly in a liquid scintillator, preventing accurate determination of the radioactivity. Liquid scintillation cannot accurately measure the radioactivity of phase-separated samples. Thus, by using a liquid collector and a liquid scintillation counter, the author devised a method to measure the concentration of β-emissive radioactive chemical compounds, especially tritiated compounds and radon gas. The liquid collector is suitable for quantitative and qualitative analysis with a liquid scintillation counter.

9. Methodology of the liquid scintillation measurements

The liquid scintillation measurement of gaseous radioactive materials requires at least three steps. The first step is the collection of the radioactive airborne materials in a sampling medium. The second step is the uniform mixing of the medium in the liquid scintillator. The third step is measuring the medium in the liquid scintillation counter at the maximum efficiency with the lowest quenching.

In this work, a liquid scintillation methodology for determining the radioactivity of gaseous materials is described. The selection of the sampling medium, the practical measurement of vaporized tritiated water ($\cong 3.7\times10^{-3}$ Bq cm^{-3} (10^{-7} μCi cm^{-3})) below the tritium LPRHR limit of 5×10^{-1} Bq cm^{-3} to over its limit in air and airborne radon over the concentration range from ≅0 to 8000 Bq m^{-3}, the development of a scintillation absorbent collector, as well as the performance of the method are also discussed.

10. Summary of the content in each chapter according to the development of this study

Chapter 1. The first step in the liquid scintillation measurement is the determination of air contaminated by tritiated chemical compounds. Using a traditional liquid collector, ethylene glycol, the radioactive chemical compound [methyl-^{3}H]-thymidine was quantitatively measured in air 31).

Chapter 2. Using a second liquid collector, silicone oil, the radioactive chemical compounds [methyl-^{3}H]-thymidine and [U-^{14}C]-leucine were measured in air, and the material properties of the liquid collector and the scintillator solvent were considered 32).

Chapter 3. The quenching effect of a liquid scintillator was considered mathematically 33) in relation to the quenching phenomenon of liquid scintillation using the Stern-Volmer equation 34). This phenomenon occurs when the sample in the collector material is mixed into the scintillation cocktail. This step is important in the development of liquid collectors.

Chapter 4. A game-changing liquid collector, i.e., a nonvolatile liquid scintillation absorbent, was developed 35). This is the most important development in this work. The

molecular properties and chemical structure of the scintillator solvent are presented. The measurements in the following chapter show that the measurement method proposed herein is suitable.

Chapter 5. Using the scintillation absorbent, vaporized tritiated water in air is measured 36).

Chapter 6. The qualitative analysis of air contaminated with the self-decomposition product of [^{35}S]-methionine was demonstrated using the liquid collector methanol. The degradation mode of a biological molecule upon internal exposure to the β-emitter was indicated. The self-decomposition gaseous compounds produced by β-emitter irradiation from [^{35}S]-methionine and [^{35}S]-cysteine were identified 9).

Chapters 7 and 8. Atmospheric radon was quickly measured by α-spectrometry. The radon measurements were performed using the nonvolatile liquid scintillation absorbent developed in Chapter 4.

In Chapter 7, the performance of a general and quick practical process for measuring atmospheric radon based on ^{214}Po α-spectrometry is detailed 37).

In Chapter 8, the performance of a novel, quick and practical process for measuring atmospheric radon based on ^{222}Rn-^{218}Po α-spectrometry is detailed 38).

References

1) Radiation Protection in Uranium and other Mines. *ICRP Publication* **24**, Annals of the ICRP, **1**(1) Pergamon Press, Oxford (1977).

2) Report of Committee Ⅱ on Permissible Dose for Internal Radiation (1959). *ICRP Publication* **2**, Annals of the ICRP, Pergamon Press, Oxford (1960).

3) Recommendation of the International Commission on Radiological Protection. *ICRP Publication* **26**, Annals of the ICRP, **1**(3), Pergamon Press, Oxford (1977).

4) Limits for Intakes of Radeoradionuclides by Workers. *ICRP Publication* **30**, Annals of the ICRP, **2**(3/4); **4**(3/4); **6**(2/3), Pergamon Press, Oxford (1979-1982)

5) *The Law concerning Prevention from Radiation Hazards due to Radioisotopes, etc., Japan* (2005).

6) *Regulation concerning Prevention from Radiation Hazards due to Ionizing Radiation, Japan* (2005).

7) Heath, R. L., Hofstadter, R and Hughes, E. B. (1979) Ⅸ. Scintillation detectors Inorganic scintillators. A review of techniques and applications, *Nucl. Instr. and Meth.* **162**, 431-476.

8) Horrocks, D. L. (1975) Standardizing ^{125}I sources and determining ^{125}I counting efficiencies of well-type gamma counting systems, *Clinical Chemistry* **21**, 370-375.

9) Kato, T., Saito, K. and Kurihara, N. (1994) Self-decomposition Components Generated from ^{35}S-labeled Amino Acids, *Int. J. Appl. Radiat. and Isot.* **45**, 693-698.
10) Jalbert, R. A. and Hiebert, R. D. (1971) Gamma Insensitive air monitor for Radioactive gases, *Nucl. Instr. and Meth.* **96**, 61-66.
11) Jalbert, R. A. (1975) A Monitor for tritium in air containing other beta emitters, *Proc. 23rd Conf. on Remote System Technology*, 89-93.
12) Reynold, G. T. Harrison, F. B. and Salvini, G. (1950) Liquid scintillation Counters, *Phys. Rev.* **78** 488.
13) Sannes, F. and Banville, B. (1965) A portable tritium-in-air monitor, *Atomic Energy of Canada Limited* **2283**, 1-20.
14) Kallman, H. and Furst, M. (1950) Fluorescence of solutions bombarded with high radiation (energy transport in liquids) *Phys. Rev.* **79**, 857-870.
15) Raymond, C. S. and Irvine, J. W., Jr. (1956) Study of organic scintillators, *J. Chem. Physics* **24**, 670-715.
16) Davidsib, J. D. and Feigelson, F. (1957) Practical aspects of interal-sample liquid – scintillation counting, *Int. J. Appl. Radiat. and Isot.* **2**, 1-18.
17) Brooks, F. D. (1979) Development of organic sintillators, *Nucl. Instr. and Meth.* **162**, 477-505.
18) Noaks, J. E., Neary, M. P. and Spaulding, J. D. (1979) Tritium measurements with a new liquid scintillation counter, *Nucl. Instr. and Meth.* **109**, 177-187.
19) Furst, M. and Kallman, H. (1955) Enhancement of fluorescence in solutions under high-energy irradiation, *Phys. Rev.* **97**, 583-587.
20) Furst, M. and Kallman, H. (1955) Increasing Fluorescence Efficiency of Liquid Scintillation Solutions, *Nucleonics.* **13**, 58-60.
21) Furst, M., Kallman, H. and Brown, F. H. (1955) Fluorescence Behavior of solutions containing more than one solbent, *J. Chem. Phys.* **23**, 607-612.
22) Libby, W. L. (1946) Atmospheric Helium Three and Radiocarbon from Cosmic Radiation, *Phys. Rev.* **69**, 671-672.
23) Kaufman, S and Libby, W. L. (1954) The Natural Distribution of Tritium, *Phys. Rev.* **93**, 1337-1344.
24) Goldsmith, P. and Brown, F. (1961) World-wide circulation of air within the stratosphere, *Nature* **191**, 1033-1037.
25) Hagemann, L., Gray, J. Jr., Machta, L. and Turkevich, A. (1959) Stratospheric carbon-14, carbon dioxide, and tritium, *Science* **130**, 542-552.
26) William, J. J. and Rhines, P. B. (1980) Tritium in the deep North Atlantic Ocean, *Nature* **286**, 877~880.

27) Rapkin, E., and Gibbs, j. A. (1962) A system for continuous measurement of radioactivity in flowing streams, *Nature* **194**, 34~36.
28) Moghissi, A. A., Kelley, H. L., Phiillips, C. R. and Regnier, J. E. (1969) A tritium monitor based on scintillator, *Nucl. Instr. and Meth.* **68**, 159.
29) Osborne, R. O. (1970) Detector for tritium in water, *Nucl. Instr. and Meth.* **77**, 170~171.
30) Alvarez, L.W. and Cornog, R. (1940) Radioactive Hydrogen, *Phys. Rev.* **57**, 248.
31) Kato, T. (1979) Measurement of tritium in air by adsorbent, *Nucl. Instr. and Meth.* **163**, 463-465.
32) Kato, T. A. (1979) Monitoring of radioactive gases in air by adsorption, *Int. J. Appl. Radiat. and Isot.* **30**, 349-351.
33) Stern, V. O. and Volmer, M. (1919) Über die abklingszeit der fluoreszenz, *Physik. Zeitschr.* **XX**, 183-188.
34) Kato, T. (1980) Quenching equation for scintillation, *Nucl. Instr. and Meth.* **172**, 597-599.
35) Kato, T. and Hatagami, T. (1981) Nonvolatile Liquid Scintillator, *Anal. Chem.* **52**, 586-587.
36) Kato, T. (1983) Analysis of tritiated water vapor by non-volatile liquid scintillant sorbent, *Int. J. Appl. Radiat. and Isot.* **34**, 1953-1595.
37) Kato, T, Janik, M., Kanda, R., Ishikawa, T., Kawase, M. and Kawamoto, T. (2016) Measurement of radon in air using a radon-^{218}Po calibration curve determined by an absorptive non-volatile liquid scintillator, Radiation Measurement, **95**, 25-30.
38) Kato, T, Janik, M., Kanda, R., Ishikawa, T., Kawase, M. and Kawamoto, T. (2018) "Environmentally friendly measurement of airborne radon using a non-volatile liquid scintillation absorbent", Health Physics Journal. **115**(2), pp. 203-211.

Chapter 1

Measurement of Tritium in Air using a Sorbent

1. Introduction

This chapter describes a method for obtaining samples of very low concentrations of tritium in air by sorption, and after adsorption, the samples are mixed in a liquid scintillator and measured with a liquid scintillation counter 1, 2).

The measurement of tritium in gases and liquids has been described in many previous reports 3~8). Low concentrations of tritium in air are usually measured by flowing a fixed volume of atmospheric air into an ionization chamber 9, 10). This instrument has good accuracy and is able to measure tritium concentrations on the order of 3.7×10^{-1} Bq/mL (10^{-5} μCi/mL). This method has limited sensitivity due to the volume limits of the chamber and suffers from increasing background in the chamber upon repeated use.

Ethylene glycol was initially selected as the liquid collector because of its sorbent properties and ability to gather gaseous chemical compounds from air. Active carbon, for instance, is an excellent adsorbent; however, being black and opaque reduces its efficiency as a liquid scintillator.

Ethylene glycol (CH_2OHCH_2OH) has two hydroxyl units and easily dissolves many chemical compounds. Based on its chemical formula, two rotamers, staggered and eclipsed conformations, exist as a result of rotation about the carbon–carbon bond 11). Each rotamer has three geometric isomers. Fig. 1-1 shows the isomers; eclipsed isomers are not possible because of steric hindrance between the hydroxyl units and hydrogen.

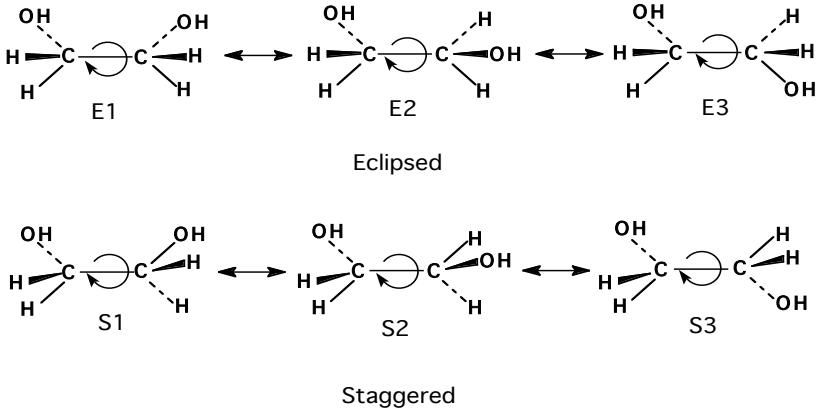

Figure 1-1 Considered conformational isomers of ethylene glycol.

The S2 conformation in the staggered rotamer is the most stable and has a center of symmetry, that is, it is nonpolar and can sorb both hydrophilic and lipophilic compounds.

Ethylene glycol not only satisfies the conditions mentioned in the general introduction but is also one component of Bray's liquid scintillation cocktail (Bray's solution is composed of naphthalene, ethylene glycol, and dioxane) 12). 4). In Bray's liquid scintillation cocktail, ethylene glycol provides a freezing-point depression. It is not necessary for energy transfer in the scintillation process but acts as a low quenching solvent. When ethylene glycol sorbs (adsorbs and/or absorbs) a radioactive chemical component and is mixed in the scintillator, it is effective for the measurement of radioactivity. Ethylene glycol is, however, a quencher. When excess ethylene glycol is mixed in the scintillator, the sensitivity and accuracy are lowered. Based on these considerations, the most suitable volume of ethylene glycol was determined.

In this study, [methyl-^{3}H]-thymidine was used as the volatilized chemical compound. [Methyl-^{3}H]-thymidine is one of the most useful radioactive chemical compounds in radiation facilities. Tritium is commonly used in a variety of applications in the life sciences. Thus, there is a continuous need to measure its concentration both in tracer applications and as a contaminant in air.

From these results, the optimum volume of sample for mixing was determined, the sorbent that gives the maximum sensitivity was established, and the detectable concentration of tritium in air was found to be less than 3.7×10^{-3} Bq/mL (10^{-7} μCi/mL).

2. Experimental and Results

The method is as follows: a measured amount of tritiated thymidine was dissolved in the scintillator solution, and its activity was estimated. This source was placed in a closed desiccator of the known volume. A 10 mL aliquot of ethylene glycol was placed in an open vessel in the desiccator. The source was allowed to volatilize, thus forming tritiated air. The source was made up to its original volume, and its activity was measured again. Thus, the activity of the air was calculated. During the experiment, 0.2 mL samples of glycol were periodically withdrawn and added to 9.8 mL of Bray's solution, and the activity was measured with a liquid scintillation counter.

These measurements were repeated several times. The initial measurement period per cycle was approximately two months. To speed up subsequent cycles, an air pump was employed in the closed desiccator, and as a result, the period was shortened to less than a day.

The results with ethylene glycol are shown in Fig. 1-2. The curve indicates that the

amount of sorbed tritium is directly proportional to the amount volatilized, which is proportional to the volatilization time. Using these data, the amount of volatilized tritium in ethylene glycol and the sorption coefficient can be estimated. The following typical values were obtained. The activity of the tritium source is 8.58×10^{3} Bq (0.232 μCi). The activity of the volatilized tritium from the source is 5.40×10^{2} Bq (1.46×10^{-2} μCi). The tritium concentration in the desiccator was 1.76×10^{-1} Bq/mL (4.76×10^{-6} μCi/mL). The sorption coefficient was thus calculated to be 2.77×10^{-3} Bq, which is the amount of sorbed tritium divided by 1.46×10^{-2} Bq, giving a fraction of 19.0%.

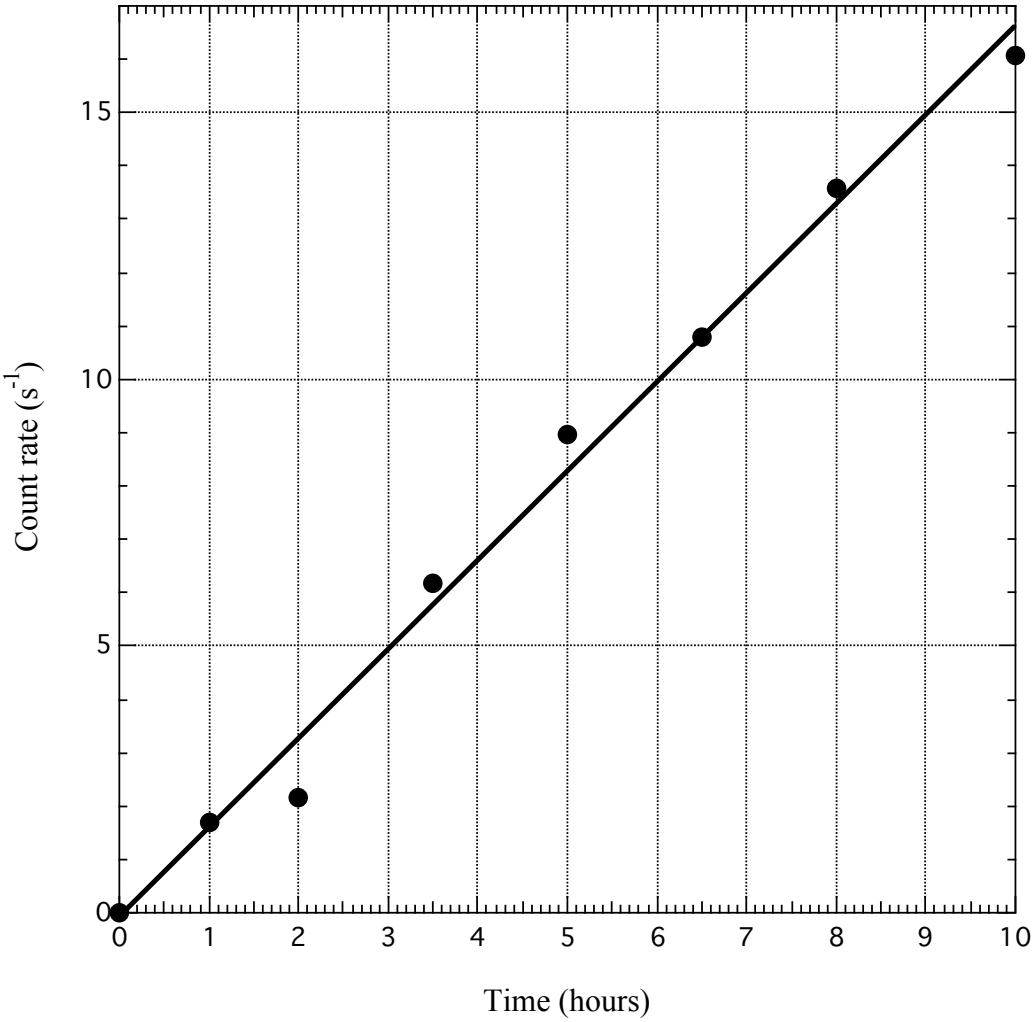

Figure 1-2 Collected amount of tritium vs. the collection time in hours for ethylene glycol.

In the first experiment as described above, tritium for sampling was trapped using ethylene glycol as a sorbent. Measurements were conducted with a liquid scintillation

counter using Bray's dioxane solution in which the sorbent was used at a 2%.

To increase the sensitivity of this method, the following experiment was performed. In the sampling, if a sorbent sorbs a fixed concentration of tritium, the activity of tritium per vial will be proportional to the amount of sorbent in the vial. Therefore, if the quantity of sorbent in the scintillator is increased, the quantity of tritium per vial will be greater. This in turn will increase the counting rate of the sample in the vial, enhancing the sensitivity of the analysis.

In the second experiment, the counting rate was varied and the sorbent mixture in each scintillator sample vial was increased. The sorbent with tritium was added to increasing amounts of Bray's scintillator solution, from 0.2 mL to 10 mL per vial. The counting rates due to activities in these samples were measured. The same procedure was also used in the measurement of the toluene scintillator solution.

The results are shown in Fig. 1-3. Curve I is the toluene scintillator solution and curve II is obtained with Bray's solution. A fixed concentration of tritium was added to

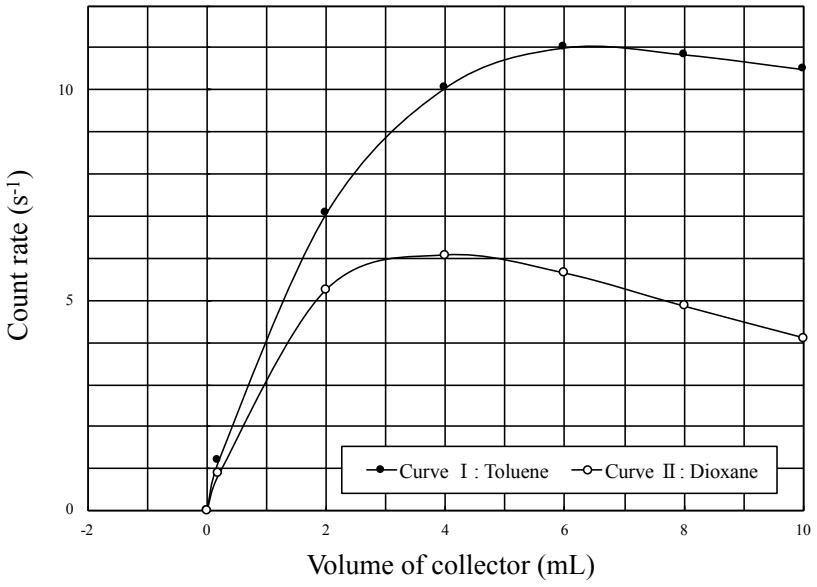

Figure 1-3 The variation in the counting rate as a function of the volume of tritium-loaded ethylene glycol in a vial containing a liquid scintillator. Closed circles are for the toluene scintillator solution, and open circles are for the dioxane solution.

varying volumes of ethylene glycol in the liquid scintillator. At low concentrations of sorbent, the curve is linear, i.e., the counting rate is proportional to the concentration, but as the concentration increases, the count rate becomes nonlinear. Saturation of ethylene

glycol was reached in a mixture of 10 mL of scintillator solution containing approximately 4 mL of dioxane and 6 mL of toluene. This concentration of dioxane scintillator solution is 20 times the standard amount (0.2 mL) in Bray's solution. Accordingly, the quantity of tritium that could be absorbed by the ethylene glycol was 20 times greater, but because the counting efficiency decreases due to the increased quenching, the counting rate is only approximately 7 times greater; therefore, the sensitivity also increases by a factor of 7. Since the sensitivity with 0.2 mL of the standard was on the order of 3.7×10^{-2} Bq/mL (10^{-6} μCi/mL), it is possible to increase the sensitivity to on the order of 3.7×10^{-3} Bq/mL (10^{-7} μCi/mL). As indicated in curves I and II of Fig. 1-2, the sensitivity with the toluene scintillator solution (curve I) can be a factor of 10 greater that that with standard Bray's solution (curve II).

3. Discussion

Ethylene glycol is a good sorbent for tritium in air because of its homogeneity and low volatility. Because of its miscibility and high efficiency, it is an effective scintillator solution.

The sensitivity of the method depends upon the concentration of tritium trapped in the sorbent, the sample volume and the efficiency of the detector. In this method, the sorbing efficiency of ethylene glycol was found to be 19.0%. Therefore, in practice, the product of the total amount of tritium in the room and this coefficient is the maximum amount of sample needed to increase the sensitivity.

If contaminated air with the maximum concentration of tritium is trapped in this sorbent and if the optimum sample volume, which corresponds to the saturation point for the maximum counting rate, is measured, the highest counting sensitivity can be obtained.

4. Conclusion

A liquid scintillation method was used to measure tritium volatilized from a tritiated chemical compound in air using a liquid sorbent. The sorbent was effectively used as one component of the liquid scintillator solution.

5. Summary

A scintillation method that measures tritium contamination in air using a liquid sorbent is described. In this method, tritium in the atmosphere is sorbed onto a sorbent, which is then mixed in a liquid scintillator and measured using a liquid scintillation counter. The sorbent has two roles: first, to sorb tritium and second, to be one component of the liquid scintillation cocktail. According to this method, the accumulated quantity of tritium is

proportional to the sampling period and to the sample volume of sorbent in which tritium is uniformly sorbed. A variation in the counting rate with different volumes of mixed sample in the liquid scintillator was tested using a liquid scintillation counter. From the results, the optimum volume of mixed sample was determined, the sorbent that gave maximum sensitivity was established, and the detectable concentration of tritium in air was found to be less than 3.7×10^{-3} Bq/mL (10^{-7} μCi/mL).

References

1) Kallman, H. and Furst, M. (1950) Fluorescence of solutions bombarded with high radiation (energy transport in liquids) *Phys. Rev.* **79**, 857-870.

2) Noaks, J. E., Neary, M. P. and Spaulding, J. D. (1973) Tritium measurements with a new liquid scintillation counter, *Nucl. Instr. and Meth.* **109**, 177-187.

3) Herberg, R. J. (1960) Determination of carbon-14 and tritium in blood and other whole tissues: liquid scintillation counting of tissues, Anal. Chem. **32**, 42-46.

4) Butler, F. E. (1961) Determination of tritium in water and urine, *Anal. Chem.* **33**, 409-414.

5) Patterson, M. S. and Greene, R. (1965) Measurements of low energy beta-emitters in aqueous solution by liquid scintillation counting of emulsions, *Anal. Chem.* **37**, 854-857

6) Benson, R. H. (1966) Limitation of tritium measurements by liquid scintillation counting of emulsions, *Anal. Chem.* **38**, 1353-1356.

7) Gupta G. N. (1966) A simple in-vial combustion method for assay of hydrogen-3, carbon-14 and sulfur-35 in biological, biochemical, and organic materials, *Anal. Chem.* **38**, 1356-1359.

8) Greene, R. C., Patterson, M. S. and Estes, A. H. (1968) Use of alkylphenol surfactants for liquid scintillation counting of aqueous tritium samples, *Anal. Chem.* **40**, 2035-2037.

9) Jalbert, R. A. and Hiebert, R. D. (1971) Gamma Insensitive air monitor for Radioactive gases, *Nucl. Instr. and Meth.* **96**, 61-66.

10) Jalbert, R. A. (1975) A Monitor for tritium in air containing other beta emitters, *Proc. 23rd Conf. on Remote System Technology*, 89-93.

11) James B. Hendrickson, Donald J. Cram and Geore S. Hammond, (19**) Organic Chemistry, 3rd Edition, MacGRAW-HILL KOGAKUSHA, LTD.

12) Bray, G. (1961) A simple efficient liquid scintillator for counting aqueous solutions in a liquid scintillation counter, *Anal. Biochem.* **1**, 279-285.

Chapter 2

Monitoring of Radioactive Gases in Air by Sorption

1. Introduction

The experiments in this chapter were conducted with silicone vacuum oil, which fulfills almost all the conditions for collectors of radioactive gases by sorption 1). The chemical structure of the silicone oil, HIVAC F-4, is illustrated in Fig. 2-1. The oil is also nonpolar due to rotation about the oxygen-silicon bond. In practice, the sorbent agent, silicone oil, is exposed to a contaminated atmosphere, and it gradually sorbs radioactive gases from the environment. Then, the oil is mixed with a liquid scintillator for counting. When mixed in a toluene scintillator solution, no quenching effect was observed for the sample through coupling to a pulse height analyzer. Any β-emitting nuclides can easily be identified by their spectra 2~6), allowing the development of a nonvolatile liquid scintillator sorbent, as discussed in Chapter 4.

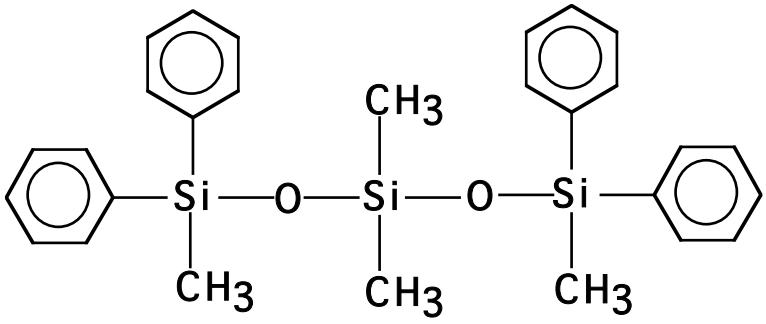

HIVAC F-4

Figure 2-1 Chemical structure of methyl-phenyl silicone oil.

2. Experiments and Results

To generate an environment similar to an atmosphere contaminated with radioactive gases, for this experiment, a fixed quantity of sorbent, sources of radioactive gases with predetermined activities and a stirring electric air pump to accelerate the evaporation and sorption of radioactive materials were sealed in a container. In the container, radioactive gases are vaporized, contaminating the air, and this material is gradually sorbed onto the

sorbent. After a predetermined time, a fraction of the sorbent that has absorbed the radioactive gases was removed and mixed into the liquid scintillator, and thus, the quantities of sorbed radioactive gases were determined. The activities of the radioactive contaminants were evaluated. [Methyl-^{3}H]-thymidine and [^{14}C]-L-leucine were used as the sources of gaseous radioactive compounds. Toluene was used as the liquid scintillator (toluene 0.71, ethanol 0.31, 1,5-diphenyloxaole (PPO) 4.0 g/L, 2,2'-phenylenebis(5-phenyloxazole) (POPOP) 0.1 g/L. Table 2-1 shows the typical results for tritium-contaminated air and air contaminated by a mixture of radioactive gases.

Table 2-1 Measurement results for contaminated air by tritium and by a mixture of tritium and ^{14}C radioactive gases.

	Contaminated material		
		Mixture (Tritium and ^{14}C)	
	Tritium	Tritium	^{14}C
Vaporized quantity (Bq)	1.65E+03	1.28E+02	7.03E+01
Concentration in air (Bq/mL)	6.62E-01	5.14E-02	2.81E-02
Adsorbed quantity (Bq/10 mL)	1.48E+01	2.98E+00	1.10E+00
Adsorbed fraction (%)	1.79	2.32	1.55

Volume of Container :2500 mL

To increase the counting sensitivity, the silicone oil sample loaded with radioactive gases was added to a liquid scintillator to increase its volume before its counting rate was measured. The results are shown in Fig. 2-2. As anticipated, the counting rate is proportional to the amount of sorbent being analyzed. This result confirms that no quenching effect is occurring in the liquid scintillator due to the addition of the sorbent even when the volume was increased until it was equal to the volume of the liquid scintillator. Furthermore, increasing amounts of inactive pure silicone oil were added to a scintillator loaded with a fixed activity, and variations in the counting rate observed (see Fig. 2-3 which shows no reduction in activity).

The same phenomenon was observed in the β-scintillation spectra of the above samples. As shown in Fig. 2-4(a) and -4(b), the shapes of the scintillation spectra do not change as a function of the volume of silicone oil, which was admixed with a fixed volume of scintillator loaded with fixed β-activities of tritium and ^{14}C. Based on the characteristics of silicone oil, multiple types of coexisting β-emitting air contaminants can be separately detected with high sensitivity.

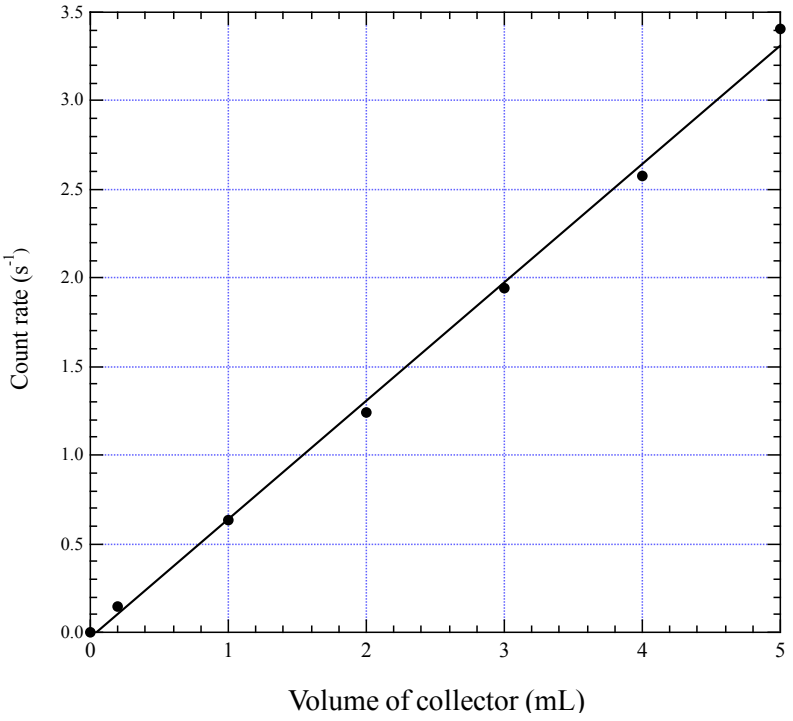

Figure 2-2 Variation in the counting rate as a function of the volume of sorbed tritiated gas in the toluene scintillator.

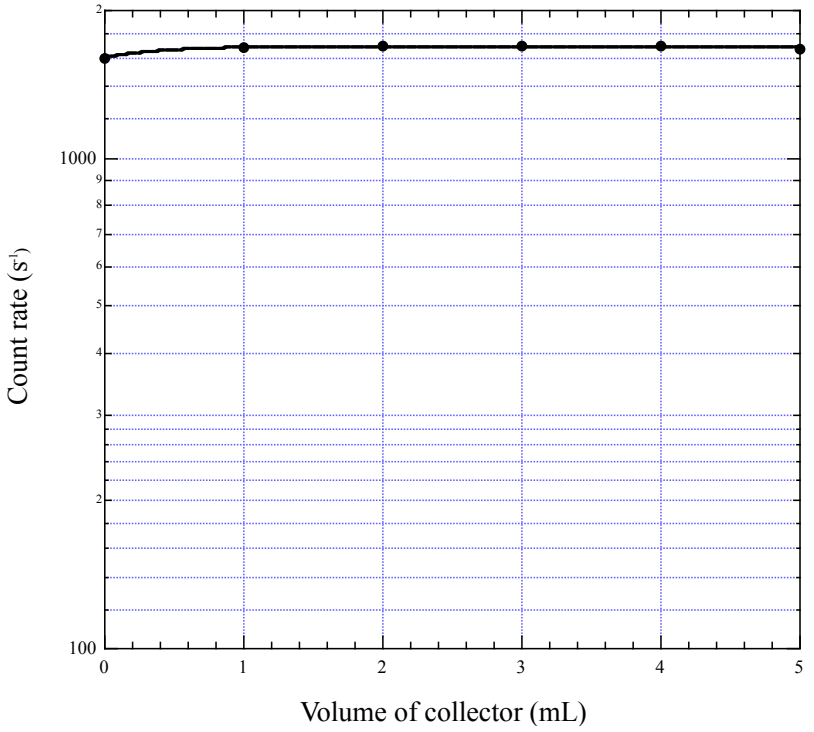

Figure 2-3 Counting rate vs volume of silicone oil with a fixed sorbed activity mixed with

the toluene scintillator.

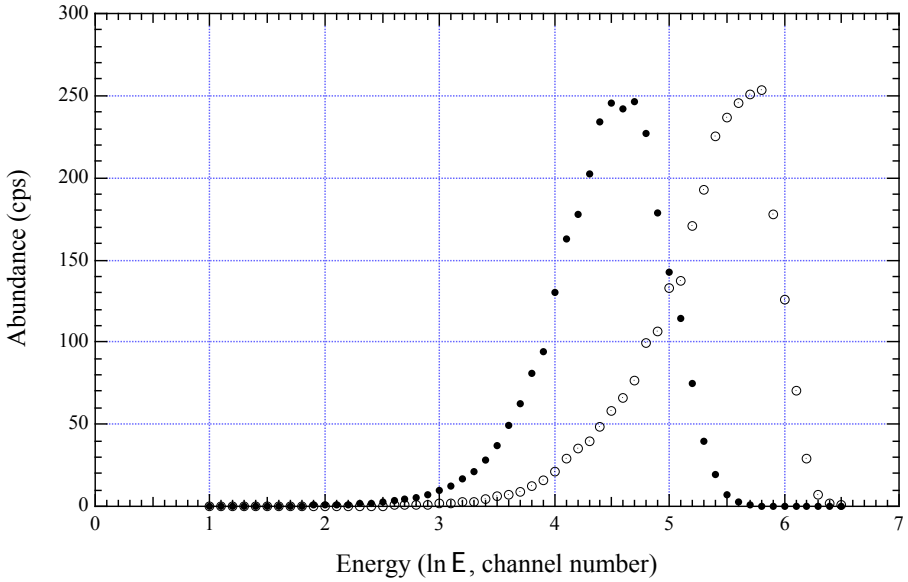

Fig. 2-4(a)

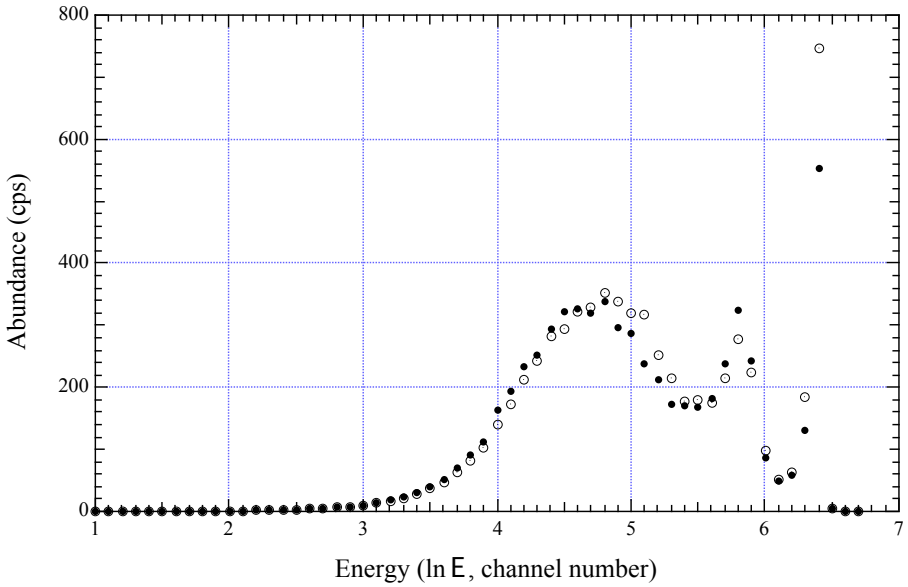

Fig. 2-4(b)

Figure 2-4 Two curves showing the liquid scintillation spectra obtained with an Intertechnique Liquid Scintillation Spectrometer Model SL-30. The abscissa is the energy of the β-emitters on an arbitrary scale; (a) for tritium (left curve) and for ^{14}C (right curve) and (b) for the tritium and ^{14}C mixture. The dotted curves with open circles represent the measurements without silicone oil and those with solid circles correspond to 5 mL of silicone oil added to 5 mL of scintillator.

3. Discussion

In this method, to obtain high sensitivity, the sorbent must absorb as much contaminant gas from the air as possible until saturation is reached; the sample must also be added to the maximum amount of liquid scintillator that the vial will accommodate.

The collector has two roles: it catches the gases, and it is needed to prepare the sample and mix it into the liquid scintillator. For such a collector, the following additional prerequisites should be satisfied:

To catch radioisotopes,

1. strong adsorptive and absorptive interactions with radioactive gases,
2. liquid and homogeneous adsorptive and absorptive power,
3. extremely low vapor pressure and no evaporation during sampling.

To be a component of the scintillator solution,

1. miscible and uniformly dissolvable in a liquid scintillator,
2. transparent and colorless,
3. free from quenching effects.

Two kinds of liquid collectors have been tested herein, ethylene glycol in Chapter 1 and silicone vacuum oil in Chapter 2, and these both fulfill almost all these conditions unlike other collectors such as active carbon and silica gel, which fulfill too few of these conditions. The former is polar and hydrophilic, and the latter is nonpolar and lyophilic. In practice, ethylene glycol and silicone oil as adsorbing and absorbing agents are exposed to the contaminated atmosphere and gradually sorb radioactive gases from the environment. Then, they are mixed with a liquid scintillator to prepare the samples for counting.

Since the sorptive function of the liquid sorbent is uniform, the radioactive concentration can be measured very accurately.

Moreover, the selected sorbent, silicone oil, is free from quenching effects (as mentioned above), so the contaminant radioactive gases are easy to identify from their scintillation spectra.

4. Conclusion

A more effective sorbent, methyl-phenyl silicone oil, was used for the liquid scintillation measurements of airborne tritium- and carbon-14-containing compounds. The sorbent was nonquenching.

5. Summary

A method to measure low levels of radioactive gases in air with a liquid scintillation counter using silicone oil as the sorbent is described. With this method, one can measure the total concentration or separately detect the different β-emitters in air at a much higher sensitivity than can be achieved with usual methods. In the presence of multiple nuclides, the detection can be performed with a β-emitter scintillation spectrometer. In this chapter, tritium- and carbon-14-containing compounds in air with contamination levels of 3.7×10^{-3} Bq/mL (10^{-7} μCi/mL) are measured and analyzed.

References

1) Kato, T. (1979) A Monitoring of radioactive gases in air by adsorption, *Int. J. Appl. Radiat. and Isot.* **30**, 349-351.

2) Noaks, J. E., Neary, M. P. and Spaulding, J. D. (1973) Tritium measurements with a new liquid scintillation counter, *Nucl. Instr. and Meth.* **109**, 177-187.

3) Jalbert, R. A. and Hiebert, R. D. (1971) Gamma Insensitive air monitor for Radioactive gases, *Nucl. Instr. and Meth.* **96**, 61-66.

4) Jalbert, R. A. (1975) A Monitor for tritium in air containing other beta emitters, Proc. 23rd Conf. on Remote System Technology, 89-93.

5) Tanaka E. (1965) Optimum Window Setting in a Spectrometer for Low-level Activity Counting, *Int. J. appl. Radiat. Isot.* **16**, 405~412.

6) Curran, S. C., Angus J. and Cockroft, A. L. (1949)Ⅲ. Investigation of soft radiations of tritium, *Phil. Mag.* **40**, 53.

7) Horrocks, D. L. (1964) Measurement of sample quenching of liquid scintillator solutions with X-ray and gamma-ray sources, *Nature* **202**, 78~78.

Chapter 3

Quenching Equation for Scintillation

1. Introduction

Quenching is the largest obstacle in liquid scintillation counting 1~3). Quenching occurs when a compound without a scintillation element for energy transfer is mixed in the scintillator fluor, which leads to a decreased fluorescence intensity. As a result, the count rate decreases, and the spectrum shifts toward lower energy. In Chapter 1, the sample itself was found to be a quencher, and the sample decreased the counting efficiency by reducing the fluorescence intensity.

The relationship between the fluorescence intensity and the quencher concentration in the gas was originally derived by Stern and Volmer 4) and has current applications 5~10). The equation is generally valid when the quencher volume is much smaller than the volume in the fluor. Many studies have shown that the equation is also valid for scintillation due to radiation 11~14). However, according to the relationship, higher concentrations of quencher in the scintillator result in greater counting errors.

In this chapter, the notable effects of concentration-dependent quenching are demonstrated. To generalize the effects, a mathematical expression was derived, and it is applicable in such cases and is in agreement with the Stern-Volmer equation in cases of low quencher concentrations.

2. Experiment

The relationship between fluorescence and quencher concentration was determined by measuring the count rate as a function of the concentration of the quenching agent used in this experiment. The quenching agents used in this experiment were ether, ethanol, ethylene glycol, acetic acid, water and acetone. Figs. 3-1 and 3-2 show the effects of increased concentration on the fluorescence of the sample. The solid curves are nearly linear. Accordingly, this effect can be expressed as follows:

$$\boldsymbol{I} = \boldsymbol{I_0}\, e^{-bQ} \qquad (1)$$

where $\boldsymbol{I}_0$ is the fluorescence intensity of the light from the unquenched solution; $\boldsymbol{I}$ is the fluorescence intensity of the light from the quenched solution; $\boldsymbol{Q}$ is the quantity of the

quencher; and *b* is the coefficient of the quencher concentration.

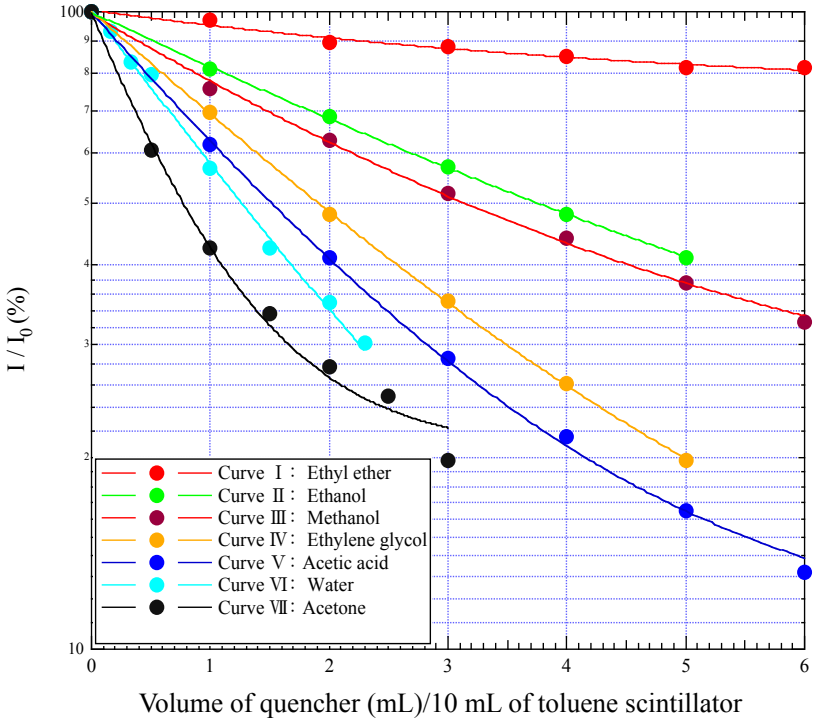

Figure 3-1 The effects of increasing concentration of quencher on the counting efficiency for several quenchers. Starting from the top curve, I is for ether, II is ethanol, III is methanol, IV is ethylene glycol, V is acetic acid, VI is water, and VII is acetone.

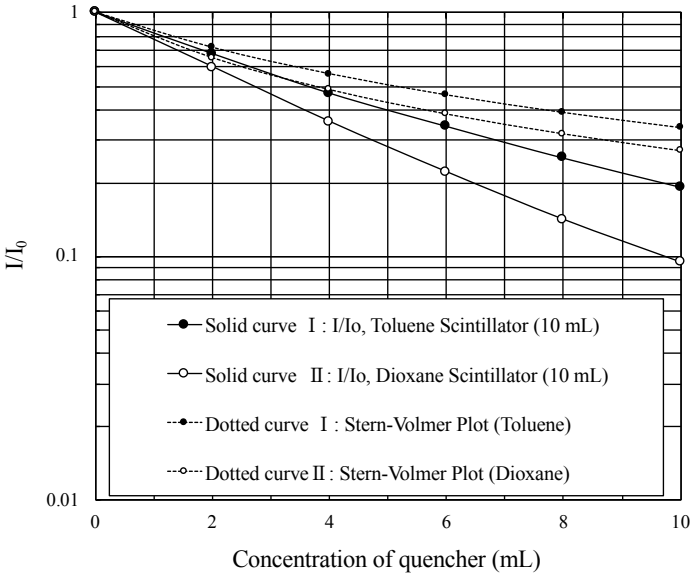

Figure 3-2 Counting efficiency at increasing quencher (ethylene glycol) concentrations. Solid curve I is with toluene as the scintillator, and curve II is for a dioxane scintillator.

The dotted curves represent the Stern-Volmer equation.

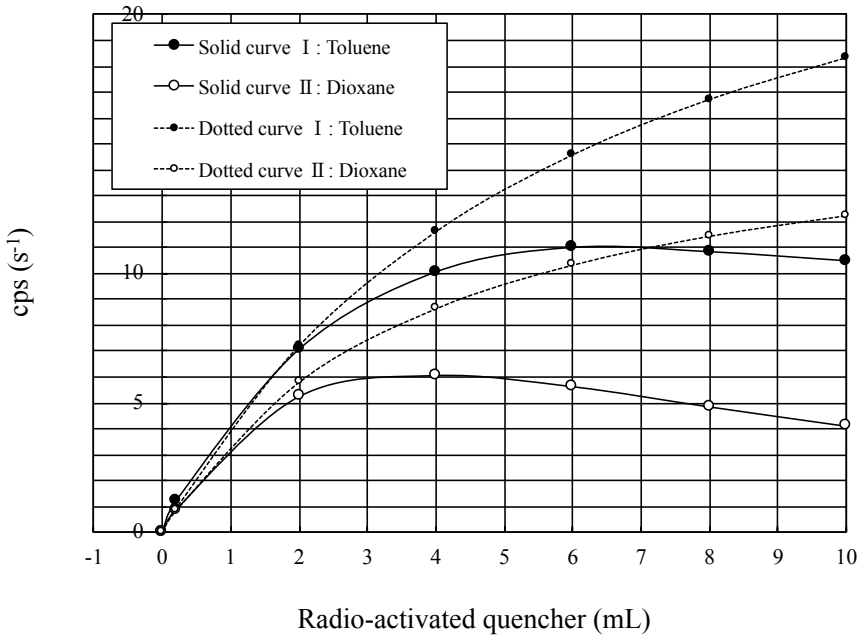

Figure 3-3 Variation in the counting rate with increasing volume of radioactive quencher (ethylene glycol) in toluene and dioxane scintillators. The solid curves are experimental values; curve 1 is for the toluene scintillator and 2 is for dioxane. The corresponding dotted curves are based on the Stern-Volmer equation.

To measure the radioactive samples using a liquid scintillation counter, the quenching materials were dissolved in a nonactive scintillant. As the sample volume added to the liquid scintillator is increased, the radioactivity in the detector increases, and quenching is observed. The variation in the counting rate as a function of the quantity of quenching solution is shown by the solid curves in Fig. 3-3, and the quenching solution was loaded with a fixed concentration of tritium activity and was mixed with 5 mL of liquid scintillator.

3. Calculation

Considering the experimental results in Fig. 3-3, the activity, $\boldsymbol{I_0}$, of radioactive material in the sample should theoretically be proportional to the quantity of quencher, $\boldsymbol{Q}$,

$$\boldsymbol{I}_0 = k\boldsymbol{Q} \,, \qquad (2)$$

where k is the activity of the unit volume of the sample. Since the variation in fluorescence intensity due to quenching is expressed by eq. (1), the solid curves are expressed by the following equation, which is a combination of eq. (1) and eq. (2),

$$\boldsymbol{I} = k\boldsymbol{Q}\, e^{-b\boldsymbol{Q}} \ , \tag{3}$$

where I is the counting rate.

The Stern-Volmer quenching equation is

$$\frac{\boldsymbol{I}}{\boldsymbol{I_0}} = \frac{1}{1+b\boldsymbol{P}} , \tag{4}$$

where $\boldsymbol{I}_0$ is the fluorescence intensity of light without quenching; $\boldsymbol{I}$ is the fluorescence intensity of light with quenching; b is the Stern-Volmer coefficient of the concentration of the quencher; and $\boldsymbol{P}$ is the concentration of quencher.

When the concentration of the quencher, $b\boldsymbol{Q}$ in eq. (1), is much less than unity ($b\boldsymbol{Q}$<<1), then from eq. (1)

$$\frac{\boldsymbol{I}}{\boldsymbol{I_0}} = \frac{1}{e^{b\boldsymbol{Q}}} = \frac{1}{1+b\boldsymbol{Q}+\frac{bQ^2}{2!}+\cdots} \tag{5}$$

Therefore, eq. (5) approximates eq. (4) as follows:

$$\frac{\boldsymbol{I}}{\boldsymbol{I_0}} = \frac{1}{1+b\boldsymbol{Q}} \qquad (b\boldsymbol{Q}<<1).$$

Thus, eqs. (1) and (5) are identical to the Stern-Volmer quenching equation when $\boldsymbol{Q}$ is substituted in eq. (4).

The dotted curves in Fig. 3-2 show the comparison between eq. (1) and eq. (4).

When $\boldsymbol{I}_0 = k\boldsymbol{Q}$ is substituted in eq. (4) then

$$\boldsymbol{I} = \frac{k\boldsymbol{Q}}{1+b\boldsymbol{Q}} \tag{6}$$

This equation is plotted in Fig. 3-3 as dotted lines. Comparing the experimental curves (I and II) with those of the Stern-Volmer relationship, the curves are in very good agreement at low concentrations of quencher. As the concentration increases, the Stern-Volmer equation deviates further from empirical values and becomes invalid at high concentrations. The experimentally determined equation is valid throughout the tested quencher concentration range.

4. Application

Two parameters, k and b, in eq. (3) can be experimentally determined by measuring the

counting rates of liquid samples containing different quantities of quencher ($\boldsymbol{Q}$) by mixing them in the same scintillator.

$\boldsymbol{Q}$, the peak of each solid curve in Fig. 3-3, represents the maximum counting rate, which corresponds to the optimum sample volume to obtain the maximum sensitivity of scintillation detection. Furthermore, by multiplying e^{bQ} by the counting rate, $\boldsymbol{I}$, from eq. (3), the original unquenched activity for the self-quenching sample volume can be obtained. The quenching due to the scintillator component can be accounted for by multiplying by the efficiency of the scintillator in an unquenched state.

If eq. (3) is differentiated with respect to $\boldsymbol{Q}$, the maximum sensitivity is theoretically given by the following.

$$b\boldsymbol{Q}_{\max} = 1 \qquad (7)$$

The value of $\boldsymbol{Q}_{\max}$ agrees with the experimental results: b is 0.16 and $\boldsymbol{Q}_{\max}$ is 6.3 mL for the toluene scintillator and b is 0.26 and $\boldsymbol{Q}_{\max}$ is 3.9 mL for dioxane, whereas no maximum value appears in the Stern-Volmer plot.

5. Conclusion

The quenching effect in liquid scintillation measurements can be expressed through a mathematical equation.

6. Summary

A mathematical expression giving the relationship between the counting rate and the quenching agent concentration in a liquid scintillation solution was determined. The expression is better suited to a wider range of quenching agent concentrations than the Stern-Volmer equation. The quencher correction was estimated using the expression.

References

1) Furst, M. and Kallman, H. (1955) Enhancement of fluorescence in solutions under high-energy irradiation, *Phys. Rev.* **97**, 583-587.

2) Kipsky, S. and Burton, M. (1959) Comparison of high-energy and ultraviolet-radiation induced luminescence in liquid systems, *J. Chem. Phys.* **31**, 1221~1226.

3) Berlman, I. (1961) Luminescence in a scintillation solution excited by α and β particles and related studies in quenching, *J. Chem. Phys.* **34**, 598~603.

4) O. Stern and M. Volmer (1919) Über die abklingungzeit der fluoreszenze, *Physik. Zeitschr.* **20**, 183.

5) Higashiura, T., Yamada, O., Nohara, N. and Shidei, T. (1962) External standard method for determination of the efficiency in luquid scintillation counting, *Int. J. Appl. Radiat. and Isot.* **13**, 308~309.
6) Horrocks, D. L. (1964) Measurement of sample quenching of liquid scintillator solutions with X-ray and gamma-ray sources, *Nature* **202**, 78~78.
7) Korarov, V., Le Gallic, Y. and Vatin, R. (1970) Measure absolute directe de l'activité des emetteurs ß purs par scintillation liquide, *Int. J. Appl. Radiat. and Isot.* **21**, 443-452.
8) Yura, O. (1971) Absolute activity measurement of tritium by liquid scintillation counting, *Radioisotopes* **20**, 493~497.
9) Houtermans, H. (1973) Probability of non-detection in liquid scintillation counting, *Nucl, Instr. and Meth.* **112**, 121~130.
10) Chikkur, G. C. and Umakantha N. (1973) A new method of determining the Compton in liquid scintillators, *Nucl, Instr. and Meth*. **107**, 201~202.
11) Melhuish, W. H. (1961) Quantum efficiencies of fluorescence of organic substances: effect of solvent and concentration of the fluorescent solute, *J. Phys. Chem.* **65**, 229~235.
12) J. B. Birks (1967) The theory and Practice of Scintillation Counting (Pargamon, Oxford)
13) Lami, H. and Laustriat, G. (1968) Eximer formation with polar molecules: oxazole and oxadiazole derivatives, **48**, 1832~1841.
14) Takiue, M. and Ishikawa, H. (1974) Quenching analysis of liquid scintillation, *Nucl. Instr. and Meth.* **118**, 51-54.

Chapter 4

Nonvolatile Liquid Scintillator

1. Introduction

Chapters 1 and 2 discuss gas sampling for liquid scintillation counting of air contaminated with radioactive gases 1, 2). The sampling was carried out using a nonvolatile or hard-to-volatilize liquid sorbent, and the counting was performed after mixing with a volatile liquid scintillator. The most common scintillators are nonpolar or weakly polar organic liquids, e.g., toluene, dioxane, xylene 3~8), pseudocumene or di-isopropyl-naphthalene, each of which is somewhat volatile. If the liquid scintillator used to sorbs the radioactive gases is itself a sample, the measuring process for monitoring radioactive gases in air can be shortened. As discussed in Chapter 2, when silicone oil is used as the collector, the sample did not exhibit the quenching effect observed with other solvents, such as toluene and xylene. 2). In this chapter, a silicone oil-based liquid scintillator containing wavelength shifters PPO and POPOP was prepared and tested on low-energy β-emitters, namely, tritium and carbon-14.

2. Experimental

1. Method and Materials. The reagents were prepared from the following: 1,5-diphenyloxaole (PPO), 2,2'-phenylenebis(5-phenyloxazole) (POPOP), and methyl-phenyl silicone oil HIVAC F4 from Nakarai Chemicals, Ltd.

An Intertechnique Liquid Scintillation Spectrometer Model SL-30 was used for counting, as were 20-mL low-potassium glass vials (Wheaton Glass Co.).

The radioactive materials were aqueous [methyl-^{3}H]thymidine solution and aqueous L-[U-^{14}C]leucine solution containing 2% ethanol.

The composition of the silicone oil scintillator was as follows: silicone oil, 100 mL; PPO, 0.7 g/100 mL; and POPOP, 0.2 g/100 mL.

2. Determination and Spectral Analysis. ^{3}H-Thymidine and ^{14}C-leucine were dissolved in 1-mL aliquots of ethanol. Then, 0.02~0.2 mL of each solution was added separately to the silicone oil scintillator, to toluene (toluene 700 mL ethanol 300 mL, PPO 4.0 g/L, POPOP 0.1 g/L) and to dioxane 3), and the samples were measured by liquid scintillation counting. The γ-ray spectrum of the silicone scintillator was measured with a ^{137}Cs external standard source 5), and the results are plotted. Decays per minute (DPM)

corrections for the toluene and dioxane scintillators were calculated, and a similar correction for the silicone scintillator was applied by substituting the toluene quenching standard correction curve for the silicon curve. Such correction is, however, an approximation. The counting values and results are shown in Table 4-1.

In Table 4-1, counts per minute (CPM), DPM, and the ratios for the different windows are indicated. The DPM for the silicone scintillator is shown in parentheses because the quench approximation used. These results indicate that the silicone scintillator functions as well as toluene.

Table 4-1 Count and decay rates and ratios

		β-emitters			γ-ray	
		carbon-14	tritium		cesium-137	
window	upper lower	6.50 1.70	6.00 1.00		5.90 4.74	8.86 4.88
	silicone scintillator	372/(390)=0.95	19/(31)=0.60		470	1548
CPS[a]/DPS[b]						
	toluene scintillator	46/(50)=0.91	272/(494)=0.55		511	1186
	silicone scintillator	46/(50)=0.91	272/(494)=0.55		361	1827
CPS/DPS						
	dioxane scintillator	63/66=0.95	318/749=0.42		265	1751

[a] Counts per minute. [b] Decays per minute.

In Table 4-1, counts per minute (CPM), DPM, and the ratios for the different windows are indicated. The DPM for the silicone scintillator is shown in parentheses because the quench approximation used. These results indicate that the silicone scintillator functions as well as toluene.

To compare the β-particle spectrum of the silicone scintillator with that of toluene, the same amounts of ^{14}C-leucine sample were mixed with the silicone and toluene scintillators. In each case, the ^{14}C spectrum was analyzed with a pulse height analyzer. The spectra are shown in Figs. 4-1 and 2. Fig. 4-1 shows the spectrum of an unquenched standard, and Fig. 4-2 shows two curves for the quenched spectra. The dotted curve with open circles represents the silicone scintillator and that with solid circles represents the toluene scintillator. The silicone spectrum shows less quenching than that of toluene.

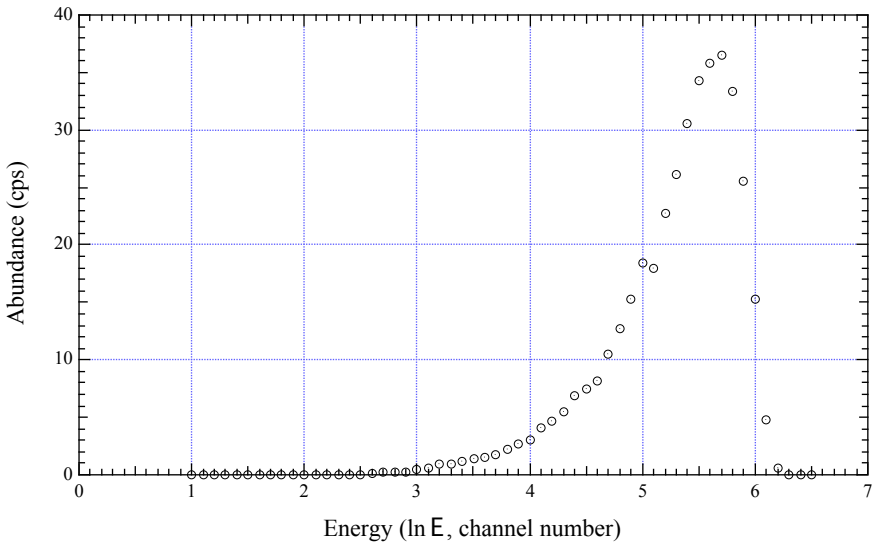

Figure 4-1 The standard spectrum from unquenched carbon-14 β-emitters liquid scintillation.

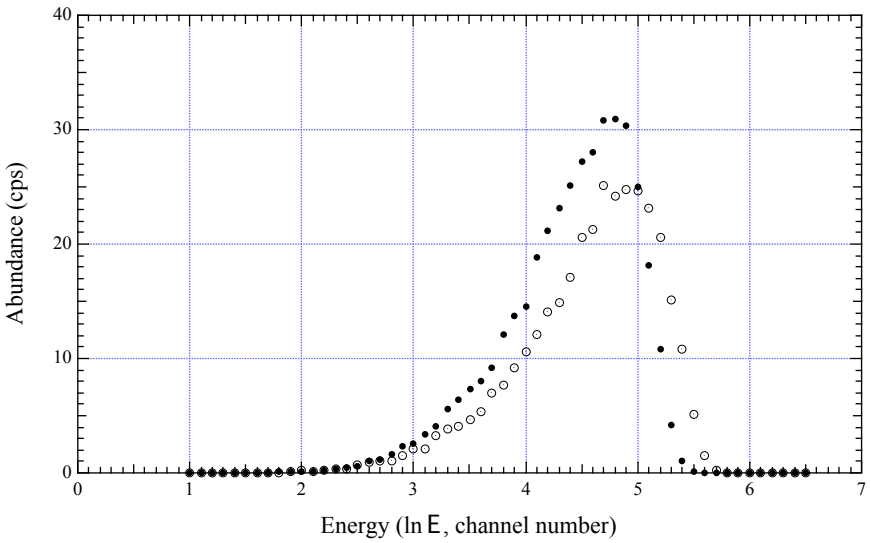

Figure 4-2 Curves showing the spectra of quenched carbon-14 β-emitters. The dotted curve with open circles represents the silicone scintillator, and the solid circles represent the toluene scintillator. The silicone spectrum curve shows less quenching than that of toluene.

3. Discussion

As shown in Table 4-1, the counting function of the silicone scintillator approximates those of toluene and dioxane. This silicone solvent acts as an excellent absorbent for radioactive gases in air and can also be used as a scintillator. As seen from the spectrum shift in Fig. 4-2, the silicone solution exhibits less quenching than that in the toluene solution.

5. Conclusion

A nonvolatile liquid scintillation absorbent was generated by mixing the scintillator PPO and the energy shifter POPOP in methyl-phenyl silicone oil, and this absorbent was tested with low-energy β-emitters, namely, tritium and carbon-14.

6. Summary

A nonvolatile scintillator derived from methyl-phenyl silicone oil was produced for the analysis of radioactive gases. This scintillator, which absorbs radioactive gases, can function as a sampling and measuring medium for radioactive gases in air. Tritium and carbon-14 β-emitters and cesium-137 γ-rays can be measured by the addition of energy transfer agents. The low-energy β-emitters spectrum of carbon-14 was analyzed using this scintillator and compared with that obtained from a toluene solution.

References

1) T. Kato (1979) Measurement of tritium in air by adsorbent, *Nucl. Instr. and Meth.* **163**, 463-465.
2) T. Kato (1979) Monitoring of radioactive gases in air by adsorption, *Int. J. Appl. Radiat. Isot.* **30**, 349-351.
3) Kallman, H. and Furst, M. (1950) Fluorescence of solutions bombarded with high radiation (energy transport in liquids) *Phys. Rev.* **79**, 857-870.
4) Kallman, H. and Furst, M. (1951) Fluorescence of solutions bombarded with high radiation (energy transport in liquids) part Ⅱ *Phys. Rev.* **81**, 853-864.
5) Furst, M. and Kallman, H. (1952) High energy induced fluorescence in organic liquid solutions (energy transport in liquids). Ⅲ *Phys. Rev.* **85**, 816-825.
6) Furst, M. and Kallman, H. (1955) Fluorescent behavior of solutions containing more than one solvent, *J. Chem. Physics* **23**, 607~612.
7) Furst, M. and Kallman, H. (1955) Enhancement of fluorescence in solutionsunder high-energy irradiation, *Phys. Rev.* **97**, 816~825.
8) Bray, G. (1961) A simple efficient liquid scintillator for counting aqueous solutions in a liquid scintillation counter, *Anal. Biochem.* **1**, 279-285.

Chapter 5

Analysis of Tritiated Water Vapor by Nonvolatile Liquid Scintillator Sorbent

1. Introduction

As discussed in Chapters 1 and 2, the application of a tracer technique, i.e., the sorption of a radioactive gas, was applied to sample airborne radioactive contaminant gases, which were measured by a liquid scintillation counter 1, 2). In such applications, airborne tritiated and ^{14}C-labeled chemical compounds were analyzed using a liquid sorbent. The development of a new liquid scintillator sorbent was discussed in Chapter 4 3). In this chapter, the concentration of tritiated water vapor in air is measured using the developed scintillator. The measurement using this method showed high sensitivity and accuracy. However, to quantitatively analyze the sorbed radioactive gases by the tracer technique using the sorption method, fundamental principles related to the sorption of tritiated water and the applicable characteristics of the sorption of a nonvolatile solvent must be considered.

Radioactive tracer techniques for the study of surface adsorption have been applied by Dixon et al. 4) and numerous other researchers 5~15). They showed that the Gibbs theoretical adsorption isotherm equation, which expresses the relationship between the adsorbed gas on the liquid surface and its surface tension, was consistent with their experimental results 10). In addition to the above application for liquid solutions, this technique can also be used for the adsorption of solids 16, 17), i.e., to confirm the Langmuir adsorption isotherm 18), which describes the relationship between gas adsorption by a solid material and the pressure of the adsorbed gas.

Gases usually dissolve in liquids via a two-step process. In the first step, the gas molecules are adsorbed on the surface of the liquid, forming an adsorbed gaseous molecular layer, similar to that on a solid. In the second step, the adsorbed gas molecules gradually migrate toward the bulk of the liquid in a uniform manner, leading to a slightly different phenomenon, namely, absorption instead of adsorption. Adsorption and absorption cannot be distinctly separated in this case, and they are therefore combined under the term sorption. When adsorbed molecules attached to the surface of the liquid transfer from the surface into the bulk, the number of molecules on the surface begins to decrease. Therefore, since the surface cover is removed, additional molecules can be adsorbed. If the sorbent liquid is nonvolatile, it will be a suitable sorbent. Thus, the

relation between the sorption isotherm and the nonvolatile liquid solvent was experimentally determined.

2. Experiments and Results

The experiments were carried out in a constant temperature/humidity room. A known volume of tritiated water with a predetermined specific activity was loaded into a 20-mL low-potassium glass vial, and this solution was used as the source. The nonvolatile silicone liquid scintillator sorbent (10 mL) 3) in an identical vial was measured to determine the background with an error of ±2%. An electric pump was used both for stirring the sorbent solution through blowing air and for promoting vaporization. Table 5-1 shows the air temperature and humidity in the room. In the sealed container, the evaporation of the tritiated water was accelerated by the electric pump, thus filling the container with tritiated water and ordinary water vapors from the source, along the vapors present in the atmosphere. The vapors were continuously blown over the scintillator sorbent and allowed to sorb. After 24 h, the container was opened, and the radioactivity of the tritiated water sorbed by the scintillator sorbent was directly measured by a liquid scintillation counter. The remaining radioactivity in the source vial was also measured by adding 10 mL of dioxane scintillator. The difference between the source and the amount remaining after vaporization was calculated.

Table 5-1 The vaporized amounts, activity of the source, and the sorbed activity of the tritiated water and the related temperature and humidity.

	Experimental number	1	2	3	4	5
(1)	Volatilized amounts of tritiated water (μg)	6.00	9.00	11.00	25.00	50.00
(2)	Amounts of natural water vapor in the container (2450 mL) (μg),	16.90	17.80	19.10	19.10	19.10
	the temperature (℃) and	20	20	20	20	20
	humidity (%)	40	42	45	45	45
(3)	Total amounts of (1) and (2) in the container (μg)	22.90	26.80	30.10	44.10	69.10
(4)	Volatilized tritium activity at (3) (Bq)	5.14E+01	7.33E+01	9.51E+01	1.85E+02	4.00E+02
(5)	Sorbed tritium activity (Bq)	4.59E-01	6.77E-01	9.62E-01	2.23E+00	4.74E+00

The sorption of tritiated water by the scintillator was stable for at least half a year, but it could be totally desorbed by heating the scintillator sorbent at 50 °C for several hours. These results suggest that the sorption occurs entirely through van der Waals interactions. The activity of the sorbed tritiated water in the scintillator sorbent was approximately 1% of the tritium vaporized from the source in the container, as shown in Table 5-1. While

there was some humidity fluctuation in the container during the measurements, the activity of the sorbed tritium was proportional to the activity vaporized from the source, as shown in Fig. 5-1. The variation in the sorption of radioactive gases in air by a nonvolatile solution is directly proportional to the partial vapor pressure of the solution at a constant temperature.

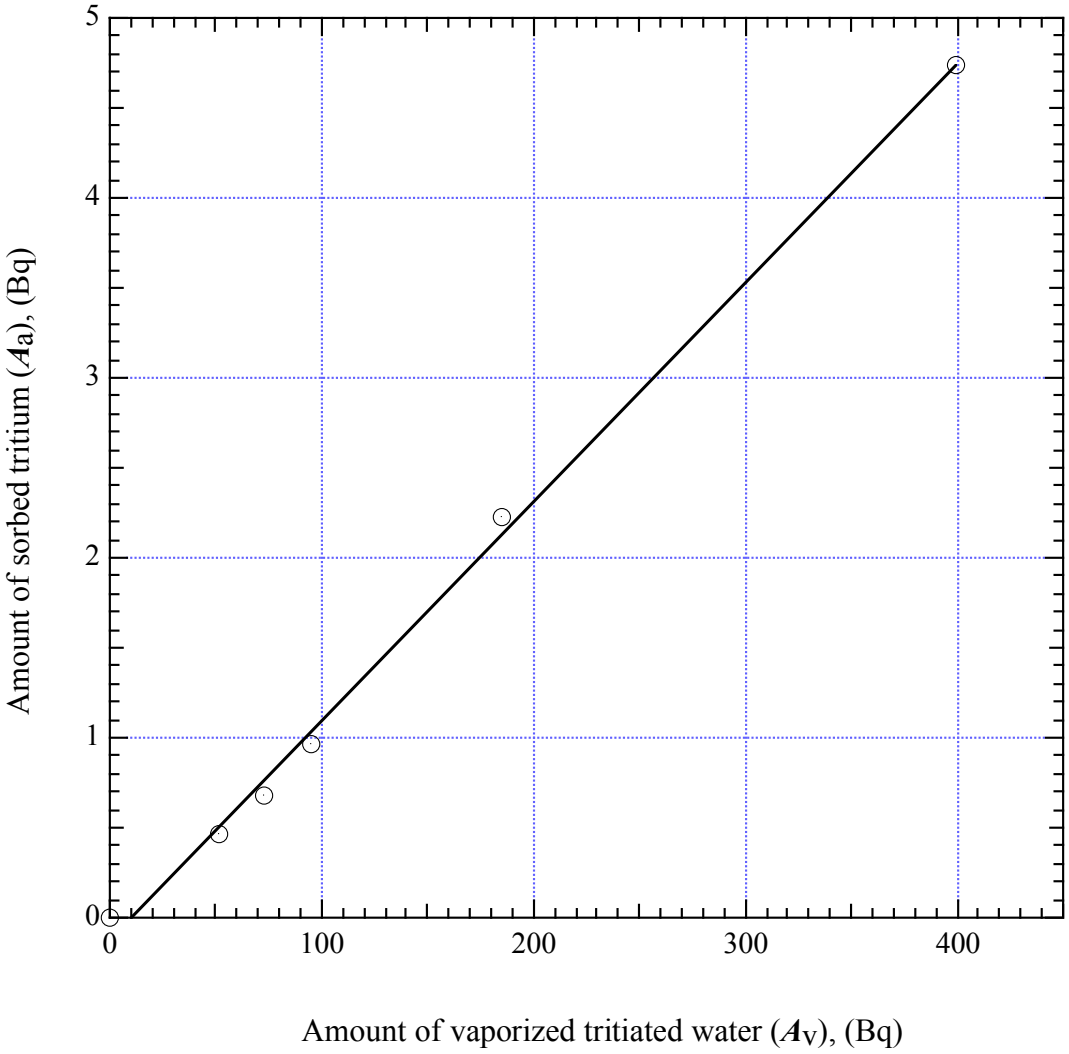

Figure 5-1 Plot of the amount (A_a) of tritiated water sorbed by the sorbent solution (also use as the scintillant) vs the amount of tritiated water (A_v) vaporized from the tritium source (liquid water contained in a vial).

The variation over a limited range of sorbed amounts is given by the following empirical expression:

$$A_a = K \cdot P \qquad (1)$$

where is A_a the amount of gas sorbed by a constant volume of sorbent at partial pressure P, and K is the constant for the given gas and sorbent at the particular temperature. The equation is a sorption isotherm that is valid for sorption by nonvolatile liquid sorbents at a constant temperature.

3. Discussion

The experimental results indicate that the vapor of tritiated water was adsorbed on the surface and then absorbed into the bulk of the nonvolatile silicone scintillator. This scintillator solvent, which traps radioactive gases present as air contaminants, is a sample and at the same time a good detector for analyzing the contaminants. Therefore, a scintillation counter is used to determine the radioactivity of the sample, eliminating some of the chemical or physical processes typically needed. Such simplification of the experimental procedure prevents leakage of the sample material.

The results of this isotherm equation [eq. (1)] for gas sorption by a solution will now be compared with the adsorption isotherm for adsorption on the surface of a solid. In the latter case, the variation in gas adsorption (A_s) with pressure at constant temperature can be represented by the Langmuir adsorption equation:

$$A_s = k_1 P / (k_2 P + 1) \qquad (2)$$

where k_1 and k_2 are constants. If the pressure of the gas is extremely low, it is possible to disregard $k_2 P$ in the denominator. This equation then becomes

$$A_s = k_1 P \qquad (3)$$

Eq. (3), the Langmuir adsorption isotherm in the special case of extremely low gas pressures and a solid adsorbent, has the same formula as eq. (1) for the sorption of gas in the nonvolatile solution. In the former case, which involves sorption on a solid surface, at any particular moment, a fraction of the adsorbing surface is covered with gas molecules. It follows that the rate of adsorption of the gas molecules decreases with increasing pressure; when the entire adsorbing surface is covered with molecules, the adsorption is considered saturated. Hence, the denominator of eq. (2) is larger than one, and the curve of the adsorbed amount (A_s) vs pressure (P) deviates below a straight line. Consequently, eq. (2) is approximated as eq. (4).

$$A_S = k_1 P^n \quad (4)$$

n < 1 for intermediate or high pressures and n = 1 for extremely low pressures. However, in the case of liquid adsorbents, by allowing the adsorbed gas molecules on the surface to migrate into the bulk of the liquid, the adsorption immediately progresses to absorption, resulting in the adsorbing surface becoming almost devoid of adsorbed molecules at any given moment. Consequently, the rate of adsorption of the gas molecules remains almost constant. Therefore, eq. (1), which shows the sorption isotherm for nonvolatile liquid solutions, should be valid over a wide range of pressures, i.e., beyond the limits of concentration.

As indicated in the second column of Table 5-1, the humidity fluctuated by approximately 10%, but this had little effect on the sorption of tritiated water vapor. This suggests that the presence of common water vapor does not influence the sorption of tritiated water.

4. Conclusion

With this sorption method, the concentration of tritium in the atmosphere can be measured. Sampling occurs through sorption by a nonvolatile scintillator, and the activity is measured with a liquid scintillation counter. The concentration is determined by comparing the measured values of subtracted backgrounds with the sorption calibration curve in Fig. 5-1, which was prepared by plotting the results with known amounts of tritiated vapor.

5. Summary

The quantitative analysis of tritiated water vapor in air was investigated by sorption into a nonvolatile liquid scintillator sorbent derived from silicone oil. The activity of β-emission from the sorbed tritiated water vapor, 3.7×10^{-3} Bq/mL (10^{-7} μCi/mL) in air, was directly measured using a scintillator solution that also served as the sorbent. The variation in the partial vapor pressure of the tritiated water in air was proportional to the amount of vaporized tritiated water sorbed by the liquid scintillator sorbent. The relation was expressed as a sorption isotherm and was compared to the Langmuir adsorption isotherm, supporting the suggested adsorption by the solid adsorbent.

References

(1) Kato, T. (1979) Measurement of Tritium in air by adsorbent, *Nucl. Instr. and Meth.*

163, 463-465.
(2) Kato, T. (1979) Monitoring of radioactive gases in air by adsorption, *Int. J. Appl. Radiat. Isot.* **30**, 349-351.
(3) Kato, T. and Hatagami, T. (1980) Nonvolatile liquid scinitllator, *Anal. Chem.*, **52**, 586-587.
(4) Dixon, J. K., Weith, A. J., Afgyl, A. A. and Salley, D. J. F. (1949) Measurement of adsorption of surface-active agent at solution-air, *Nature*, **163**, 845.
(5) Aniansson, G. and Lamm, O. (1950) A radioactive method for measuring the adsorption of dissolved substances on liquid surfaces, *Nature (London)***, 165**, 357- 358.
6) Lewis, W. K., Gilliland, E. R., Chertow, B. and Hoffman, W. H., (1950) Vapour-adsorbate equilibrium. Ⅰ. Propane-propylene on activated carbon on silica gel, *J. Amer. Chem. Soc.* **72**, 1153~1157.
7) Lewis, W. K., Gilliland, E. R., Chertow, B. and Hoffman, W. H. (1950) Vapour-adsorbate equilibrium. Ⅱ. Acetylene-ethylene on activated, *J. Amer. Chem. Soc.* **72**, 1157~1159.
8) Lewis, W. K., Gilliland, E. R., Chertow, B. and Hoffman, W. H. (1950) Vapour-adsorbate equilibrium. Ⅲ. The effect of temperature on the binary systems ethylene-propane, ethylene-propylene over silica gel, *J. Amer. Chem. Soc.* **72**, 1160~1163.
9) Judson, C. M., Lerew, A. A., Dixon, J. K. and Salley, D. j. (1951) Radiotracer study of cationic surface-active agents by measurement of gegenion adsorption, *J. Chem. Phys.* **19**, 378~379.
10) Hill, T. L. (1951) On Gibbs' theory of surface tension, J. Chem. Phys. **19**, 1203.
11) Judson, C. M., Lerew, A. A., Dixon, J. K. and Salley, D. j. (1952) The surface adsorption of small ions in solutions of surface-active agents, *J. Chem. Phys.* **20**, 519~520.
12) Mignolet, J. C. P. (1953) Charge-transfer no-bond adsorption of inert atomsor molecules on metals, *J. Chem. Phys.* **21**, 1298~1299.
13) Roe, C. P. and Brass, P. D. (1954) The adsorption of ionic surfactants and their gegenions at the air-water interface, *J. Am. Chem. Soc.* **76**, 4703~4708.
14) Nilsson, G. (1957) The adsorption of tritiated sodium dodecyl sulfate at the solution surface measured with a windowless , high humidity gas, flow proportional counter, *J. Phys. Chem*. **61**, 1135-1142.
15) Muramatsu, M., Tokunaga, N. and Kyano, A. (1967) End-window counting of tritium radio activity by scintillation phosphor combined with prismatic light guide, *Nucl. Instr. and Meth.* **52**, 148~152.
16) Tabushi, I., Kobuke, Y. and Nisiya, T. (1979) Extraction of uranium from seawater by polymer-bound macrocyclic hexaketon, *Nature* **280**, 665-666.

17) Tabushi, I., Kobuke, Y. and Nisiya, T. (1979) Macrocyclic hexaketone as a specific host of uranyl ion, *Tetrahedron Lett.* **37**, 3515-3518.
18) Langmuir, I. (1916) The constitution and fundamental properties of solid and liquid *J. Am. Chem. Soc.* **38**, 2221-2295.

Chapter 6

Self-decomposition Components Generated from ^{35}S-labeled Amino Acids

1. Introduction

In this chapter, the qualitative analysis of airborne self-decomposed organic compounds was demonstrated. Analyzed gases were several self-decomposition chemical compounds of ^{35}S-labeled amino acids generated by the irradiation of β-emitters from the disintegration of neighboring ^{35}S-labeled amino acids. The used liquid collector was methanol because of the effect on the analysis of high-performance liquid chromatography.

When the author surveyed both internal and external exposure to a molecule, the external exposure to organic compounds was found to be due to the indirect generation of degraded chemical compounds by the attack of radicals produced by the radiation 1~8). External exposure to organic compounds gives a rise to grafted copolymers by direct effect on, for example, DNA and induces single- or double-strand damage due to the direct influence as well as the indirect effect of radicals 9~15).

Abundant examples of internal exposure to self-decomposed organic compounds labeled with radioactive isotopes have been reported over the years, suggesting that radioactive organic compounds, widely used as tracers in biological chemistry, should be carefully stored. Meisenhelder and Hunter 16) recently noted the contamination of laboratories and the human body associated with the release of a radioactive volatile component from ^{35}S-labeled amino acids having an extremely high specific activity. The mode and the products of this self-decomposition induced by β-emitters, however, have not been elucidated. It is necessary to characterize the gas component released from the ^{35}S-amino acid solution not only to improve the storage conditions and to eliminate contamination accidents involving radioactive organic compounds but also to elucidate the fundamental self-decomposition mechanism. The generated self-decomposition compounds and the self-decomposition mode resulting from internal exposure to β-emitters by ^{35}S was, therefore, elucidated. The results are indispensable for human health

Since the specific activity of ^{35}S-labeled compounds is often greater than 48 TBq/mmol (1300 Ci/mmol) and their decomposition products containing ^{35}S also have high

specific radioactivity, it should be easier to identify the decomposition products in ^{35}S-compounds than those in ^{3}H- and ^{14}C-labeled compounds.

By identifying the gas components released from ^{35}S-labeled amino acids, the author ascertained that one principle self-decomposition mode of ^{35}S-labeled compounds is similar to the electron-impact fragmentation of chemical compounds, as in organic mass spectrometric processes. Degradation by irradiation of unlabeled amino acids by external ^{60}Co source γ-rays was examined. The author also shows that self-decomposition by β-emitters differs from the degradation of unlabeled amino acids by external γ-ray irradiation.

2. Experimental

Labeled compounds

L-[^{35}S]Methionine(1.5~18.5 GBq/mmol (4.1~50×10^{-2} Ci/mmol), 18.5 MBq/33 μL of H_2O (5×10^{3} μCi/μL) without stabilizers), L-[^{35}S]methionine (>48 TBq/mmol, 18.5 MBq/33 μL of H_2O stabilized by 15 mmol pyridine-3,4-dicarboxylic acid containing 0.1% 2-mercaptoethanol), and L-[^{35}S]cysteine (>48 TBq/mmol, 18.5 MBq/33 μL of H_2O stabilized by 5mmol dithiothreitol and 15 mmol pyridine-3,4-dicarboxylic acid containing 20 mmol potassium acetate) were purchased from Amersham International. These ^{35}S-amino acids had been biologically prepared by using a growing microorganism species, followed by purification and storage in a large quantity at -80 °C for 2-3 weeks until further processing. One week before the shipping, a part of the stock solution was diluted with water, transferred into a vial and sealed, and then the stabilizer was added when needed. They were stored again at -80 °C for the sample with stabilizers and -70 °C for that without stabilizers. The packed solution in the vial was sent to us with dry ice for the sample with stabilizers, and at room temperature for that without stabilizers. The total transport process normally took 4~5 days.

Analysis of the radioactive gas component generated from ^{35}S-amino acids

The 1.45-mL head-space of the vial containing each labeled compound was shown out with an air-tight syringe and dissolved in 0.12 mL of methanol. The gas component dissolved in methanol was analyzed by means of high performance liquid chromatography (HPLC): pump-Waters, model 6000Å; column-Waters, Nova-Pac C_{18} reversed-phase column (ϕ 3.9×300 mm length); detector-Waters, differential refractometer, R-401. Three eluents were used: CH_3CN/H_2O (6:4, v/v), CH_3OH/H_2O (7:3, v/v) and tetrahydrofuran(THF)/CH_3CN/H_2O (3:3:4, v/v/v). The eluate from the column was collected in small fractions at regular (10-s) intervals. The radioactivity

level in each fraction was determined with a liquid scintillation counter (LKB 1219 Rack Beta Spectral SM). Using all three eluents independently, the author identified respective radioactive gaseous components by comparing their retention times with those of 22 authentic sulfur compounds, most of which are volatile: hydrogen sulfide (H_2S), sulfur dioxide (SO_2), methyl mercaptan (CH_3SH), ethyl mercaptan (CH_3CH_2SH), propyl mercaptan ($CH_3CH_2CH_2SH$), isopropyl mercaptan [$(CH_3)_2CHSH$], dimethyl sulfide (CH_3SCH_3), methyl ethyl sulfide ($CH_3SCH_2CH_3$), methyl propyl sulfide ($CH_3SCH_2CH_2CH_3$), methyl butyl sulfide ($CH_3SCH_2CH_2CH_2CH_3$) diethyl sulfide [$(CH_3CH_2)_2S$], methyl allyl sulfide (CH_3SCH_2CH=CH2), carbon disulfide (CS_2), dimethyl disulfide [$(CH_3S)_2$] , 1,2-ethanedithiol ($HSCH_2CH_2SH$), 2-mercaptoethanol (($HSCH_2CH_2OH$), thioglycolic acid (($HSCH_2COOH$) , thioacetic acid ((CH_3COSH), dimethyl sulfoxide [$(CH_3)_2SO$], trithiane ($C_3H_6S_3$), methionine [$(CH_3SCH_2CH_2CH(NH_2)COOH$), and sulfuric acid ($H_2SO_4$). A portion of the original solution containing ^{35}S-amino acid was analyzed by HPLC with an Opti-Pac CE column (Waters, ϕ 3.9×150 mm) using perchloric (pH 2) as an eluent to determine its radiochemical purity.

External irradiation of unlabeled amino acid solution by ^{60}Co γ-rays

Unlabeled methionine (20 mg/10 mL) and cysteine solution (20 mg/10 mL) were separately sealed in 30-mL glass vials filled with air or helium. Unlabeled methionine, with added stabilizers and radical scavengers was also prepared: 0.1% 2-mercaptoethanol and 15 mmol pyridine-3,4-dicarboxylic acid as the potassium salt (pH 7.5) were irradiated by ^{60}Co γ-rays to an absorbed dose of 0~8.7×10^4 Gy (= a dose of 0~10^7 Röentgens) at room temperature. The volatile components released from unlabeled methionine and cysteine in the 20-mL head-space of the 30-mL glass vials were analyzed with GC/MS-spectrometer.

GC/MS analysis

The instruments were as follows. GC: Hewlett Packard, HP5970 Gas Chromatography; MS: Hewlett Packard 5970 mass selective detector; column-Hewlett Packard, HP-1(12[m]×0.2[mm]×0.33[μm] film thickness of crosslinked methyl silicone gum); carrier gas-helium, 20 mL/min, 20 °C.

3. Results

Upon receipt, the labeled compounds were stored at -80 °C for the specified number of days before experimental use. Stabilized labeled compounds were sent from the

manufacturer packed with dry ice, but the compounds without stabilizers were sent without dry ice. All experiments were performed under sterile conditions to identify the components generated chemically and/or physically, but not biologically. The author carried out at least duplicate runs for each experiment unless otherwise stated, but here the data from typical runs are shown here.

Labeled decomposition products generated from the respective labeled compounds

1. L-[^{35}S]Methionine, without stabilizers. After one-day storage of the received sample at -80 ℃, about 0.1% of the total radioactivity was recovered as gaseous decomposed products from the L-[^{35}S]methionine solution without stabilizers. These labeled gas components were analyzed by HPLC, and the distribution patterns of radioactivity in each chromatogram are shown in Fig. 6-1. The author could not distinguish hydrogen sulfide from sulfur dioxide with the analytical method used here. The average percentages of the labeled gas components estimated from the radioactivity in the three chromatograms (A, B and C) are shown in Table 6-1 with the standard deviation. At the time, the radiochemical purity of unstabilized L-[^{35}S]methionine (without stabilizers) in the original vial was 93% according to HPLC analysis using an Opti-Pac CE column. The major ^{35}S-impurities were methionine sulfone and methionine sulfoxide, as already reported 4, 5).

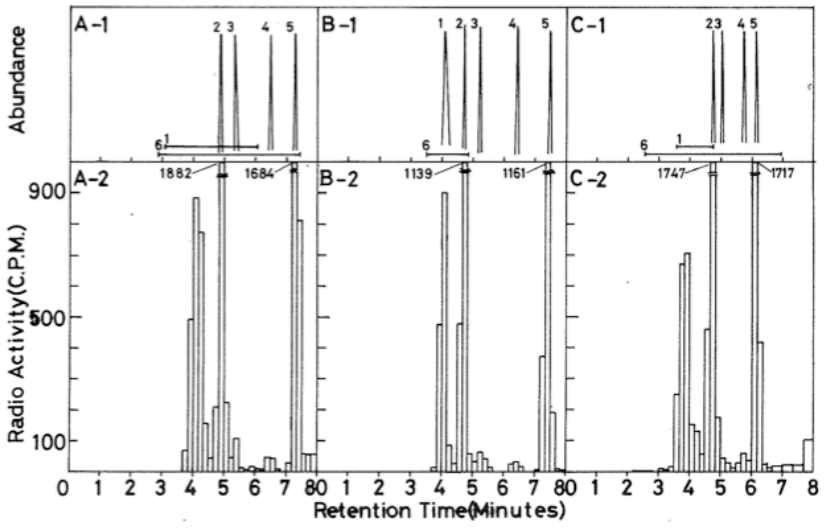

Figure 6-1. HPLC chromatograms of the gaseous self-decomposition products generated from unstabilized (without stabilizers) L-[^{35}S]methionine. Eluent: chromatogram A, acetonitrile/water (6:4, v/v); chromatogram B, methanol/water (7:3, v/v); chromatogram C, tertahydrofran/acetonitrile/water (3:3:4, v/v/v). Authentic

standards: peak or region 1, hydrogen sulfide; peak 2: methyl mercaptan; peak 3, dimethyl sulfide; peak 4, methyl ethyl sulfide; peak 5, dimethyl disulfide; region 6, sulfur dioxide.

Table 6-1 The radioactive gaseous components released from ^{35}S-amino acids, the average percentages and the standard deviations shown in parentheses.

Released components	Labeled amino acids		
	Methionine without stabilizers (%)	Methionine with stabilizers (%)	Cysteine with stabilizers (%)
Methyl mercaptan (CH_3SH)	2.3(±1.6)	70.1(±7.0)	28.7
Hydrogen sulfide (H_2S) or sulfur dioxide (SO_2)	29.8(±1.2)	13.5(±3.4)	51
Dimethyl sulfide (CH_3SCH_3)	2.1(±0.7)	3.2(±1.7)	
Methyl ethyl sulfide ($CH_3SCH_2CH_3$)	1.6(±0.2)	2.1(±0.7)	
Dimethyl disulfide $(CH_3S)_2$	33.0(±1.0)	7.8(±0.9)	3.1

2. L-[^{35}S]Methionine with stabilizers was analyzed. When L-[^{35}S]methionine with stabilizers was analyzed after storage for five days at -80 ℃, the radioactivity recovered from the gaseous components was approximately 0.1%, as observed above for the sample without stabilizers. The average percentages of the respective labeled gas components (Fig. 6-2) are shown in Table 6-1. The radiochemical purity of L-[^{35}S]methionine with stabilizers in the original vial was 90%, again comparable to the sample without stabilizers. Methionine sulfone and methionine sulfoxide were also observed as ^{35}S-impurities.

3. L-[^{35}S]Cysteine. On the day when the labeled compound arrived, only 0.01% of the total radioactivity was found in gaseous decomposition products in the head-space of the vial. Only one solvent system (CH_2CN/H_2O) was used for HPLC analysis of the gaseous components. Three decomposition products were identified among five radioactive peaks, as shown in Fig. 6-3. The percentages of the respective labeled gas components identified are shown in Table 6-1. The radiochemical purity of L-[^{35}S]cysteine with stabilizers was 91%, and one third of the radioactive impurities were

cystine.

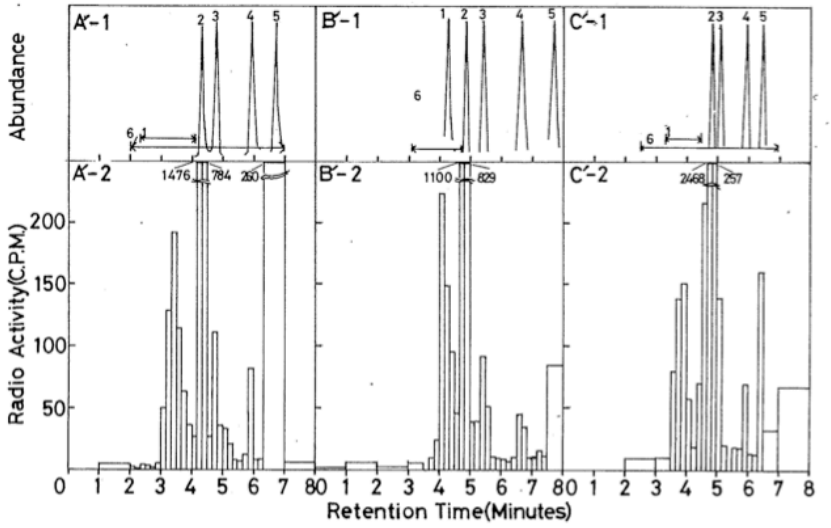

Figure 6-2. HPLC chromatograms of gaseous self-decomposition products generated from stabilized L-[^{35}S]methionine. Each symbol is as illustrated in the footnote to Fig. 6-1. Panels A, B and C correspond to those in Fig. 6-1.

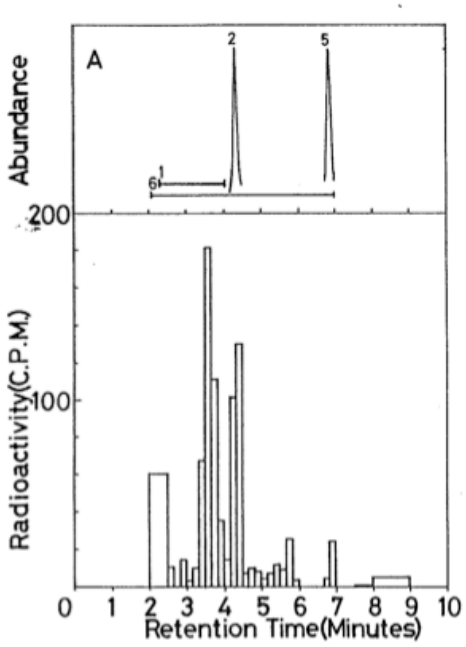

Figure 6-3. HPLC chromatograms of gaseous self-decomposition products generated from stabilized L-[^{35}S]cysteine with stabilizers was 91%, and one third of the radioactive

impurities were cystine.

Degradation products of unlabeled methionine or cysteine irradiated by ^{60}Co γ-rays

1. Methionine. The gaseous component released from unlabeled methionine irradiated ^{60}Co γ-rays was analyzed with a GC/MS spectrometer. In the head-space filled with air but without stabilizers, dimethyl disulfide was the sole degradation component, as shown in Fig. 6-4. The amount of dimethyl disulfide generated was proportional to the dose of irradiation (Fig. 6-5). No degradation products were detected either when the head-space of the vial was filled with helium or when stabilizers were added to the methionine solution.

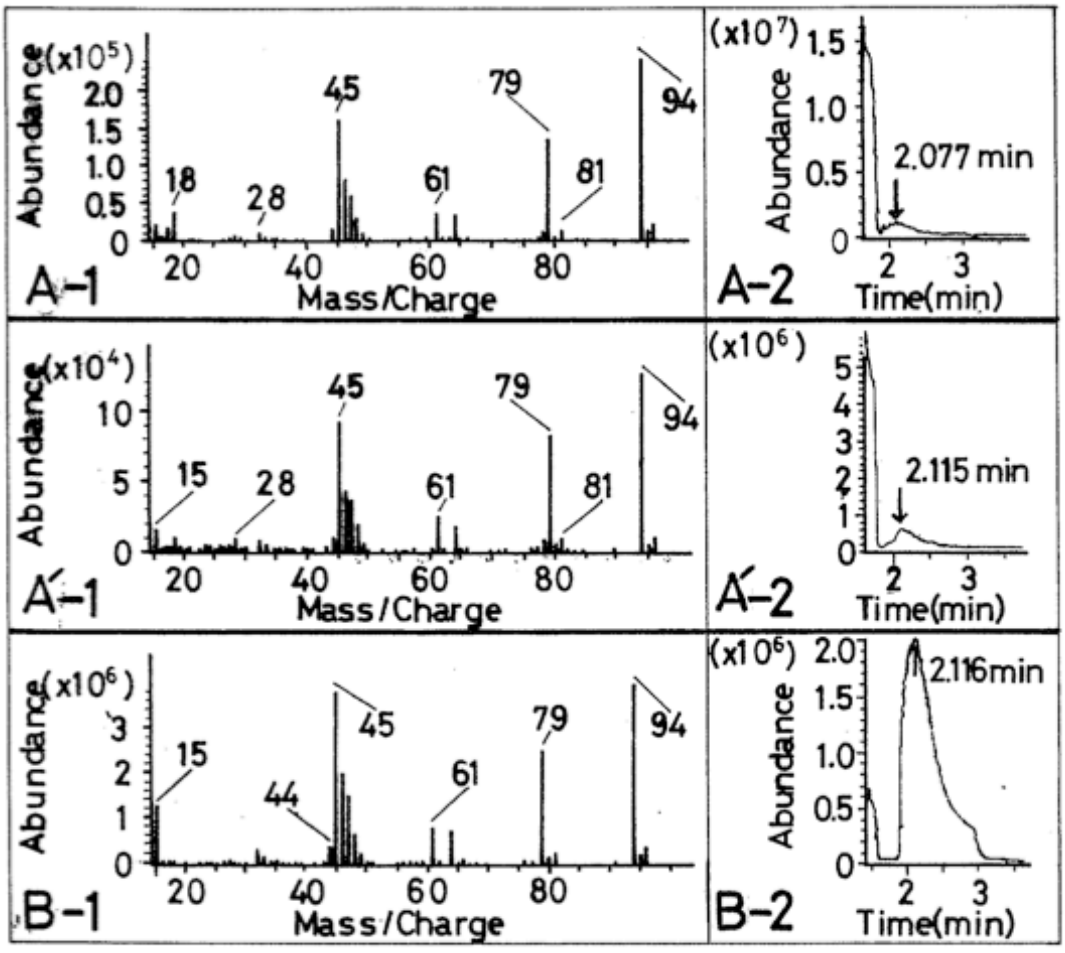

Figure 6-4. Charts A-1 and A-2 show the mass spectrum and the gas chromatogram of the gaseous degradation compound of unlabeled methionine solution irradiated with ^{60}Co γ-rays. Charts B-1 and B-2 were obtained by analyzing authentic dimethyl disulfide described as above (A-1 and A-2). Analytical conditions are described in the text.

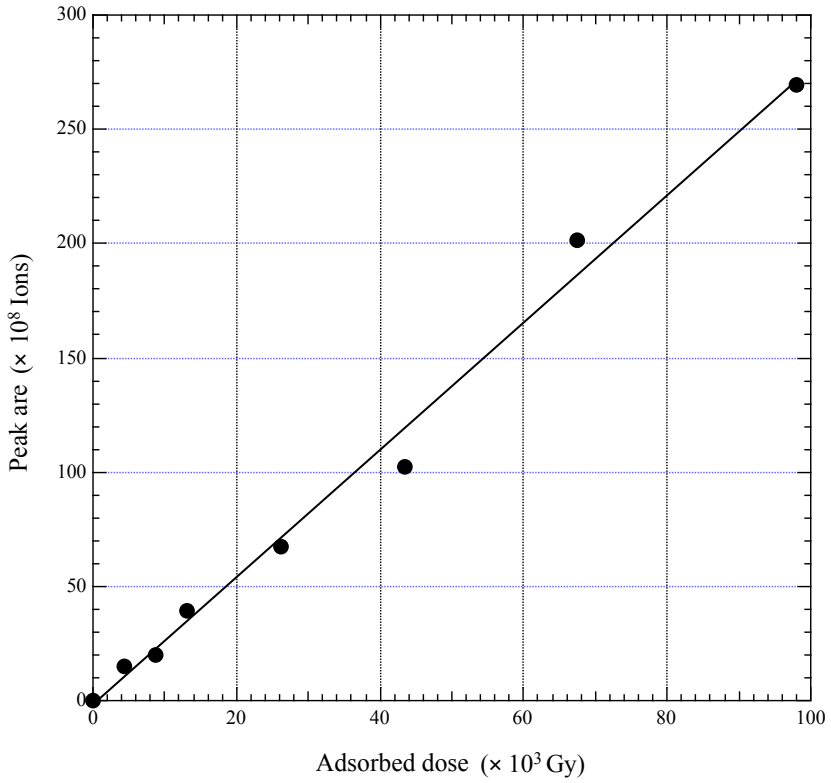

Figure 6-5. The relationship between the amount of dimethyl disulfide produced (total ions/ml) and the dosage of ^{60}Co γ-rays. The amount of dimethyl disulfide produced was proportional to the ^{60}Co γ-radiation absorbed dose (Gy) or dose (R).

2. Cysteine. No gaseous degradation products were detected in the cysteine sample under any of the irradiation conditions tested.

4. Discussion

The gaseous self-decomposition products, except dimethyl disulfide, generated from [^{35}S]methionine or [^{35}S]cysteine corresponded to the respective fragments which are supposed to be formed by the cleavage of chemical bond(s) in the skeletal structure of each amino acid (Fig. 6-6). Similar fragmentation occurs when organic compounds undergo electronic bombardment, for example, in an organic mass spectrometric process. Figure 6-7 shows those fragments when methyl propyl sulfide, whose structure is a part of L-methionine, was analyzed with GC/MS. Proportions of the respective fragments are shown in Table 6-2. There was considerable similarity between the self-decomposition products of [^{35}S]methionine and fragments formed by the electron impact of methyl propyl sulfide, although there is supposedly a big difference in the chemical and/or physical conditions between the two fragmentation processes.

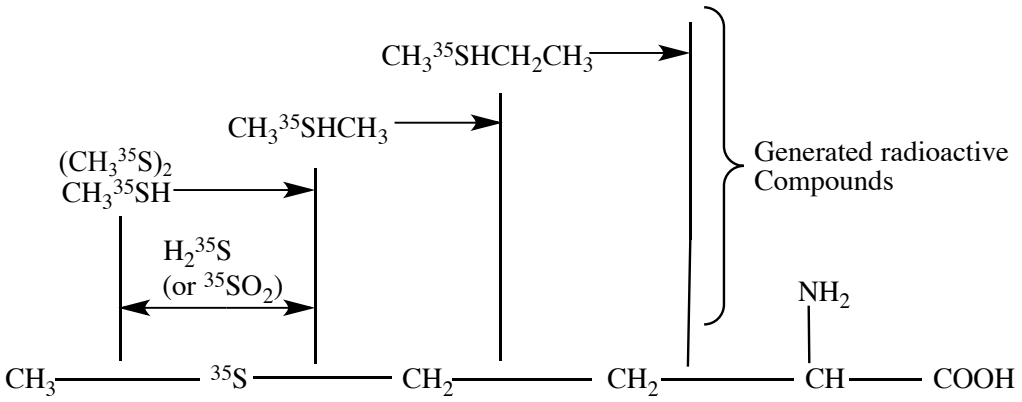

L-Methionine

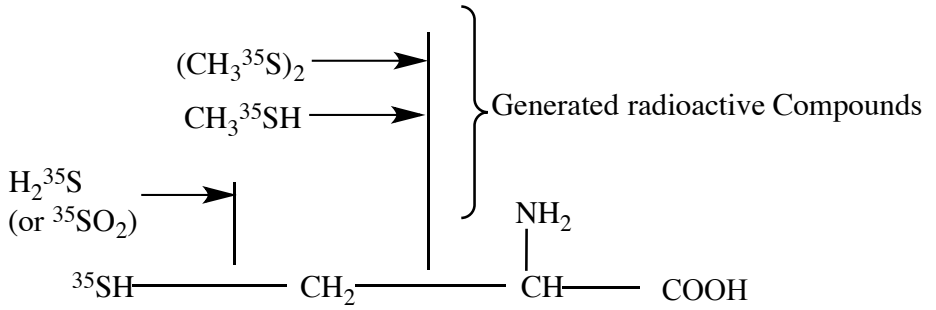

L-Cysteine

Figure 6-6. An illustration of the self-decomposition mechanism of L-methionine and L-cysteine. The dotted lines show the location of bond cleavage by electron impact, and the arrows show the compounds generated by the respective cleavages.

Table 6-2. Fragments of methyl propyl sulfide analyzed by GC/MS and their percentages. The skeletal structure of methyl propyl sulfide is a part of L-methionine.

Fragments of methyl propyl sulfide by GC/MS	Percentage (%)
CH_3S— or —SCH_2—(m/z = 47, 46)	16.9
CH_3SCH_2— or —CH_2CH_2S—(m/z = 61, 60)	15.0
$CH_3SCH_2CH_2$— or $CH_3CH_2CH_2S$—(m/z = 75)	1.95
$CH_3SCH_2CH_2CH_3$ (m/z = 90)	5.34
CH_3— or —CH_2— (m/z = 15, 14, 13)	12.1
CH_3CH_2— or —CH_2CH_2— (m/z = 29, 28, 27, 26)	15.1
$CH_3CH_2CH_2$— (m/z = 43, 42, 41)	14.4

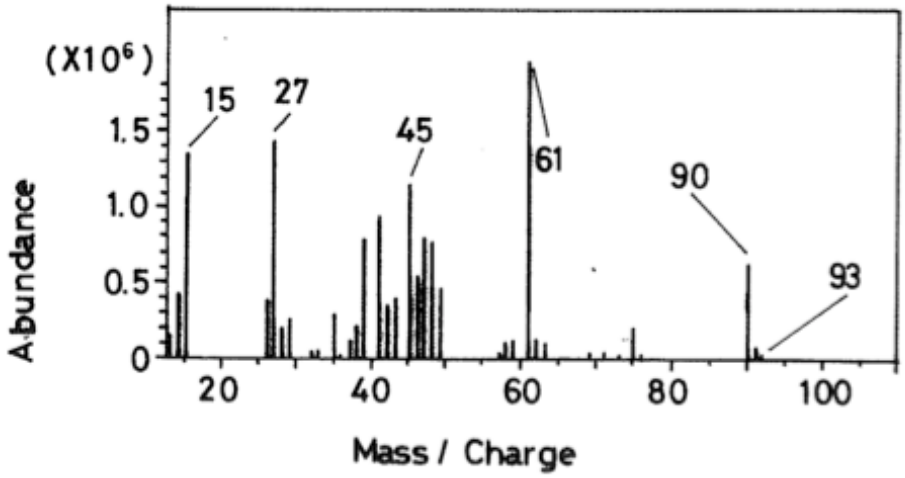

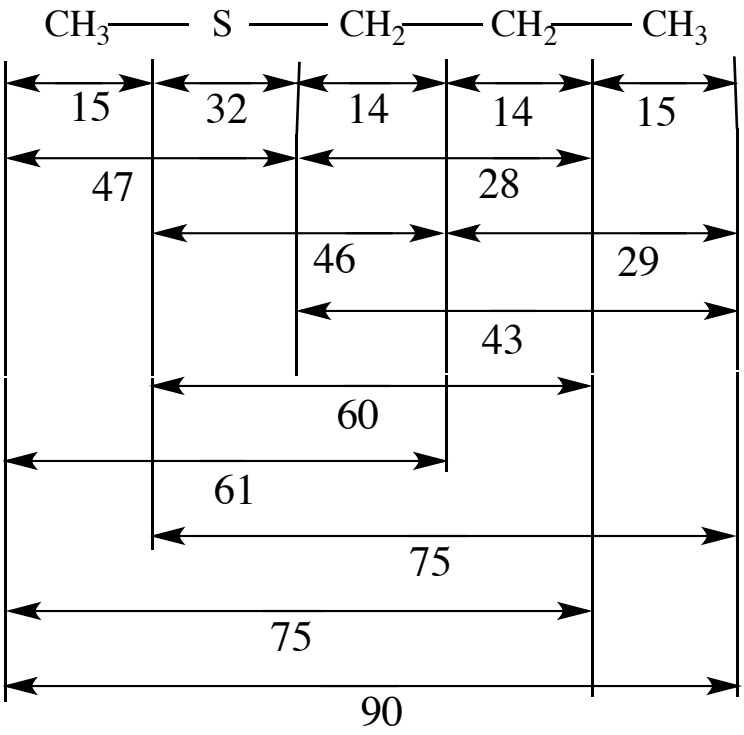

Mass unite of methyl propyl sulfide

Figure 6-7. Mass spectrum and fragmentations in the GC/MS analysis of authentic methyl propyl sulfide.

Dimethyl disulfide was major self-decomposition product released into the head-space of a vial that contained [^{35}S]methionine without stabilizers (Fig. 6-1). Disulfide is generally produced by condensation of the corresponding thiols under mild oxidative conditions 17). Dimethyl disulfide seems to be generated not as a primary

decomposition product of methionine but as a secondary product 1) resulting from the oxidative condensation of methyl mercaptan, a putative primary decomposition product of methionine. This assumption may explain the finding that the added stabilizers caused a decrease in dimethyl disulfide formation, resulting in an increase of methyl mercaptan (Fig. 6-2). Similarly, much less labeled dimethyl disulfide was generated from stabilized [^{35}S]cysteine than labeled methyl mercaptan. This assumption is also consistent with finding that dimethyl disulfide was formed from methionine irradiated by ^{60}Co γ-rays under aerobic conditions, but not when stabilizers were added to unlabeled methionine solution and the head-space of a vial containing methionine solution was filled with helium.

Next the author discusses the difference between the dose of ^{60}Co γ-ray irradiation and the exposed dose of β-emitters of ^{35}S. This difference cannot be directly estimated. One way is to compare the number of ion pairs generated by the two systems. The exposure to ^{60}Co γ-rays for the unlabeled methionine and cysteine solution was 10^7 Röentgens for 40 days. By definition, 1R (Röentgen)(= 8.7×10^4 Gy) is equal to 2.58×10^4 C/kg, which corresponds to the generation of 1 e.s.u. electric charge in 1 cm^3(= 0.001293 g) of dry air under standard conditions. The average electrolytic dissociation energies of air and water are 33.73 and 30.02 eV, respectively. Therefore, the number of ion pairs generated in 1 mL water by irradiation of ^{60}Co γ-rays would be approximated by the following:

$$\frac{1[e.s.u.]\times10^7}{4.8\times10^{-10}[e.s.u./ion\ pair]}\cdot\frac{1}{0.001293}\cdot\frac{33.73[eV]}{30.02[eV]}\cdot\frac{1}{40\times24\times60\times60} \quad (1)$$
$$=5.24\times10^{12}[ion\ pairs/g\cdot s]$$

where the value 4.8×10^{-10} e.s.u. is the electric charge of one electron.

On the other hand, the number of ion pairs generated by ^{35}S β-emitters wa estimated as follows. The β-emitters produced by the decay of ^{35}S nuclei are directly emitted into water. Supposing most of the energy of the β-emitters is lost in water, the number of ion pairs generated in 1 mL of an ^{35}S-amino acid solution can be calculated from equation (2) using several factors: the number of β-emitters emitted in 1 s (18.5×10^6[disintegration/s]), the amount of ^{35}S-amino acid solution (33 μL≅ 0.33 g), and, using the average energy of ^{35}S β-emitters (48.6 keV) 18),

$$\frac{48.6\times10[eV/disintegration]\times18.5\times10^6[disintegration/s]}{30.02[ion\ pairs]}\cdot\frac{1}{0.033[g]} \quad (2)$$
$$=9.07\times10^{11}[ion\ pairs/g\cdot s]$$

Thus the number of ion pairs formed in a ^{35}S-amino acid solution is thought to be roughly comparable to those formed in the unlabeled amino acid solution irradiated by ^{60}Co γ-

rays. On the other hand, there was no qualitative difference in the degradation products in an unlabeled amino acid solution irradiated by ^{60}Co γ-rays through doses between 0 and 8.7×10^{11} Gy (=10^7 Röentgens). These facts suggest that the level of the irradiated dose has no effect on the decomposition mode of the amino acid. The author also confirmed that the storage temperature (4 °C or -80 °C) resulted in no difference in the gaseous self-decomposition compound from the ^{35}S-amino acid. The detailed mechanism of the decomposition of organic compounds caused by ionizing radiation 19~22) of different qualities (such as β-emitter and γ-ray) remains to be investigated.

In this study, the author demonstrated that there were practically no differences in the degree and the product distribution in the self-decomposition of [^{35}S]-methionine between stabilized and unstabilized (without stabilizers) solutions, although the specific radioactivities were quite different (＞48 TBq/mmol vs. ~18.5 GBq/mmol). However, in fact, the stabilizers actually compensated for the high degree of self-decomposition which should be inevitable in L-[^{35}S]methionine with extremely high {more than 2 thousand times that of the un-stabilized (without stabilizers) sample} specific radioactivity.

5. Conclusion

The author confirmed that ^{35}S-labeled amino acids with high specific activity are very unstable. The radiochemical purity of L-[^{35}S]methionine, stabilized or not, and of stabilized L-[^{35}S]cysteine was approximately 90% even at the time of their arrival at the user's laboratory.

Methyl mercaptan, hydrogen sulfide (or sulfur dioxide) and dimethyl disulfide were the major self-decomposition products generated from un-stabilized (without stabilizers) [^{35}S]methionine. When stabilizers were added, the fraction of methyl mercaptan considerably increased, and the other two decomposition products decreased. On the other hand, methyl mercaptan and hydrogen sulfide (or sulfur dioxide) were the major self decomposition products in stabilized L-[^{35}S]cysteine.

Stabilizers can retard the self-decomposition of ^{35}S-amino acids but cannot completely stop it. The headspace of a vial containing an original solution of ^{35}S-amino acid always contains a considerable number of gaseous radioactive components. Therefore, the physical and chemical properties of radioactive compounds with high specific radioactivity must be carefully handled before they are purchased, stored and used at high specific radioactivity. The author hopes that these findings will be useful in arranging for the safe handling of radio-labeled compounds of high specific activity.

6. Summery

The author examined the fragment molecules in the gaseous components generated from ^{35}S-amino acids with high specific radioactivity. The one self-decomposition mode of a molecule labeled with β-emitters was principally similar to the fragmentation mode of organic compounds impacted by accelerated electrons as in organic mass spectrometry. Degradation products of unlabeled amino acids irradiated by ^{60}Co γ-rays indicated that the degradation mode induced by external γ-ray irradiation was different from the self-decomposition mode of ^{35}S-labeled compounds.

Acknowledgement－This investigation was supported in part by a Grant-in-Aid for Scientific Research by the Ministry of Education, Science and Culture of Japan (Project No. 034531444).

References

1) Bayly R. J. and Weigel H. (1960) Self-decomposition of compounds labeled with radioactive isotopes, *Nature* **188**, 384.
2) Ekert B. (1962) Effect of γ-rays on thymine in de-aerated aqueous solutions, *Nature* **194**, 278.
3) Evans E. A. and Stanford F. G. (1963) Stability of thymidine labeled with tritium of carbon-14, *Nature* **199**, 762.
4) Kolousek J., Liebster J. and Babicky A. (1957) Radiochemical degradation of DL-methionine, *Nature* **179**, 521.
5) Kopoldova J., Kolousek J., Babicky A. and Liebster J. (1958) Degradation of DL-methionine by radiation, *Nature* **182**, 1074.
6) Szirard L. and Chalmers T. A. (1934) Chemical separation of the radioactive element from its bombarded isotope in the Fermi effect, *Nature* **22**, 452.
7) Tolbert B. M., Adams P. T., Bennett E. L., Hughes A. M., Kirk M. R., Jemmon R. M., Noller R. M., Ostwald R. and Calvin M. (1953) Observation on the radiation decomposition of some ^{14}C-labeled compounds, *J. Am. Chem. Soc.* **75**, 1867.
8) Wolfgang R. L., Anderson R. C. and Dodson R. W. (1956) Bond rupture and nonrupture in the beta decay of carbon-14 studied by double isotopic labeling, *J. Chem. Phys.* **24**, 1
9) Michael G. Debije, Yuri Razskazovskiy, and William A. Bernhard (2001) The yield of strand breaks resulting from direct-type effect in crystalline DNA X-irradiated at 4 K and room temperature, *J. Am. Chem. Soc.* **123**, 2917.

10)Betsy M. Sutherland, Paula V. Bennett, and John C. Sutherland (1996) Double strand breaks induced by low doses of γ rays or heavy ions: Quantitation in nonradioactive human DNA, *Analytical Biochemistry* **239**, 53.
11) Williams J. L. Stannett V. at. Al. (1975) Graft copolymers as elastomric fibers-II. Mechanical properties and morphology of grafted copolymers, *Int. J. Appl. Radiat. Isoto.* **26**, 169.
12) Khan Ferdous, Ahmad S. R. and Kronfli E. (2006) γ-Radiation induced changes in the physical chemical properties of lignocellulose, *Biomacromolecules* **7**, 2303
13) Matzner M. Schober D. L. and Mcgrath J.E. (1976) Polystyrene-nylon 6 graft copolymers, *European Polymer Journal* **9**, 469.
14) Hal S. Blair and Kam Moon Lai (1982) Graft copolymers of polysaccharides: 1. Graft copolymers of alginic acid, *POLYMER* **23**, 1838.
15) McGrath R. A. and William R. W. (1966) Reconstruction in vivo of irradiated escherichia coli deoxyribonucleic acid; the rejoining of broken pieces, *Nature* **212**, 534.
16) Meisenhelder J. and Hunter T. (1988) Radioactive protein-labeling techniques, *Nature* **335**, 120.
17) Wallace T. J. and Schriesheim A. (1962) Solvent effects in the base-catalyzed oxidation of mercaptans with molecular oxygen, *J. Org. Chem.* **27**, 1514.
18) Mantel J. (1964) The beta ray spectrum and the average beta energy of several isotopes of interest in medicine and biology, *Int. J. Appl. Radiat. Isot.* **23**, 407.
19) Bexendale J. H. (1964) Effects of oxygen and pH in the radiation chemistry of aqueous solution, *Radiat. Res. Suppl.* **4**, 114.
20) Matheson M. S. (1964) The formation and detection of intermediates in water radiolysis, *Radiat. Res. Suppl.* **4**, 1.
21) Schwarz H. A. (1964) Intensity effects, pulsed-beam effects, and the current status of diffusion kinetics, *Radiat. Res. Suppl.* **4**, 89.
22) Trump J. G. and Van De Graaff R.J. (1948) Irradiation of biological materials by high energy Roentgen rays and cathode rays, *J. Appl. Phys.* **19**, 599.

Chapter 7

Environmentally friendly measurement of airborne radon using a nonvolatile liquid scintillation absorbent

Radon (^{222}Rn) measurement I.

General quick measurement of radon based on ^{222}Rn and ^{214}Po radioactive equilibrium.

1. Introduction

The health hazards posed by ^{222}Rn (radon) in the past are described in the general introduction section, but atmospheric radon is still the subject of much research. Radon measurements are indispensable for protecting humans from internal exposure at places of work and in residential environments, e.g., radiation institutes, dwellings and mines.

In Chapter 7, radon in air is quickly measured by liquid scintillation. The equivalent radioactivity of radon was attained using the ^{214}Po radioactive equilibrium method calculated by successive decay equations via α-particle spectrometry based on the immediate; 1-hour measurement of the generated ^{214}Po α-spectrum after radon was sampled.

Many researchers have used the liquid scintillation measurements of airborne radon using a liquid absorbent to determine the presence of radon. The method was first proposed by Noguchi M. 1) in 1964, who performed a few measurements using a scintillator after extraction using a large quantity of toluene. Since Noguchi's experiments, Prichard H.M. 2) furthered this method and measured radon in air using 20 mL of hexane as the solvent and cooling to -78 ℃ with dry ice for sample collection. The determination was made by measuring ^{214}Po 3), 4), 5) after at least a 4-h waiting period and then counting for 100 min. Gudjónsson G. et al. 6) reported progress using a mineral oil-based scintillator. Radon was extracted from the air with 20 mL of a mineral oil-based solvent with a low volatility in an open scintillation vial by natural diffusion for 24 h, and the concentration was determined based on the measurement of the ^{214}Po α-spectrum for 11 h after equilibrium with radon was reached.

This work presents an improved measurement method that considerably shortens the sampling and measurement periods by accumulating radon via the bubbling of a large volume of air for 30 min, achieving a higher measurement quality relative to prior methods for the determination of atmospheric concentrations and effectively decreasing the number of procedural steps. Our medium for sampling radon in air acts as both the collector of airborne radon by absorption and the nonvolatile liquid scintillator 7). The

nonvolatile liquid scintillator acts as an absorbent, and a suitable radon sample can be collected in a short time with only 10 mL of the nonvolatile liquid scintillation absorbent (NLSA) by bubbling a large volume of radon-containing air through the NLSA. The accumulation shortens the time required for measurement with a liquid scintillation counter (LSC). Furthermore, the quenching index is based on the exposure of an external standard source fixed within the LSC, and the source remains unchanged before and after the sampling and measurement. The NLSA fluor is colorless and transparent and therefore will not increase the quenching or decrease the efficiency. In addition, NLSA is safe to humans, environmentally friendly, and can be used repeatedly. The greatest advantage of this NLSA is that the entire volume of the scintillator within the 20-mL scintillation vial effectively serves as the sample.

The practicality of using a liquid scintillation method with an NLSA for the measurement of airborne radon in a residence was examined. The relationship between the radioactivity absorbed by the NLSA and the atmospheric radon concentration in a calibrated walk-in radon chamber was investigated. The amounts of radon absorbed in the NLSA were proportional to the radon concentration in the air. The calibration curve showed reliable quantitative linearity from 500 to 8000 Bq m^{-3} in air using the least-squares method, and these data were used to extrapolate the curve to the region between 0 and 500 Bq m^{-3}. The validity of the extrapolated curve at less than 500 Bq m^{-3} was confirmed by comparisons of the measured radon concentrations in the room and the atmosphere with those determined using an existing ionization chamber. Variations in the absorption of radon were observed due to changes in temperature and humidity. The health and environmental safety of the NLSA were also considered.

Keywords: radon, liquid scintillation counting, radioactivity, α-spectrometry, scintillation absorbent

2. Experimental methods and results

2-1. Sampling apparatus

The sampling process is illustrated in Fig. 7-1. The apparatus is portable and can be transported to residences or to field sites.

2-2. Reagents and materials

The reagents were prepared from the following: Crystal Fluor (cat. no. 882419, Parc d'Innovation, Illkirch, France), 1,5-diphenyloxazole (PPO)/p-bis-(o-methylstyryl)-benzene (bis-MSB) (95:5, w/w) and methyl-phenyl silicone oil (HIVAC F4, purchased from Shin-Etsu Chemical Co., Ltd, Tokyo, Japan). The silicone oil NLSA was composed of silicone oil (100 mL) and Crystal Fluor (cat. no. 882419) (0.6 g/100 mL). With this

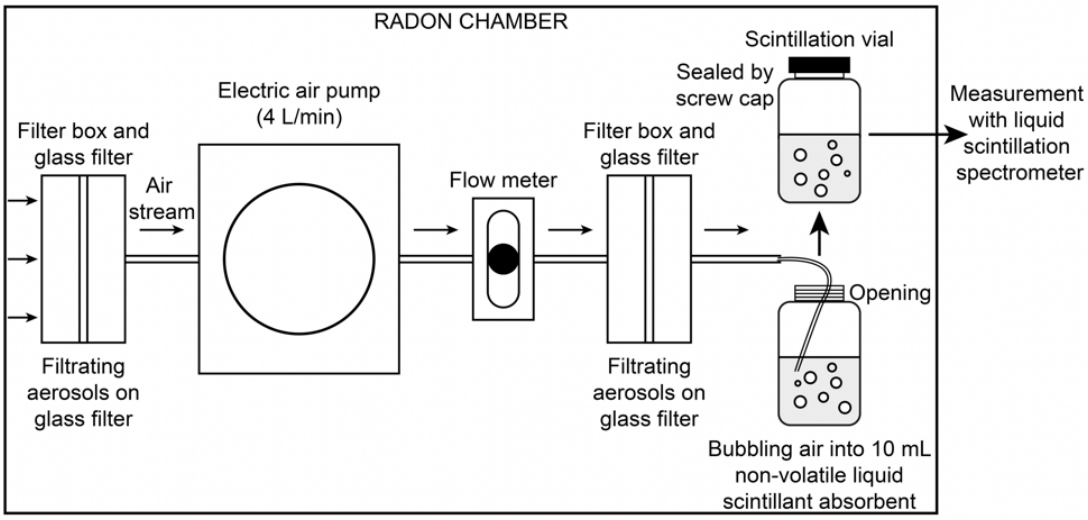

Figure 7-1 Illustration of ^{222}Rn sampling in a nonvolatile liquid scintillation absorbent (NLSA) by bubbling air.

solute combination, the NLSA has the same measurement efficiency and radon spectrum as those of tritium, ^{14}C and other nuclides, and the quenching was unchanged compared with that of the combination described by Kato, T. and Hatagami, T. (PPO: 0.7 g/100 mL, POPOP: 0.02 g/100 mL). Charcoal (activated charcoal, CHR-30, No. 079-12, specially prepared reagent purchased from Nakarai Chemicals, Ltd., Tokyo, Japan) for NLSA recovery, CHC-50, glass filters (GF/F, diameter ø: 55 mm, Whatman, Kent, U.K.), a bubbling nozzle with an immersion filter (ø: 18 mm, length: 229 mm, glass particle No. 1, 100~120 μm hole size for the largest bubble size and glass particle No. 4, 4~5.5 μm hole size for the smallest bubble size, Sogorikagaku Glass Works, Osaka, Japan), and a glass tube (ø: 8 mm, Sogorikagaku Glass Works, Osaka, Japan) were used for radon sampling.

2-3. Measurements

2-3-1. Measurement methods

Liquid scintillation analyzers Tri-Carb 3100TR (Perkin Elmer, Boston, U.S.A.) and Tri-Carb 2770TRSL (Packard Instrument Co., U.S.A.) in conjunction with 20-mL Teflon vials purchased from Kagaku Kyoeisha, Ltd., Osaka, Japan were used for counting. Sampling was performed in a radon chamber at the internationally recognized National Institute of Radiological Science (NIRS) 8) as well as in natural settings. Thoron was not present in the atmosphere in the chamber. In the chamber, the radioactivity of radon was measured and controlled with an AlphaGUARD ionization chamber (SAPHYMO GmbH, Frankfurt a.M., Germany). The temperature and humidity (20 °C/60%) in the air were calibrated and held constant. The temperature and humidity levels were set to standard

ground-level atmospheric conditions. The established radioactivity in the chamber varied with an uncertainty of ±4% at 500-8000 Bq m^{-3} and with an uncertainty greater than ±5% at concentrations less than 500 Bq m^{-3}. Sampling was performed at radioactivity levels of approximately 200, 500, 1000, 3000, 5000, 7000 and 8000 Bq m^{-3}. The radon in the chamber air was thoroughly and uniformly absorbed into 10 mL of NLSA in a 20-mL Teflon scintillation vial using nozzle No. 1 with a 100~120 μm hole size at a flow rate of 4 L/min for 30 min. This flow rate was optimal for achieving good sensitivity and precision in these measurements. The point of the nozzle was immersed at the deepest point in the NLSA (the bottom of the vial). Air was blown through the nozzle and was in direct contact with the NLSA, providing the most effective absorption. When the nozzle released smaller bubbles, the absorption rate by the NLSA higher. When the smallest bubbles were used (nozzle No. 4 with a 4~5.5 μm hole size), the absorptive rate was approximately 3-fold higher than that achieved with nozzle No. 1. However, the bubbles overflowed from the sampling vial even at a flow rate of 0.1 L min^{-1}. The total amount of radon extracted from 0.12 m^3 of air while bubbling at 4 L/min for 30 min could not be extracted in more than 6.7 h when the bubbling was less than 0.1 L min^{-1}. To shorten the sampling time, nozzle No. 1, with the largest holes size (100~120 μm), was selected. The counting vial was used as the sampling vessel because of its simple operation before and after radon accumulation. To prevent bubbling over, an NLSA volume of 10 mL and a flow rate of 4 L min^{-1} were used as the maximum values. After the bubbling was completed, the vial was tightly closed with a cap and an inner liner, and the NLSA sample was immediately – generally within 1 h, but within no more than 4 h – measured for a period of 1 h using an LSC in a normal room (not a radon chamber).

2-3-2. Count estimation for radon determination by spectrometry

When the radon in the natural atmosphere is measured, thoron will be present, and the influence and progeny of thoron should be considered. Examination of the spectra of radon, ^{218}Po, ^{214}Po, thoron (^{220}Rn), ^{216}Po, ^{212}Bi, and ^{212}Po α-particles showed that the radon α-particle spectrum overlaps with those of ^{218}Po, thoron, ^{216}Po and ^{212}Bi, and the actual integrated counts of radon could not be separated 9), 10). To avoid similar overlaps and the generally long sampling time required for measuring ^{214}Po, our established LSC system used instantaneous measurements obtained before the radioactive equilibrium state of ^{214}Po was attained. However, count results were obtained immediately following an hour of sampling. The actual count contributed by radon can be recalculated using the count rate after the ^{214}Po equilibrium was achieved using counts estimated from the decay product equations rather than the radioactive equilibrium of ^{214}Po 11). The (recalculated) actual ^{214}Po α-count contribution after equilibrium was set to $C^{a}_{eqPo214}$; the actual count

immediately after the sampling of ^{214}Po was set to $C^{a}_{0-1Po214}$; the estimated count rate for ^{214}Po calculated using the successive decay equations after equilibrium was achieved was set to $C^{v}_{eqPo214}$; and the equation-based estimated count rate for ^{214}Po immediately after sampling was set to $C^{v}_{0-1Po214}$. The (recalculated) actual radon count contribution, C^{a}_{0-1Rn}, is represented as follows:

$$C^{a}_{0-1Rn} \equiv C^{a}_{eqPo214} = C^{a}_{0-1Po214} \cdot \frac{C^{v}_{eqPo214}}{C^{v}_{0-1Po214}}.$$

2-3-3. Measurement results

The measurements of the absorbed radioactivity for levels from 500-8000 Bq m^{-3} in the air are presented in Table 7-1. The absorbed radioactivity of radon based on ^{214}Po in 10 mL of NLSA for each actual measurement in the chamber is shown. The errors in the radioactivity measurements in the chamber in the range of 500-8000 Bq m^{-3} were within the electric current fluctuations shown in Table 7-1. The practical measurement at approximately 200 Bq m^{-3} (Table 7-2) exhibited a radon radioactivity of 236 Bq m^{-3} with an error of ±76.4 Bq m^{-3}; thus, this measurement is not reliable. The indicated Ostwald coefficients are shown under bubbling conditions. The temperature and humidity are the average during the 30-min sampling period.

2-3-4. Generating the calibration curve

The calculated absorbed radioactivity of radon alone, $C^{a}_{eqPo214}$, shown in Table 7-1, is plotted in Fig. 7-2 as a function of the level of radon radioactivity in the radon chamber, which contained unmixed ^{218}Po and its progeny. Open circles represent the radon radioactivity absorbed in 10 mL of NLSA in a 20-mL scintillation vial measured with an LSC based on the radioactivity of radon in 1 m^3 of air. The absorbed radioactivity of ^{214}Po in the NLSA was proportional to the radioactivity of radon in the air. The straight line ($Y=9.00\times10^{-5}\cdot X+7.13\times10^{-3}$) and R correlation factor were approximated using the least-squares method from each of the data points from 500-8000 Bq m^{-3}. The line was extrapolated to the lower range (below 500 Bq m^{-3}) using an approximation based on the values from 500-8000 Bq m^{-3} with the least-squares method.

2-3-5. Assessment of validity and practicality

The average concentrations in indoor air and the atmosphere are less than 50 Bq m^{-3}; for example, the averages are 15 Bq m^{-3} (minimum: 2; maximum: 208) in Japan 12), 8-84 Bq m^{-3} in 18 European countries 13) and 25 (1.85-7,770) Bq m^{-3} in the United States14). The radon concentration can vary over a considerably larger range than mentioned above due to considerable temporal variations. Regarding regulations, however, the effective measurement of concentrations near 300 Bq m^{-3} is essential. This concentration range is covered by the calibration curve in Fig. 7-2. Therefore, to perform

Table 7-1 The ratio of radon absorption by the nonvolatile liquid scintillation absorbent (NLSA) to the test radon concentration in the air determined using a liquid scintillation counter (LSC). The radioactivity of ^{222}Rn was calculated using the successive decay equations for ^{214}Po after equilibrium was achieved. Each concentration of radon in the air was calibrated within the electric current fluctuations. The Ostwald coefficient refers to after 30 min of bubbling at a flow rate of 4 L/min and using bubbling nozzle No. 1 with an immersion filter (ø 18) and glass particles (100–120 μm).

C: Concentration of ^{222}Rn in radon chamber air ($Bq \cdot m^{-3}$) (20°C, relative humidity 60%), ±Error		539.1	±117.3	1046.3	±151.6	3017.0	±321.5	5097.0	±474.5	7349.2	±672.0	7538.3	±665.0	8046.6	±712.8
^{222}Rn absorbed radioactivity in 10 mL Liquid Scintillation Absorbent determined by calculation from the α-spectrum of ^{214}Po in radiation equilibrium, ±Uncertainty	$Bq \cdot m^{-3}$	0.0339	±0.0031	0.1121	-±0.0056	0.3634	±0.0100	0.3972	±0.0105	0.6400	±0.0138	0.7320	±0.0135	0.7369	±0.0140
	NET Counts $\cdot(h \cdot 10mL)^{-1}$	122.0	±11.0	403.5	±20.1	1308.4	±36.2	1423.3	±37.7	2454.6	±49.5	2350.4	±48.5	2556.8	±50.6
A: Absorbed Radioactivity of ^{222}Rn in 1.0 m^3 LSA ($Bq \cdot m^{-3}$), ±Uncertainty		3389.1	±58.2	11207.4	±105.9	36345.0	±190.6	39724.1	±199.3	63996.6	±253.0	73201.3	±270.6	73694.2	±271.5
$A \cdot C^{-1}$: Ostwald Coefficient $A \cdot C^{-1}$		6.3		10.7		11.8		7.8		8.7		9.7		9.2	
Transfer Time Period from Sampling Point to the Location of Liquid Scintillation Spctrometer (min)		5.6		5.0		4.2		4.2		5.6		5.0		3.5	
Tenperature (℃)		21.8		22.1		22.1		22.1		22.0		22.1		22.0	
Humidity (%)		57.4		55.8		55.9		55.3		56.4		56.0		56.3	

Table 7-2 Comparison of the radon concentrations in air measured using an NLSA in the indicated atmosphere and in rooms measured with a Tri-Carb 2770TRSL and an AlphaGUARD ionization chamber. This comparison confirms the validity of the straight line extrapolated to lower concentrations near 500 Bq m^{-3} by approximation based on the values obtained from 500-8000 Bq m^{-3} using the least-squares method with practical measurements. The new NLSA is indicated by "ⓝ"; NLSA regenerated at least twice was used in all other determinations. The identification limit of this measurement was 36.3 Bq m^{-3}.

	Poorly Ventilated Outdoors, Drift ⓝ	Ventilated First Basement Floor Underground Room	Ventilated First Basement Floor Underground Room	First Floor Room (No Ventillation System) ⓝ	Ventilated Second Basement Floor Underground Room	Poorly Ventilated First Basement Floor Underground Room	Poorly Ventilated First Basement Floor Underground Room	Poorly Ventilated Second Basement Floor Underground Room ⓝ	Poorly Ventilated Second Basement Floor Underground Room	Poorly Ventilated Second Basement Floor Underground Room	Poorly Ventilated Second Basement Floor Underground Room	Poorly Ventilated Second Basement Floor Underground Room	Poorly Ventilated Semi-third Basement Floor Underground Room ⓝ	Poorly Ventilated Semi-third Basement Floor Underground Room	Poorly Ventilated Semi-third Basement Floor Underground Room ⓝ	Poorly Ventilated Semi-third Basement Floor Underground Room ⓝ	Radon Chamber in NIRS ⓝ
Radon Concentration in Air by **AlphaGUARD** (Bq·m^{-3}) Diffusion Mode ±Error	17.3 ±4	16.8±10	19.8±10.5	41.0 ±10	41.5±18.3	66.8±27.5	66.8±23.3	96.0 ±16	117.3±36	118.5±40.0	137.0±42.0	137.0±42	157.6 ±22	170.8±49	188.9 ±24	187 ± 50	236.1 ± 76.4 (more than 12)
Radon Concentration in Air by **LSA Absorption** (Bq·m^{-3}) ±Uncertainty	< 36.3 (22.0 ±5.0)	< 36.3 (0)	< 36.3 (17.2±4.1)	45.0 ±7.0	<36.3 (23.8±4.9)	65.0±8.1	78.1±8.8	145.1±12	110.0±10.5	135.6±11.7	121.9±11.0	163.8±12.8	129.7 ±11	200.5±14.2	179.7 ±13.4	231.6.7 ± 15.2	222.1 ±14.9
Transfer Time from the Measurement Point to the LSA (min)	4.00	5.17	4.50	2.75	5.17	5.33	5.50	3.17	4.20	5.00	4.17	4.33	3.50	8.33	3.38	4.80	5.03
Temperature (°C)	27.9	17.5	19.4	25.9	16.5	15.6	17.3	25.8	13.7	14.0	13.3	13.3	25.6	13.7	25.8	27.0	21.7
Humidity (%)	61.0	41.9	37.9	66.0	44.2	55.8	48.1	68.0	52.3	50.3	56.7	56.7	74.5	57.2	74.0	75.0	57.8
Atmospheric Pressure (mb)	999.1	1019.4	1016.2	1008.6	1022.0	1025.0	1023.5	1007.7	1019.4	1023.0	1023.8	1023.8	1005.3	1023.8	1005.5	1010.0	1012.4

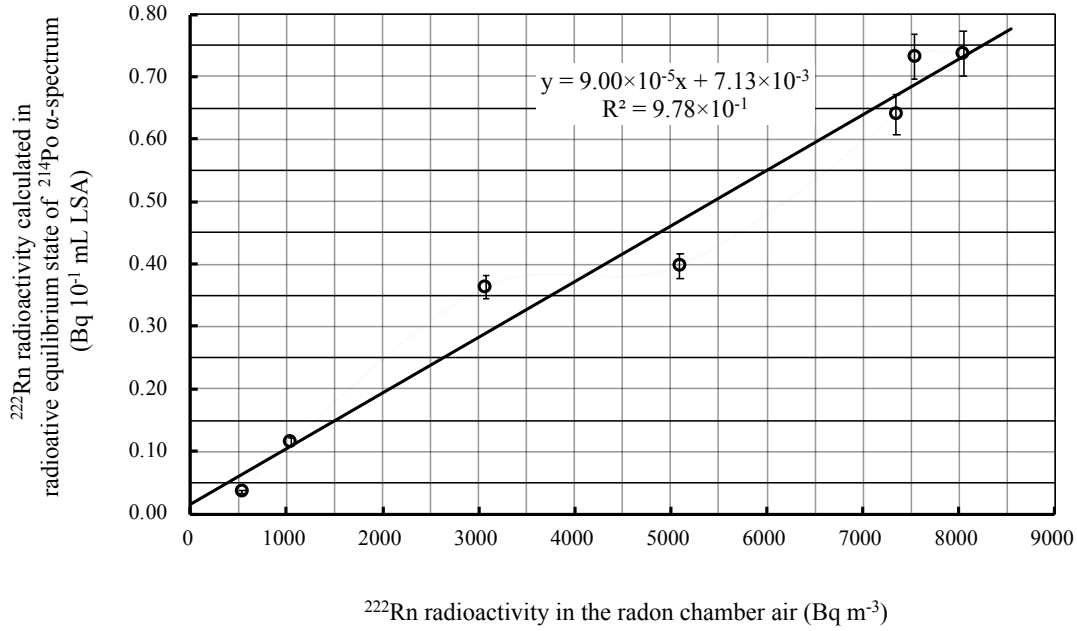

Figure 7-2 Radioactivity of ^{222}Rn absorbed in a nonvolatile liquid scintillation absorbent (NLSA)/radioactivity of ^{222}Rn in air. The radioactivity of ^{222}Rn was the radioactivity of ^{214}Po after radioactive equilibrium was reached, which was calculated using successive decay equations from ^{214}Po with measurements collected immediately after bubbling. The absorbed radioactivity of ^{222}Rn in 10 mL of NLSA (Bq m^{-3}) is proportional to the radioactivity of ^{222}Rn in air (Bq m^{-3}). The line was extrapolated to concentrations less than 500 Bq m^{-3}.

this measurement in practical settings, confirming the validity of the extrapolated linear range to less than 500 Bq m^{-3} is important. Using the calibration curve, airborne radon concentrations from 500 Bq m^{-3} to 8000 Bq m^{-3} can be determined. For concentrations between 0 and 500 Bq m^{-3}, the calibration curve is unsuitable because calibrated concentrations in this range could not be prepared in the radon chamber. The curve from 0 to 500 Bq m^{-3} must be established in the near future based on practical experimental measurements using precisely calibrated concentrations. Currently, the best approach for addressing this issue is to extrapolate the straight line of the calibration curve obtained with the least-squares method from the data in the 500 to 8000 Bq m^{-3} range to the range below 500 Bq m^{-3} and to confirm the validity of the extrapolated line using reliable measurements of radon concentrations below 500 Bq m^{-3} in residential and atmospheric samples with NLSA and an ionization chamber. An AlphaGUARD ionization chamber

was operated in gas diffusion mode to confirm the quantitative relationship determined from the extrapolated straight line when performing the NLSA measurements at concentrations below 500 Bq m^{-3}.

2-3-6. Calibration

As shown in Table 7-2, using the valid region of the extrapolated line ($Y=9.00\times10^{-5}\cdot X+7.13\times10^{-3}$), typical liquid scintillation measurements of atmospheric radon are shown using the calculated ^{214}Po count rate based on the absorbed radon radioactivity in the NLSA sampled from atmospheric and residential samples combined with practical measurements. The concentrations were compared with direct measurements obtained using an AlphaGUARD ionization chamber. As confirmed by the data in Table 7-2, the line in Fig. 7-2 demonstrates the validity and practicality of these measurements. The identification limit in Table 7-2 was calculated based on the Currie approach 15), and the method is as follows.

When the background is 22 (counts/hour), the [uncertainty] of the background can be calculated as follows:

$[uncertainty] = \sqrt{22} \cong 4.69$

The measurement was performed for one hour (3600 s); therefore, the background [uncertainty] per second was

$$\frac{[uncertainty]}{3600} = \frac{\sqrt{22}}{3600} \cong 1.303 \times 10^{-3}$$

Here,

$$3.29 \times \frac{[uncertainty]}{3600} \cong 4.287 \times 10^{-3}$$

$$3\sqrt{2} \times \frac{[uncertainty]}{3600} \cong 5.528 \times 10^{-3}$$

The converted radioactivity (Bq 10^{-1} mL), which corresponds to the number of background counts in the NLSA (Y-axis in the graph in Fig. 7-2), is

$$\frac{22}{3600} \cong 6.111 \times 10^{-3}$$

When the interval of 3.29·[uncertainty] using the 3.29·σ method from the background count is considered, the count that can be clearly distinguished from the background count for the Y-axis in Fig. 7-2, the detection limit of 3.29·[uncertainty], corresponds to

$6.111 \times 10^{-3} + 4.287 \times 10^{-3} = 10.398 \times 10^{-3}$ (Bq 10^{-1} mL NLSA)

The concentration in air is transformed by equation $Y = 9.00\times10^{-5}\cdot X + 7.13\times10^{-3}$ as follows:

$$X = \frac{0.010398 - 0.00713}{0.0000900} \cong 36.31 \quad (\text{Bq m}^{-3})$$

2-3-7. Influences of temperature and humidity

To obtain further insights into the properties of this NLSA, the temperature- and humidity-induced fluctuations in radon absorption by the NLSA in a radon chamber were measured at the NIRS. The absorption fluctuations induced by temperature variations were determined at 10, 20 and 30 °C using a constant radon concentration of 5000 Bq m^{-3} inside the chamber and a constant humidity of 60%. The absorption fluctuations induced by humidity variations were determined at 30, 40, 50, 60, 70, 80 and 90% humidity using a constant radon concentration of 5000 Bq m^{-3} inside the chamber and a constant temperature of 20 °C.

The changes in the amounts of radon absorbed by the NLSA as a function of temperature are presented in Fig. 7-3 and are indicated by closed circles. The graph shows an inverse relationship between the amount of absorbed radon and increasing temperature. The changes in the amounts of radon absorbed by the NLSA as a function of humidity are presented in Fig. 7-3 and are indicated by open circles. The graph also indicates an inverse relationship between the amount of absorbed radon and increasing temperature. The temperature- and humidity-induced fluctuations were indicated, that is the percentage of radon absorbed in the NLSA at each temperature and humidity condition was regarded the temperature- and humidity-induced fluctuations when the humidity was 60% and the temperature was 20 °C as 100%. The influence of temperature and humidity on the airborne radon measurements is negligible because the uncertainty caused by fluctuations due to the natural heterogeneity of air is estimated to be larger than the uncertainty caused by the fluctuations in temperature and humidity, as shown in the uncertainties listed in Table 7-2.

2-3-8. Restoration of the NLSA

Methyl-phenyl silicone oil can be reused many times as an NLSA following purification. The method for restoring the NLSA involved purification using charcoal. To regenerate the NLSA, 3 g of charcoal powder was added to 100 mL of spent NLSA, and the mixture was stirred with a magnetic stirrer for 3 days. After stirring, the charcoal was removed from the NLSA by filtration through a glass fiber filter (GF/F), and additional Crystal Fluor was added to the NLSA, allowing the NLSA to be reused many times. Tritiated water and normal water could be removed by superheating the NLSA for more than 5 days at 60 °C before the above radon removal. As shown in Table 7-1, measurements marked "ⓝ" were performed using new NLSA, whereas the others were performed using NLSA that had been regenerated more than twice. The blank

(background), net count, and spectrum of the recovered NLSA (A) as well as the spectra of absorbed radon and its progeny contained in the NLSA (B) are shown in Fig. 7-4.

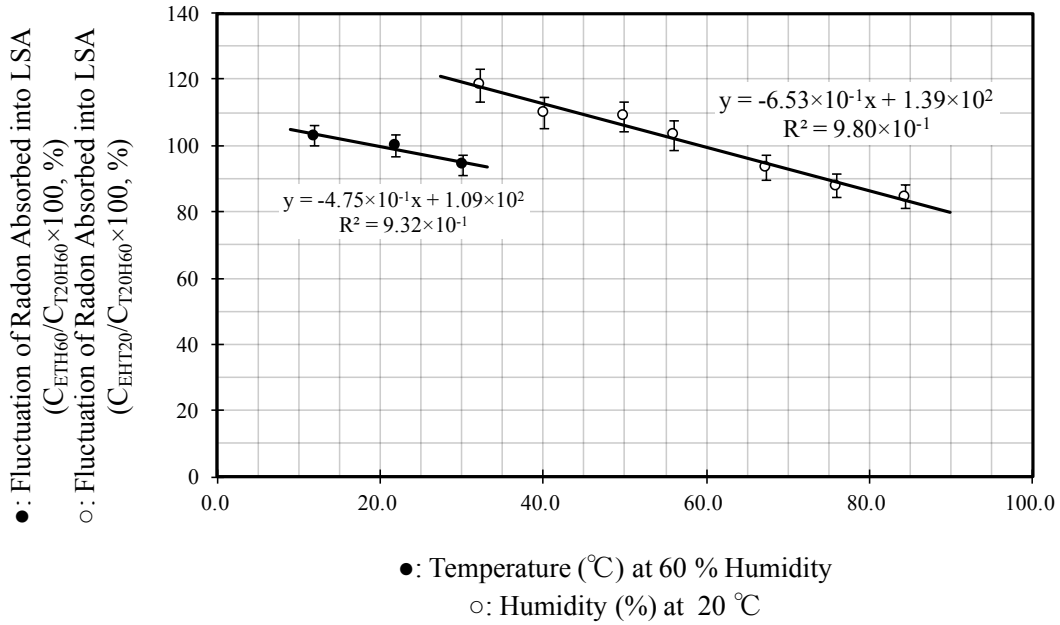

Figure 7-3 ●: Closed circles. Temperature-induced fluctuations in the amount of radon absorbed by the NLSA at a constant humidity of 60% (C_{ETH60}: count at each temperature, humidity of 60%; C_{T20H60}: count at 20 °C, humidity of 60%).
○: Open circles. Humidity-induced fluctuations in the amount of radon absorbed by the NLSA at a constant temperature of 20 °C (C_{EHT20}: count at each humidity level, temperature of 20 °C; C_{T20H60}: count at 20 °C, humidity of 60%).

3. Discussion

3-1. Safety to humans

Many commercial liquid scintillators use hazardous solvents, such as toluene, xylene and pseudocumene. These are volatile liquids that can be inhaled during bubbling, and the vapors are harmful to humans. The vapor pressure of toluene is 2.93 kPa≡390.6 kTorr, that of xylene is 0.80 kPa≡106.7 kTorr at 20 °C and that of pseudocumene is 0.21 kPa≡37.33 kTorr at 25 °C. Bubbling air through poisonous and/or toxic solvents to measure the airborne radon concentration is harmful to humans. Additionally, detrimental environmental effects are a concern. The vapor pressure of our developed silicone oil is very low, 10^{-7} Torr at 20 °C, and the potential harm is also extremely low. The oil is safe for humans and environmentally friendly.

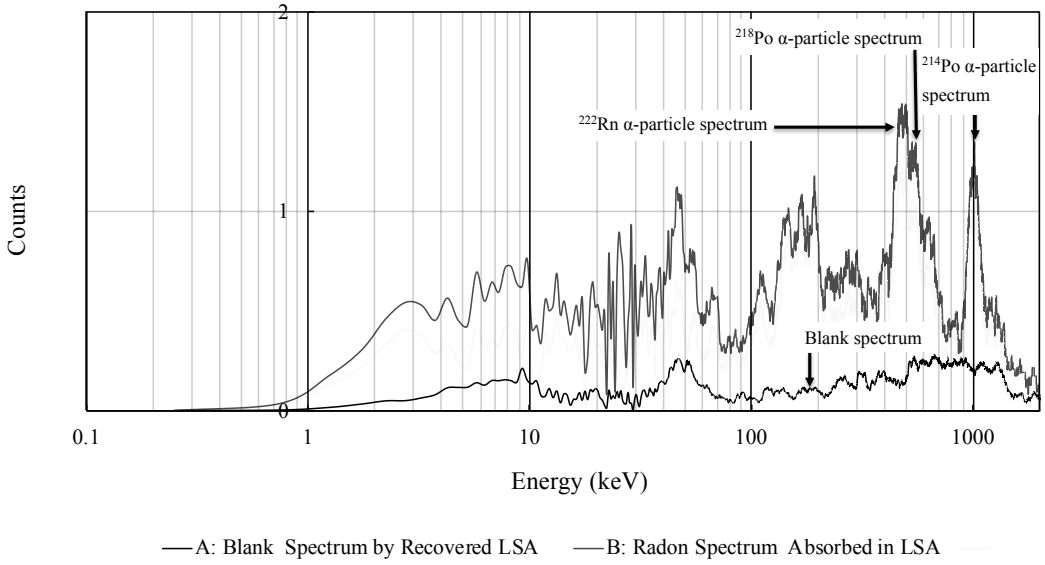

Figure 7-4 (A) The blank (background) spectrum of the LSA recovered from the radon-absorbed LSA and (B) the spectrum of ^{222}Rn absorbed in LSA coexisting with the radon progeny.

3-2. Performance of the method

The absorption ratio [absorbed radon in the NLSA/radon in air] is not the same as the Ostwald coefficient because the radon has been forcibly absorbed into the NLSA by bubbling, which prevents the absorption from reaching saturation. The average ratio was 9.2 based on 7 samples at each tested radon concentration. It is unclear whether the radon reached equilibrium in 10 mL of NLSA because radon was only present in small bubbles in the NLSA. Therefore, this degree of absorption was reached under the following conditions: bubbling period of 30 min, bubbles of the same size generated using bubbling nozzle No. 1 with an immersion filter (ø 18 mm) and glass particle with a hole size of 100~120 μm, flow rate of 4 L/min, and temperature of 20 °C.

In Table 7-1, the error in the results obtained using the ionization chamber was based on the average of the electric current fluctuations in the AlphaGUARD system with the transformation of the control mechanism over 30 min. Related to this, the parameters of the calibration curve in Fig. 7-2 include several uncertainties and errors in the corresponding sampling and counting steps. These components are mainly considered to be the electric current fluctuations in the AlphaGUARD system, the changes in the control

mechanism, variations in the absorption by the NLSA and variations in the measurement with the LSC. As a result, the parameters may vary.

As shown in Table 7-2, the pairs of concentrations obtained using the NLSA and AlphaGUARD system overlap within the error and the uncertainty in the measurements, with the exception of two pairs of values, and these values are indicated by gray shading. The errors in the measurements obtained using the ionization chamber, which are based on the electric current in the AlphaGUARD system, are reported as the average of 30 min, corresponding to the radon sampling time period used for the NLSA. However, for these measurements in natural samples, the NLSA and AlphaGUARD measurements of the sampled air differed from those of air samples taken from neighboring locations. Some uncertainty due to experimental circumstances is unavoidable. The radon concentration in the atmosphere can be detected within one hour because of the large amount of radioactivity that accumulates in the NLSA with bubbling. However, the identification limit of this measurement was somewhat higher at 36.3 Bq m^{-3} when the background was 22 counts per hour. The determination can be improved by using an LSC with a lower background signal and by increasing the counting time.

The deterioration in the quality of the oil solvent is likely due to oxidation by air. The degradation of the scintillator solvent and/or solute due to exposure to α-particles could not be confirmed. No decomposition components were found in the NLSA after exposure. To confirm the low abundance of fragmented molecules resulting from decomposition using gas chromatography/mass spectrometry and high-performance liquid chromatography, the exposure to α-particles must be equivalent to an internal irradiation of ^{35}S β-emission of 48 TBq/mmol to 18.5 GBq/mmol for more than 4 days 16). Such a high specific dose is unreasonably high for measurements of atmospheric radon. Additionally, despite recycling the LSA more than ten times and storing the sample for more than 3 months, the deterioration did not notably diminish the absorption capability or the measurement efficiency. After completion of the measurements, many kinds of radioactive impurities must be present at low concentrations in the oil solvent of the spent NLSA. The spent NLSA contained absorbed radioisotopes, e.g., radon, the progeny of radon and thoron, tritiated water and radiocarbons originating from CO_2. The amount of radioisotopes increased, which altered the background of the α-spectra. The impurities and scintillator degradation products must be removed by adsorption using charcoal. However, an extremely trace amount of some of the abovementioned radioisotopes, radon, radon and thoron progeny and tritiated water, remained, which was confirmed by the blank spectrum of the regenerated NLSA (Fig. 7-4). Therefore, the background spectrum must be reacquired when using the same NLSA lot for each measurement. Recycling is

effective for reducing environmental impacts and preserving resources.

For this method, our sampling technique and on-site measurements can be performed in locations without any special apparatus by using the hand-held LSC marketed by HIDEX (Triathler, Finland) 17). In addition, a portable LSC has been produced experimentally 18).

4. Conclusion

An advanced liquid scintillation method with a specialized NLSA was used to measure radon in air in one hour after a half-hour absorption period; this short sampling period was achievable due to acceleration by bubbling airborne radon. The radioactivity of the radon in the NLSA was immediately indirectly calculated based on ^{214}Po radioactivity using the successive decay equations. The linear relationship between the radioactivity of the radon absorbed in only 10 mL of NLSA and the radioactivity in air within the concentration range of 500-8000 Bq m^{-3} was determined. The straight line obtained by approximation based on the results for 500-8000 Bq m^{-3} using the least-squares method and extrapolated to concentrations below 500 Bq m^{-3} was reliable. The validity of this extrapolation was demonstrated by comparison with reliable measurements of indoor and outdoor air samples using NLSA and an ionization chamber. The measurements were influenced by air temperature and humidity; however, the measurements are still of practical value. NLSA is safe for humans and environmentally friendly. The NLSA measurements for radon in this study have great potential for practical applications. In addition, the relationship between safety and experimental conditions was considered.

5. Summary

The practicality of using a liquid scintillation method with an NLSA for the measurement of airborne ^{222}Rn (radon) in a residence was examined. The relationship between the radioactivity absorbed by the NLSA and the radon concentration in the air was investigated in a calibrated, walk-in radon chamber. The equivalent radioactivity of radon was calculated based on ^{214}Po radioactivity after the radioactive equilibrium was reached using successive decay equations via α-particle spectrometry based on the immediate, 1-h, indirect, selective measurement of the ^{214}Po α-spectrum acquired after radon sampling. The author confirmed that the amounts of radon absorbed in the NLSA were proportional to the radon concentration in the air. The calibration curve, which demonstrated the reliable quantitative linearity of the method from 500 to 8000 Bq m^{-3} in air, was extrapolated to concentrations below 500 Bq m^{-3} using the least-squares method based on the data from 500 to 8000 Bq m^{-3}. The validity of the extrapolated curve below

500 Bq m^{-3} was confirmed by comparison of the radon concentrations measured in indoor and outdoor air samples with those determined using an ionization chamber. Variations in the absorption of radon were observed due to changes in temperature and humidity. The health and environmental safety of the NLSA was also discussed.

References

1) Noguchi, M. (1964) New Method of Radon Activity Measurement with Liquid Scintillator. Radioisotopes, **13**, 362-366.

2) Prichard, Howard M. (1983) A Solvent Extraction Technique for the Measurement of ^{222}Rn at Ambient Air Concentration, Health Physics **45**, 493-499.

3) Salonen, L. (1993) A rapid method for monitoring of uranium and radium in drinking water. The science of the Total Environment, **130/131**, 23-25.

4) Salonen, L. (2010) Comparison of two direct LS methods for measuring ^{222}Rn in drinking water using α/β liquid scintillation spectrometer, Appl. Radiat. Isoto. **68**, 1970-1979.

5) Kato, T. (1981) Transformation of Liquid Scintillation Spectrum Shapes Obtained from Different Amplifiers, International Journal of Appl. Radiat. Isoto. **32**, 248-250.

6) Gudjónsson, G., Theodórsson, P., Sigurdsson, K., Kozak, K. and Grzadziel, D. (2009) A study of the simple open-vial scintillation method for measurement of radon in air. LSC 2008 Advances in Liquid Scintillation Spectrometry, edited by J Eikenberg, M Jäggi, H Beer, H Baehrle, 361–366.

7) Kato, T., and Hatagami, T. (1980) Nonvolatile Liquid Scintillator, Anal. Chem. **52**, 586-587.

8) Janik, M., Tokonami, S., Kovàcs, T., Kàvàsi, N., Kranrod, C., Sorimachi, A., Takahashi, H., Miyahara, N. and Ishikawa, T. (2009) International Intercomparisons of Integrating Radon Detectors in the NIRS Radon Chamber, Appl. Radiat Isoto. **67**, 1691-1696.

9) Oikari, T., Kojola, H., Nurmi, J. and Kaihola, L. (1987) Simultaneous Counting of Low Alpha- and Beta-Particle Activities with Liquid-Scintillation Spectrometry and Pulse-Shape Analysis, Appl. Radiat. Isoto. **38**, 875-878.

10) Horrocks, D. L. and Studier, M. H. (1964) Determination of Radioactive Noble Gases with a Liquid Scintillator, Anal. Chem. **36**, 2077-2079.

11) Bateman, H. (1910) The solution of system of differential equations occurring in the theory radio-active transformations, Proceeding of Cambridge Philosophical Society **15**, 423-427.

12) Sanada, T., Fjimoto, K., Miyano, K., Doi, M., Tokonami, S., Uesugi, M. and Takata, Y. (1999) Measurement of Nationwide Indoor Rn Concentration in Japan, J.

Environmental Radioactivity **45**, 129-137.
13) Air Quality Guidelines, Second Edition, WHO Regional Office for Europe, Copenhagen, Denmark, Chapter 8.3 Radon (2001).
14) Gesell, Thomas F. (1983) Background Atmospheric ^{222}Rn Concentration Outdoors and Indoors: A. Review, Health Physics **45**(2), 289-302.
15) Currie, L.A. (1968) Limits for Qualitative Detection and Quantitative Determination, Anal. Chem. **40,** 586-593.
16) Kato, T., Saito, K. and Kurihara, N. (1994) Self-decomposition Components Generated from ^{35}S-labeled Amino Acids. Int. J. Appl. Radiat. Isoto. **45**, 693-698.
17) Yasuoka, Y., Ishikawa, T., Fukuhori, N. and Tokanami, S. (2009) Comparison of Simplified Scintillation Counter (Triathler) with Conventional Liquid Scintillation Counter in the Measurement of Radon Concentration in Water, J. Hot. Spring Sci. **59**, 11-21.
18) Sato, J., Takahashi, H. and Sato, K. (1981) Portable Liquid Scintillation Counter for In-Situ Radon Measurement, Int. J. Appl. Radiat. Isoto. **32**, 592-594.

Chapter 8

Measurement of radon in air using a radon-^{218}Po calibration curve determined by an absorptive nonvolatile liquid scintillator
Radon (^{222}Rn) measurements II.
Novel measurements of radon based on ^{222}Rn-^{218}Po radioactivity.

1. Introduction

Chapter 8 of this work describes a novel method for determining ^{222}Rn (radon) in air using a radon-^{218}Po calibration curve constructed using a nonvolatile liquid scintillation absorbent (NLSA). The ability of this method to detect radon at the low concentrations found in natural environments was confirmed from the linear extrapolation of the curve between 500–8000 Bq m^{-3}. The calibration curve was generated from data obtained from measurements performed using a radon calibration chamber at the National Institute of Radiological Science (NIRS) using the least-squares method. The line had high precision and reliability, and the required detection time was less than that required for ^{214}Po. An NLSA was used to collect radon, and this strategy was found to be highly advantageous for α-spectrometry liquid scintillation measurements. The variations in the Ostwald coefficient due to changes in temperature and humidity, which affect radon absorption, were investigated and are discussed.

Keywords: Radon, Liquid scintillation, Radioactivity, α-spectrometry, Nonvolatile liquid scintillator

Generally, the radioactive equilibrium for radon is calculated, and the efficiency of ^{214}Po radioactivity based on the α-spectrum is used to determine the radon concentration in air 1) 2). This method is commonly used because the overlap of the radon spectrum interferes with the calculations when the α-spectra of ^{220}Rn (thoron) and the progeny of ^{226}Ra are combined in a scintillator for standardization 3), 4). However, the ^{214}Po α-spectrum does not overlap with radon, thoron, their decay nuclides or ^{226}Ra. Therefore, when the radioactive equilibrium between radon and ^{214}Po is reached after 4 h 5), 6), the radioactivity of radon must be determined from either air or water. A delay time of approximately 10–20 min is likely achievable when determining radon concentrations in air if the air sample is saved in a bag, which decreases both the thoron and degraded radon concentrations, making this collection method preferable. This study presents a method for determining airborne radon based on a radon-^{218}Po calibration curve that can be applied after thoron has almost completely decayed and when the amount of radon is

constant.

The radon-^{218}Po calibration curve in the region of 500-8000 Bq m^{-3} was prepared using data acquired in the radon chamber at the NIRS 7). In the region of 500-8000 Bq m^{-3}, the absorbed radioactivity in the NLSA and the radon concentration in air were proportional, as indicated by the calibration curve. The curve was extrapolated to concentrations less than 500 Bq m^{-3}. Actual radon concentrations in the atmosphere were determined by comparison with the linearly extrapolated region of the radon-^{218}Po calibration curve below 500 Bq m^{-3}. These determinations confirmed that the extrapolated line was linear at concentrations below 500 Bq m^{-3}, similar to the 500-8000 Bq m^{-3} region.

A nonvolatile liquid scintillation absorbent (NLSA) was used to sample the airborne radon. The NLSA contained a collector for airborne radon and a liquid scintillator 8). NLSAs are attractive materials because they use a nonvolatile solvent, and the components of the mixture remain unchanged during an extended sampling period 9) based on the fact that the quenching index measured relative to an external standard source (^{133}Ba) was the same before and after sampling. The mixture was transparent and colorless. Therefore, using an NLSA does not increase quenching. Radon was collected from the air using an NLSA, with the entire volume (10 mL) of the NLSA in the 20-mL scintillation vial constituting the sample. Here, a measurement method that provides higher quality results 10), 11), 12) while requiring fewer operational steps relative to previous methods is reported. In addition, to enhance the reliability of the measurements, variations in the Ostwald coefficient among the absorptive properties of the NLSA induced by temperature and humidity variations were investigated.

2. Experimental

2-1. Materials and Methods.

The absorptive NLSA was prepared as follows: 0.6 g of Cristal Fluor (cat. no. 882419, Parc d'innovation, Illkirch, France) and 1,5-diphenyloxazole (PPO)/p-bis-(o-methylstyryl)-benzene (bis-MSB) (95:5, w/w)) were dissolved in 100 mL of methyl-phenyl silicone oil (HIVAC F4, Shin-Etsu Chemical Co., Ltd., Tokyo, Japan). A glass filter was used for the GF/F (ø 55 mm, Whatman, Kent, U.K.). A 200-L sealed resin bag (Tefuron bag, Azuwan Limited, tedora-bag, Osaka City, Japan) was used for air sampling. A bubbling nozzle with an immersion filter (ø 18 mm, glass particle number 1 (100–120 μm) with a length of 229 mm) and a glass tube (ø 8 mm; Sogorikagaku Glass Works, Osaka, Japan) were used in addition to an LSS-A: Tri-Carb 3100TR (Perkin Elmer, Boston, U.S.A. (LSS-A)) and an LSS-B: Tri-Carb 2770TRSL (Packard Instrument, Co., U.S.A. LSS-B). Twenty-milliliter Teflon vials purchased from Kagaku Kyoeisha, Ltd.

(Osaka, Japan) were used for counting. An ionization chamber (AlphaGUARD SAPHYMO GmbH, Frankfurt a.M., Germany) was also used. A gas flow ionization chamber (TAM 73D, CANBERA) was used with a flow rate of 4 L/min.

2-2. Radon Sampling Method and Measurements Used to Construct the Radon-^{218}Po Calibration Curve

Radon concentrations were measured in a radon calibration chamber at the NIRS and sampled from the atmosphere. The radon collected from the chamber was not mixed with thoron. Atmospheric radon was bubbled and collected through a glass filter in 10 mL of NLSA at a flow rate of 4 L/min for 30 min. The radon in the chamber was sampled at radioactive levels of approximately 200, 500, 1000, 3000, 5000, 7000 and 8000 Bq m^{-3}. The established radioactivity levels were associated with a relative standard uncertainty of less than ±4% for the range from 500-8000 Bq m^{-3}. Radon levels below 500 Bq m^{-3} were associated with a relative standard uncertainty of more than 5%. Both the radioactivity of the radon and the air temperature and humidity (20 °C and 60%) were calibrated and held constant. The radon concentration in the sample in the vial was measured using LSS-A, and the findings were used to plot a calibration curve.

2-3. Method used to Confirm the Suitability of the Calibration Curve and its use for Practical Measurements

Air samples were collected from many rooms through glass filters and were stored in 200-L sealed resin bags for 10–20 min to allow the thoron to decay. Each stored air sample was bubbled through a filter in a vial into 10 mL of NLSA for 30 min at a flow rate of 4 mL/min. Within one hour, the sample vial was measured using LSS-B. This measurement strategy was suitable for practical measurements of indoor and outdoor air samples. The radon concentrations in the air samples stored in the 200-L sealed resin bags were measured using an ionization chamber with a gas flow rate of 0.1 L/min entering and exiting the chamber. This experiment was performed to confirm that the extrapolated line used to measure concentrations less than 500 Bq m^{-3} is quantitative. These measurements are shown in Fig. 8-1.

2-4. Ostwald coefficient

To further understand the LSA properties, the Ostwald coefficients for the temperature- and humidity-induced fluctuations in radon absorption were measured using an NLSA in a radon chamber at the NIRS. The absorption fluctuations induced by temperature variations were determined at 10, 20 and 30 °C using a constant radon concentration of 5000 Bq m^{-3} inside the chamber and a constant humidity of 60%. The absorption fluctuations induced by humidity variations were determined at 30, 40, 50, 60, 70, 80 and 90% humidity using a constant radon concentration of 5000 Bq m^{-3} inside the chamber

and a constant temperature of 20 °C.

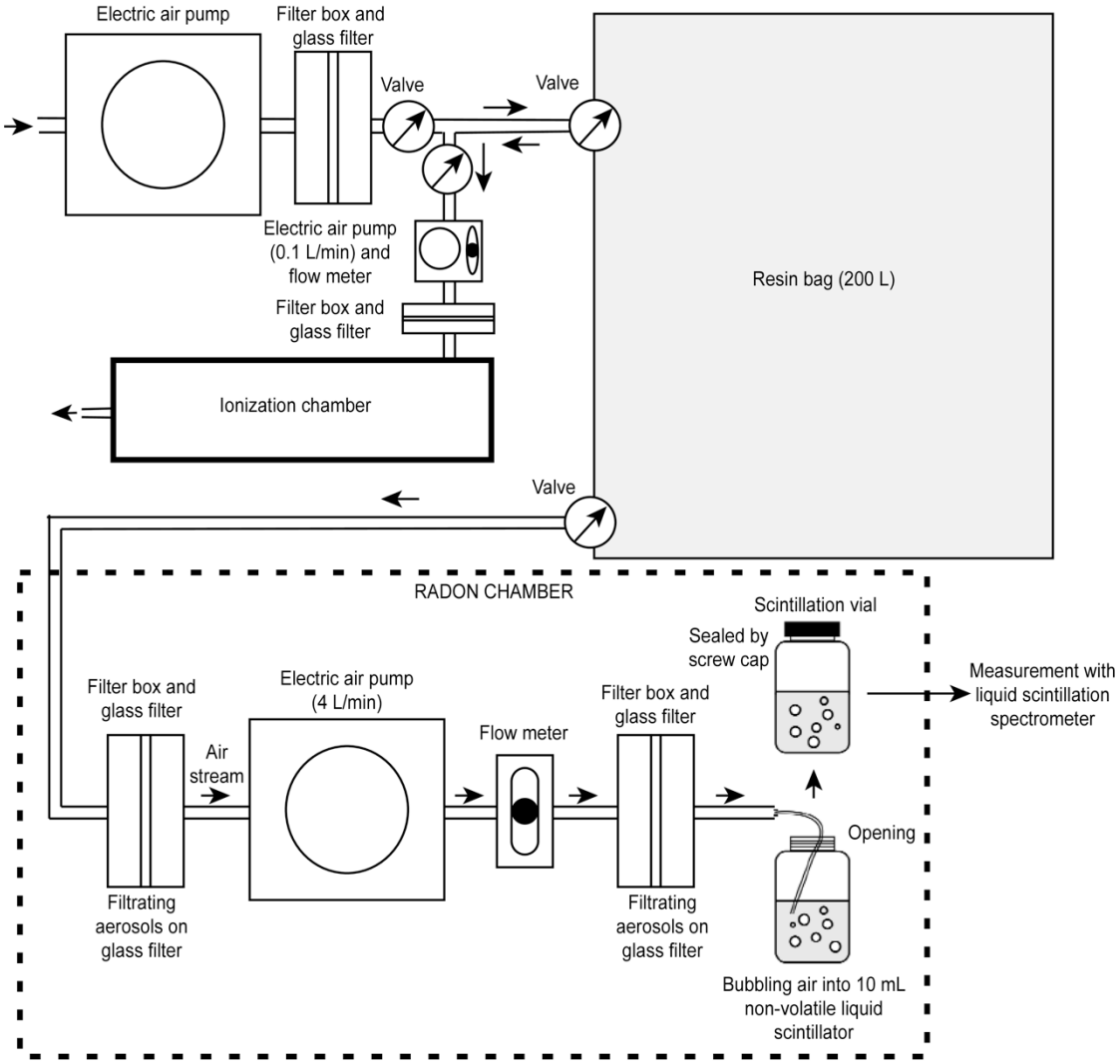

Figure 8-1 Illustration of the sampling process and ^{222}Rn measurements in an NLSA with bubbling air and a gas flow ionization chamber.

3. Results

The radon-^{218}Po radioactivity calibration curve is shown in Fig. 8-2. The data for each point are presented in Table 8-1. The line shown in Fig.8-2 indicates the relationship between the absorbed radon-^{218}Po radioactivity in 10 mL of NLSA and atmospheric concentrations between 500 and 8000 Bq m^{-3}. The line was extrapolated to concentrations less than 500 Bq/m^3 based on the data obtained for 500-8000 Bq m^{-3} by using the least-squares method.

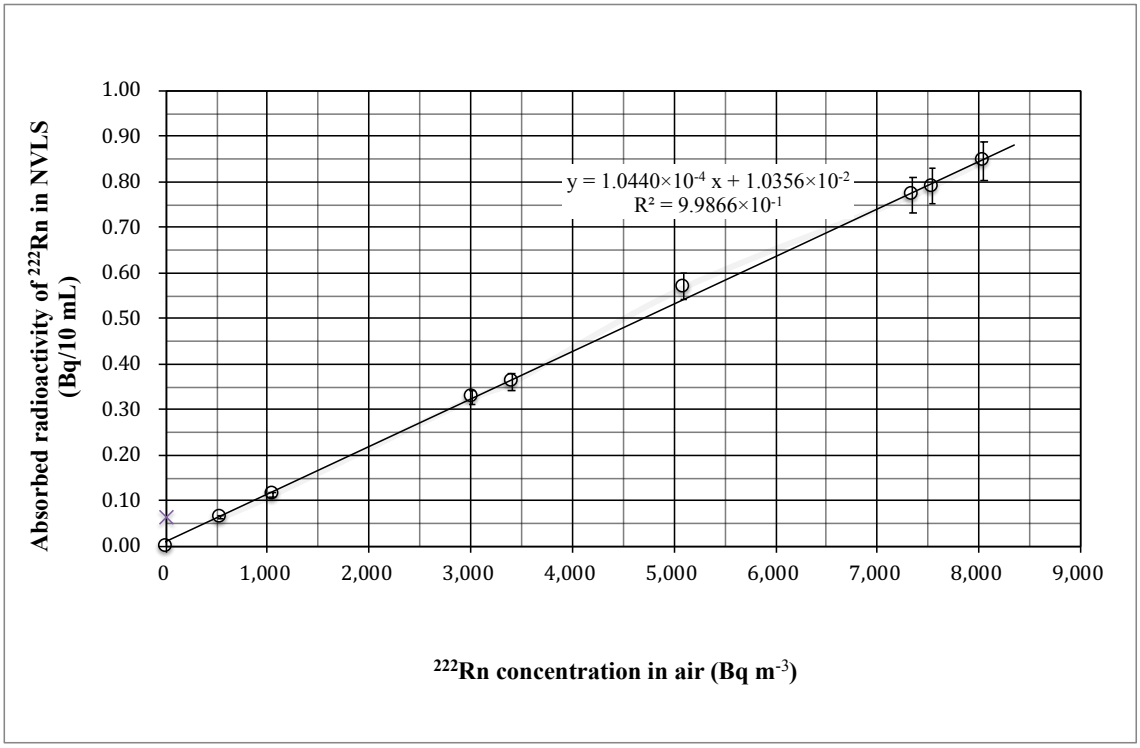

Figure 8-2 Calibration curve showing the relationship between the radioactivity of ^{222}Rn absorbed in the NLSA and the radioactivity of ^{222}Rn in the air. This investigation was conducted in a radon calibration chamber at NIRS.

The extrapolated line is used to calculate typical liquid scintillation measurements of the absorbed radioactivity of radon in atmospheric and residential samples using the NLSA (Table 8-2). These concentrations were compared with measurements performed using the AlphaGUARD ionization chamber, which also used an NLSA, based on the ^{214}Po calibration curve after radioactive equilibrium with radon was reached. The concentrations determined using the radon-^{218}Po calibration curve and measured with the NLSA fall within the uncertainties of the AlphaGUARD measurements. However, the two values measured with the NLSA using the ^{214}Po calibration curve were outside the range of the uncertainties of the AlphaGUARD radon concentrations, and these values are indicated by gray shading in Table 8-2.

The Ostwald coefficients showing the changes in the amounts of radon absorbed by the NLSA due to changes in temperature are presented in Fig. 8-3. The Ostwald coefficients showing the changes in the amounts of radon absorbed by the LSA due to changes in humidity are presented in Fig. 8-4.

Table 8-1 Detailed data describing the relationship between the radon concentration in air and the radon radioactivity absorbed in 10 mL of NLSA by bubbling. The atmospheric radon concentrations were measured using LSS-A (Tri-Carb 3100TR) and an AlphaGUARD ionization chamber in a radon calibration chamber at NIRS.

C: Concentration of ^{222}Rn in Air (Bq m^{-3}) (20℃, relative humidity 60%), Error : ±4%	539	1050	3020	3400	5100	7350	7540	8050
Absorbed Radioactivity of ^{222}Rn in 10 mL Liquid Scintillant Absorbent (LSA) (Net Counts/10 mL·hour)	230	411	1177	1299	2051	2778	2848	3049
A: Absorbed Radioactivity of ^{222}Rn in 1.0 m^3 LSA (Bq m^{-3})	6401.6	11409.6	32680.6	36089.2	56981.9	77163.0	79109.4	84683.3
A/C: Ostwald Coefficient A/C: (Average of Ostwald Coefficient =10.9)	11.9	10.9	10.8	10.6	11.2	10.5	10.5	10.5
Transfer Time Period from Sampling Point to the Place of Liquid Scintillation Spctrometer (min)	5.6	5.0	4.2	5.0	4.2	5.6	5.0	3.5
Tenperature (℃)	21.8	22.1	22.1	22.0	22.1	22.0	22.1	22.0
Humidity (%)	57.4	55.8	55.9	56.6	55.3	56.4	56.0	56.3

4. Discussion

After 20 min, the radon radioactivity had decreased by only 0.9975, which was within the range of the uncertainty and did not affect our measurements. The thoron radioactivity decreased by 5.64×10^{-4} and 3.18×10^{-7} after 10 and 20 min, respectively, and a 20-min delay was preferable over a 4-h delay. Another advantage of storing the sample air in a resin bag is the homogenization of the radon concentration in the air. Radon in air drifts in strips, similar to cigarette smoke. Radon was measured continuously at 2-s intervals using a gas flow ionization chamber (TAM 73D, CANBERA, flow rate: 4 L/min), as shown in Fig. 8-5. The radon concentration was very high, and no other fractions were monitored. The high concentration was considered to result from two types of high-concentration thin-layer drifts as well as the high-concentration mass drift of radon. When either a thin layer of radon or a mass of radon reached the ionization chamber and was bubbled through the NLSA, the measured results were similar to those obtained with a high concentration of radon. However, when only one of those high concentration bands reached the ionization chamber or was bubbled through the NLSA, the measured results obtained at high and low concentrations were different, and they were inconsistent with the samples with high radon concentrations or no radon. Collecting the air in a resin bag is thus a superior method for homogenizing the radon in the sample, which affects the stability of the measurements.

Table 8-2 Typical values of radon concentrations in indoor air samples stored in resin bags measured with both the liquid scintillation spectrometer LSS-B (Tri-Carb 2770TRSL) using the NLSA and the AlphaGUARD gas flow ionization counter after 20 min. The flow rate was set at 4 L/min for 30 min for liquid scintillation and at 0.1 L/min for 30 min for the ionization chamber. The pairs of measurements were compared. The liquid scintillation values were calculated using linear extrapolation to values below 500 Bq m^{-3} and an approximation based on the least-squares method from the data points in the range 500-8000 Bq m^{-3}. The calculated values were within the error of the ionization measurements.

Using ^{222}Rn-^{218}Po Calibration Curve Radon Concentration in Air (Bq m^{-3})	AlphaGUARD by Flow Mode (0.1L/min for 30 minutes)	11.5 ±8.3	15.2 ±9.0	30.5 ±13.5	36.5 ±15.3	48.0 ±19.8	82.3 ±26.7	96.8 ±33.2	118.5 ± 40.3	120.8 ± 39.4	144.7 ± 44.9	217.3 ± 55.5
	NVLS Absorption by Bubbling in 10 ml NVLS (4L/min for 30 minutes)	16.4 ±4.4	12.0 ±3.5	20.6 ±4.5	37.3 ±6.1	62.4 ±7.9	64.2 ±8.0	104.3 ± 10.2	78.3 ±8.9	110.5 ± 10.5	142.2 ± 11.9	237.2 ± 15.4
Temperature (℃)		19	20	16	20	17	21	13	14	16	17	15
Humidity (%)		57	57	65	40	48	57	44	55	44	47	66
Atmospheric Pressure (mb)		1011	1011	1012	1017	1025	1008	1021	1017	1022	1019	1013
Using ^{214}Po Calibration Curve Radon Concentration in Air (Bq m^{-3})	NVLS Absorption by Bubbling in 10 ml NVLS (4L/min for 30 minutes)	175.5 ± 13.5	11.0 ±3.3	20.3 ±4.5	47.8 ±6.9	46.6 ±6.8	77.3 ±8.8	113.6 ± 10.7	44.6 ±6.7	135.5 ± 11.6	171.3 ± 13.1	227.8 ± 15.1

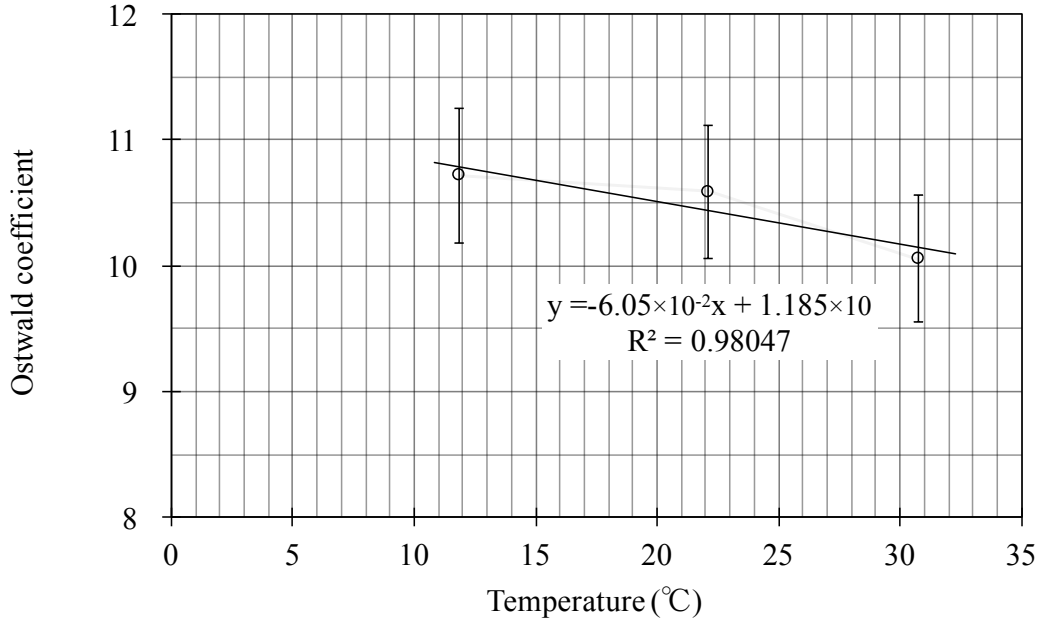

Figure 8-3 Variation in the Ostwald coefficient with temperature.

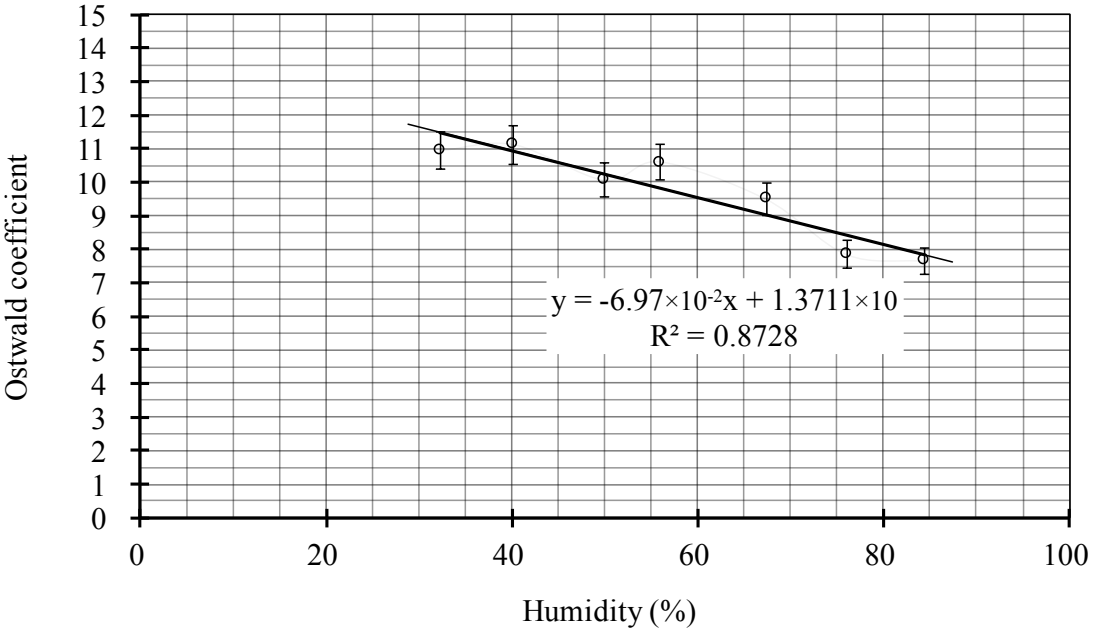

Figure 8-4 Variation in the Ostwald coefficient with humidity.

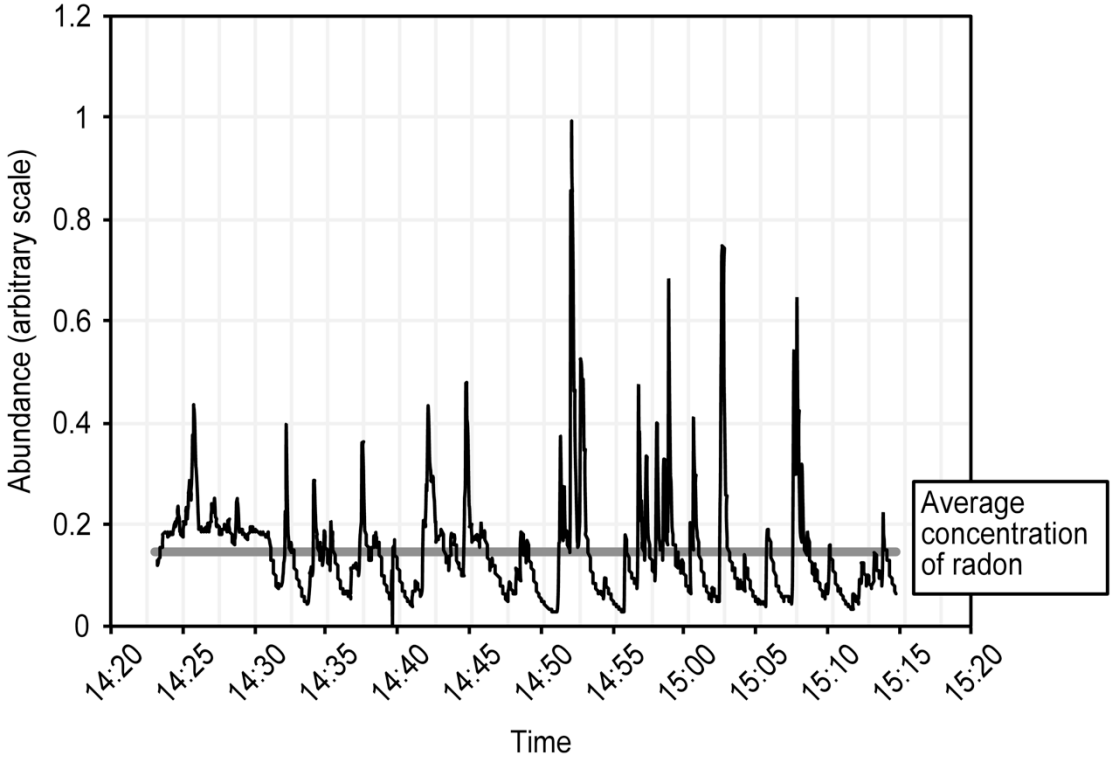

Figure 8-5 The airborne radon concentration in a room was measured continuously at two-second intervals using an ionization chamber Tam 73D, CANBERA. The radon concentration was presumed to be heterogeneous, and the radon drifts were in the form of thin layers or small masses.

The average Ostwald coefficient for temperatures of 10, 20 and 30 °C was 10.5 for the 3 samples, and the average Ostwald coefficient for humidity levels of 30, 40, 50, 60, 70, 80 and 90% was 9.7 based on 7 samples at each of the tested concentrations of radon, which was forcibly absorbed in the NLSA by bubbling. It is unclear whether the radon reached equilibrium in the 10 mL of NLSA. This degree of absorption was reached under the following conditions: a bubbling period of 30 min, bubbles of the same size generated using a No. 1 bubbling nozzle with an immersion filter (ø 18) and a glass particle 100-120 μm, a flow rate of 4 L/min, and a temperature of 20 °C. As shown by the two graphs, the Ostwald coefficient decreases as the temperature and humidity increase; thus, the relationships between the temperature and humidity and the amount of absorbed radon are both inverse, as shown in Figs. 8-3 and -4. The impacts of temperature and humidity on measurements of airborne radon are limited because the estimated uncertainty attributable to the fluctuations due to natural heterogeneity of air is larger than the

uncertainty caused by the fluctuations due to temperature and humidity.

Our handmade sampling device, which is shown in Fig. 8-6, is operated in a basket. This simple device is portable and can be used indoors or outdoors by changing the air pump's power supply to a battery. The device can be combined with a portable liquid scintillation analyzer to effectively measure radon levels outdoors 13).

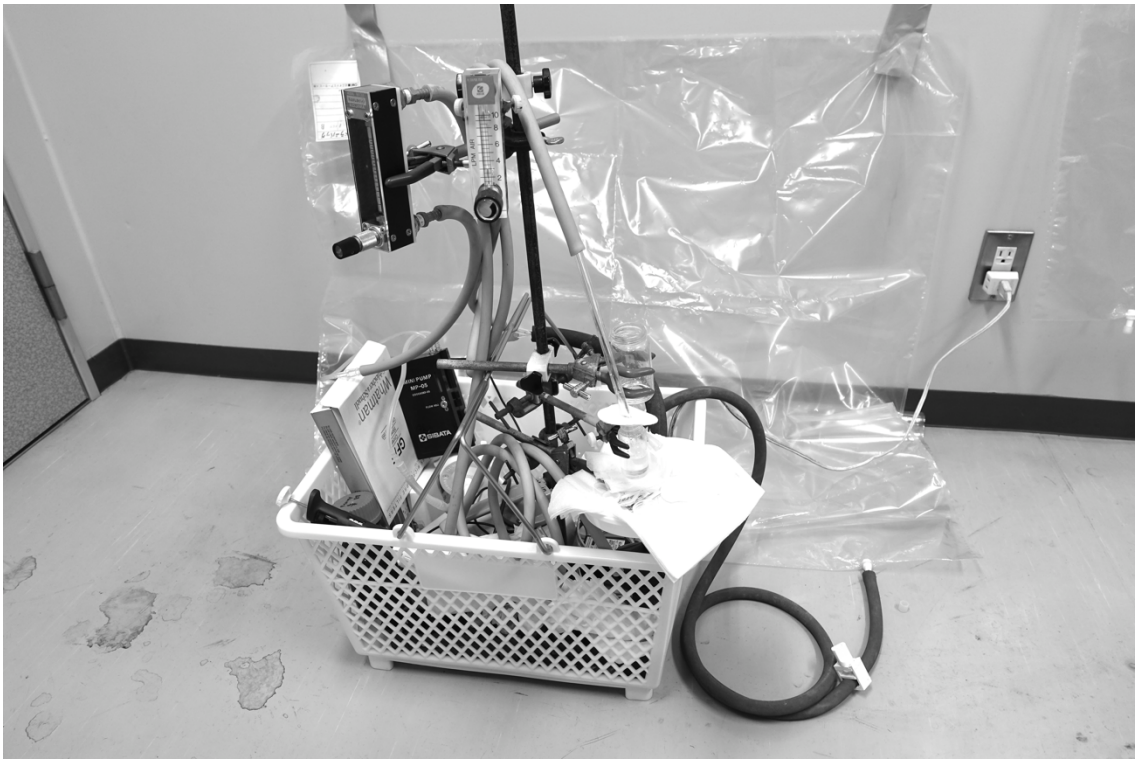

Figure 8-6 Handmade radon sampling device and the resin bag in which thoron was allowed to diminish by decay.

5. Conclusion

Atmospheric radon was measured based on a radon-^{218}Po calibration curve. The calibration curve extrapolated to concentrations below 500 Bq m^{-3} based on the data in the range of 500–8000 Bq m^{-3} using the least-squares method was both effective and useful. The air samples were stored in resin bags prior to measuring the radon to diminish the thoron concentration through degradation and homogenize the radon concentration. The measurements were influenced by air temperature and humidity; however, the practical applicability of this method is broad.

6. Summary

Radon in air can be measured based on a radon-^{218}Po calibration curve over the concentration range of ≅0 to 8000 Bq m^{-3}. The accuracy of the determination is better than that achievable with the radon-^{214}Po radioactive equilibrium method.

References

1) Prichard, H. M. (1983) A solvent extraction technique for the measurement of ^{222}Rn at ambient air concentrations, Health Phys. **45**, 493-499.
2) Vitz, E. (1991) Toward a standard method for determining waterborne radon, Health Phys. **60**, 817-829.
3) Salonen, L. (2010) Comparison of two direct LS methods for measuring ^{222}Rn in drinking water using alpha/beta liquid scintillation spectrometry, Appl. Radiat. Isot. **68**, 1970-1979.
4) Salonen, L. (1993) A rapid method for monitoring of uranium and radium in drinking water, Sci. Total Environ. **130–131**, 23-25.
5) Standard Methods for the Examination of Water and Wastewater, 20th ed., (1998).
6) Möbius Ramamonjisoa, T.L. and Möbius, S. (2002) LSC2001: Advances in Liquid Scintillation Spectrometry, University of Arizona, Tucson, pp. 253-259.
7) Janik, M., Tokonami, S., Kovács, T., Kávási, N., Kranrod, C., Sorimachi, A., Takahashi, H., Miyahara, N. and Ishikawa, T. (2009) International intercomparisons of integrating radon detectors in the NIRS radon chamber, Appl. Radiat. Isot. **67**, 1691-1696.
8) Kato, T. (1983) Analysis of tritiated water vapor by non-volatile liquid scintillant sorbent. Int. J. Appl. Radiat. Isot. 34, 1593-1595.
9) Kato, T. and Hatagami, T. (1980) Nonvolatile liquid scintillator, Anal. Chem. **52**, 586-587.
10) Cassette, P., Sahagia, M., Grigorescu, L., Lépy, M.C. and Picolo, J.L. (2006) Standardization of ^{222}Rn by LSC and canparison with α- and γ-spectrometry, Appl. Radiat. Isot. **64**, 1465-1470.
11) Horiuchi, K. and Murakami, Y. (1983) A New method for the determination of radon in Soil Air by the “Open vial” and integral counting with a liquid scintillation counter, J. Radioanal. Chem. **80**, 153-163.
12) Chalupnik, S., Meisenberg, O., Bi, L., Wang, J., Skubacz, K. and Tschiersch, J. (2010) Application of LSC and TLD methods for the measurement of radon and Thoron decay products in Air, 2010 Radiat. Protect. Dosim. **141**, 390-394.

13) Sato, J., Takahashi, H. and Sato, K. (1981) Portable liquid scintillation counter for in-Situ radon measurement, Int. J. Appl. Radiat. Isot. **32**, 592-594.

Chapter 9

General Conclusion

General Introduction.

The ability to measure radioactivity in the air, which was developed following the deaths of miners due to lung cancer, is the first step in protecting the human body and makes it possible to evaluate internal and external radiation exposure in humans. Moreover, monitoring and controlling the concentrations indoors or in environments with limited space environments can increase occupational safety for everyone involved. In this work, a liquid scintillation methodology for determining the individual radioactivity of gaseous materials, namely, ^{3}H, ^{14}C and ^{222}Rn, is described. The selection of the sampling medium, the practical measurement of vaporized tritiated water ($\cong 3.7\times10^{-3}$ Bq cm^{-3}) below the tritium limit of 5×10^{-1} Bq cm^{-3} to over its limit in air, and airborne radon over the concentration range from $\cong 0$ to 8000 Bq m^{-3}, the development of a scintillation absorbent collector, as well as the performance of the method are also discussed.

Chapter 1.

A liquid scintillation method that measures tritium contamination in air using a liquid sorbent ethylene glycol is described. In this method, tritium in the atmosphere is sorbed onto a sorbent, which is then mixed in a liquid scintillator and measured using a liquid scintillation counter. According to this method, the accumulated quantity of tritium is proportional to the sampling period and to the sample volume of sorbent in which tritium is uniformly sorbed. The detectable concentration of tritium in air was found to be less than 3.7×10^{-3} Bq/mL (10^{-7} μCi/mL).

Chapter 2.

A method is described how to measure low levels of contaminating radioactive gases in air with a liquid scintillation counter using methyl-phenyl silicone oil as the sorbent. With this method, tritium- and/or carbon-14-containing compounds in air with contamination levels of 3.7×10^{-3} Bq/mL (10^{-7} μCi/mL) are measured and analyzed. The sorbent was nonquenching.

Chapter 3.

A mathematically expressed quenching equation for liquid scintillation giving the

relationship between the counting rate and the quenching agent concentration in a liquid scintillator is described. The mathematical equation is essentially same as the Stern-Volmer quenching equation and is better suited to a wider range of quenching agent concentrations than the Stern-Volmer equation.

Chapter 4.

A nonvolatile liquid scintillator derived from methyl-phenyl silicone oil was produced for the analysis of radioactive gases. This scintillator, which absorbs radioactive gases, can function as a sampling and measuring medium for radioactive gases in air. Tritium and carbon-14 β-emitters and cesium-137 γ-rays can be measured by the addition of energy transfer agents.

Chapter 5.

The quantitative analysis of tritiated water vapor in air was investigated by sorption into a nonvolatile liquid scintillator sorbent derived from silicone oil. The calibration curve shows that the variation in the partial vapor pressure of the tritiated water in air was proportional to the amount of vaporized tritiated water sorbed by the liquid scintillator sorbent. The activity of β-emission from the sorbed tritiated water vapor, 3.7×10^{-3} Bq/mL (10^{-7} μCi/mL) in air, was directly measured using a scintillator that also served as the sorbent. The relation is expressed as a sorption isotherm and is compared to the Langmuir adsorption isotherm, supporting the suggested adsorption by the solid adsorbent.

Chapter 6.

The fragment molecules in the gaseous components generated from ^{35}S-amino acids with high specific radioactivity were examined. The molecules were methyl mercaptan, [hydrogen sulfide or sulfur dioxide], dimethyl sulfide, methyl ethyl sulfide and dimethyl disulfide. The one self-decomposition mode of a molecule labeled with a β-emitters was principally similar to the fragmentation mode of organic compounds impacted by accelerated electrons as in organic mass spectrometry. The degradation product, dimethyl disulfide, of unlabeled amino acids irradiated by ^{60}Co γ-rays indicated that the degradation mode induced by external γ-ray irradiation was different from the self-decomposition mode of ^{35}S labeled compounds.

Chapter 7.

An advanced liquid scintillation measurement of airborne ^{222}Rn was examined using the equivalent radioactivity of radon calculated based on ^{214}Po radioactivity after the

radioactive equilibrium was reached using successive decay equations via α-particle spectrometry based on the immediate, 1-h, and indirect measurement after a half-hour absorption period. The amounts of radon absorbed in the NLSA were proportional to the radon concentration (uncertainty within±4%) in the air. The calibration curve, which demonstrated the reliable quantitative linearity of the method from 500 to 8000 Bq m^{-3} in air, was extrapolated to concentrations below 500 Bq m^{-3} using the least-squares method. Variations in temperature and humidity in the absorption of radon are shown. The methods for restoring the NLSA involving purification are shown. The health and environmental safety aspects of working with the NLSA are also discussed.

Chapter 8.

Atmospheric radon can be measured based on a radon-^{218}Po calibration curve over the concentration range of ≅0 to 8000 Bq m^{-3}. The air samples were once stored in resin bags prior to measuring the radon to diminish the thoron concentration through degradation and to homogenize the radon concentration.

Conclusion.

A useful method for measuring atmospheric radioactivity was developed. A liquid scintillation method based on the accumulation of airborne radioisotopes using a liquid scintillation sorbent as the medium is described. The objective radioisotopes in the environment are tritiated chemical compounds, tritiated water, radiocarbon-containing compounds, ^{35}S-labeled compounds and radon. Using this method, radioisotopes in air at concentrations below the level described in “The Law concerning Prevention of Radiation Hazards due to Radioisotopes” or the natural level in the atmosphere can be collected. The described method allows measurements of numerous airborne radioisotopes that are hazardous to human health. Notably, the medium is composed of the liquid scintillator mixture and the sorbent. General and convenient atmospheric measurement methods will lead to great developments in this field.

PUBLICATIONS

Chapter 1.
Kato, Takahisa, "Measurement of Tritium in Air by Adsorbent", Nuclear Instruments and Methods, (1979) Vol. 163, pp. 463-465.

1979/ 3

Chapter 2.
Kato, Takahisa, "Monitoring of Radioactive Gases in Air by Adsorption", International Journal of Applied Radiation and Isotopes, (1979) Vol. 30, pp. 349-351.

1979/ 6

Chapter 3.
Kato, Takahisa, "Quenching Equation for Scintillation", Nuclear Instruments and Methods. (1980) Vol. 172, pp. 597-599.

1980/ 3

Chapter 4.
Kato, Takahisa and Hatagami, T., "Nonvolatile Liquid Scintillator", (1980) Analytical Chemistry, Vol. 52, pp. 586-587.

1980/ 3

Chapter 5.
Kato, Takahisa, "Analysis of Tritiated Water Vapor by Non-volatile Liquid Scintillant Sorbent", International Journal of Applied Radiation and Isotopes, (1983) Vol. 34, pp. 1593-1595.

1983/12

Chapter 6.
Kato, Takahisa, Saito, K and Kurihara, N., "Self-decomposition Components Generated from ^{35}S-labeled Amino Acids", Applied Radiation and Isotopes, (1994) Vol. 45, pp. 693-698.

1994/ 6

Chapter 7.
Kato, T, Janik, M., Kanda, R., Ishikawa, T., Kawase, M., and Kawamoto, T. (2018) “Environmentally friendly measurement of airborne radon using a non-volatile liquid

scintillation absorbent", Health Physics Journal. Vol. 115(2), pp. 203-211.

2018/8

Chapter 8.

Kato, T, Janik, M., Kanda, R., Ishikawa, T., Kawase, M., and Kawamoto, T. (2016) Measurement of radon in air using a radon-^{218}Po calibration curve determined by an absorptive non-volatile liquid scintillator, Radiation Measurement, Vol. 95, pp.25-30.

2016/12.

OTHER PUBLICATIONS

Kato, Takahisa, (1981) Transformation of Liquid Scintillation Spectrum Shapes Obtained from different Amplifiers, International Journal of Applied Radiation and Isotopes, Vol. 32, PP. 248-250.

1981/ 4

Kato, Takahisa and Hibasami, H., (1987) Measurement by Liquid Scintillation of $^{14}CO_2$ Absorbed in Hyamine, International Journal of Applied Radiation and Isotopes, Vol. 38, pp. 489-491.

1987/ 6

Kato, Takahisa and Saito, K., (2004) Preparation of background samples for accurate low-level measurements by liquid-scintillation spectrometry, Nuclear Instruments and Methods in Physics Research A, Vol. 524, pp.208-214.

2004/4

ACKNOWLEDGRMENT

The author would like to express a grateful acknowledgement to Dr. Minoru Yoneda, Professor of Environmental Risk Analysis, Graduate school of Engineering, Faculty of Engineering, Kyoto University, for his kind guidance, continuous encouragement, and generous support throughout this study.

The author would like to express a grateful acknowledgement to thank Dr. Takuo Kawamoto, Professor of Radioisotope Research Center, Kyoto University, for his useful discussion, kind advice and continuous encouragement.

The author would like to express a grateful acknowledgement to thank the decreased Dr. Noro Kurihara, ex-Professor of Radioisotope Research Center, Kyoto University, for his kind effective guidance and suggestions.

The author would like to express a grateful acknowledgement to thank Dr. Kazumi Saito, ex-Assistant Professor of Radioisotope Research Center, Kyoto University, for his kind guidance and suggestions.